Journal of Zhejiang University-SCIENCE A (Applied Physics & Engineering)
ISSN 1673-565X (Print); ISSN 1862-1775 (Online)
www.jzus.zju.edu.cn; www.springerlink.com
E-mail: jzus@zju.edu.cn

Review:

Development of natural gas liquefaction processes using mixed refrigerants: a review of featured process configurations and performance*

Qi SONG, Jing-peng ZHANG, Zhen ZHAO, Jie-lin LUO, Qin WANG[†‡], Guang-ming CHEN
Key Laboratory of Refrigeration and Cryogenic Technology of Zhejiang Province,
Institute of Refrigeration and Cryogenics, Zhejiang University, Hangzhou 310027, China
[†]E-mail: wangqin@zju.edu.cn
Received Apr. 11, 2019; Revision accepted Sept. 8, 2019; Crosschecked Sept. 18, 2019

Abstract: It is preferable to transport or store natural gas (NG) in a liquid state, as liquefied natural gas (LNG). In recent decades, a variety of natural gas liquefaction processes (NGLPs) using mixed refrigerants (MRs) with different configurations have been developed, which have greatly enriched the family of NGLPs. In this review, we introduce the configurations of featured commercial processes or patented designs chronologically in each category based on a modified classification framework. The corresponding refrigerant combinations and operating parameters such as operating pressures, the refrigeration temperature in each stage, and the number of evaporating pressure levels are also discussed. Specific power consumption (SPC) was considered as the major performance indicator. This review aims to clarify the development of NGLPs using MRs (MR-NGLPs) from a configurative perspective, and to provide a reference for the future improvement of their thermodynamic performance.

Key words: Natural gas (NG); Liquefaction; Mixed refrigerant (MR); Configuration; Performance
https://doi.org/10.1631/jzus.A1900143 **CLC number:** TE646

1 Introduction

Natural gas (NG) is a kind of gaseous fossil fuel rich in CH_4, and also containing some alkanes (such as C_2H_6, C_3H_8, and C_4H_{10}) and impurities (such as H_2O, N_2, and H_2S). It exists mainly in oil fields, gas fields, coal seams, and shale beds. According to the BP Statistical Review of World Energy 2017 (British Petroleum, 2017), the total proven global reserves of NG reached 186.6 trillion cubic meters by the end of 2016, while the total global production reached 3.5516 trillion cubic meters. However, worldwide NG consumption accounted for only 24.13% of global primary energy consumption in 2016, which leaves great potential for development.

NG is normally transported in gaseous phase by pipelines or in liquid phase by tankers. Pipeline transport can be easily controlled and is suitable for continuous operations, but the costs of pipeline construction and maintenance are high. In addition, NG pipelines are not allowed in some countries or regions, such as Japan, Korea, Taiwan, and some parts of European countries (Foss, 2012). According to Foss (2012), the cost of liquefied natural gas (LNG) transport is lower than that of offshore NG pipeline transport when the transport distance exceeds 1130 km, and lower than that of onshore pipeline transport when the transport distance exceeds 3540 km. Furthermore, small-scale, remote, and scattered NG resources have gained increasing attention, but the

‡ Corresponding author
* Project supported by the National Key Research and Development Program of China (No. 2016YFB0901404)
ORCID: Qi SONG, https://orcid.org/0000-0003-2004-9314

construction of pipelines for these resources is not economic. Therefore, LNG is preferred for long distance transport and recovery of remote NG resources.

In an early classification framework, NG liquefaction processes (NGLPs) were generally classified into three categories according to the refrigeration cycle employed: the cascade process, the expander process, and the mixed refrigerant process (Finn et al., 1999). Cascade processes were usually used with three sets of pure refrigerants (PRs) in early large-scale base-load LNG plants because of low power consumption, flexibility in operation, and mature technology, but the complexity and high capital cost of the system have led to few recent applications. In expander processes, the cooling capacity was provided by the compression and work-expansion of PR streams of N_2 or CH_4. Expander processes were suitable for peak-shaving plants and small-scale applications because of their applicability to rapid startups and shutdowns, but they had relatively high power consumption (Finn et al., 1999; Gu et al., 2004). In this framework, the mixed refrigerant processes (or mixed refrigerant cycles, MRCs) were originally modified from cascade processes by using a single set of mixed refrigerant (MR), usually a mixture of N_2 and hydrocarbons (HCs), instead of multiple PRs (Finn et al., 1999). Joule-Thomson (JT) expansion was still the only expansion method used, which was different from the work-expansion used in the expander processes. Later proposals of PR or MR precooled MRCs also fell into this category. They were widely used in both base-load plants and peak-shaving plants, due to their relatively simple structure, low initial cost, and high efficiency.

This early classification framework was adopted in many studies. Under this framework, Venkatarathnam (2008) provided a further classification of the MR processes according to whether precooling stages and phase separators were adopted, and emphasis was put on describing different mixed refrigerant processes and the analytical methods for choosing the optimum composition of refrigerants. Khan et al. (2017) presented a review of existing and future NG liquefaction technologies and optimization methodologies, in which expander-based, MR-based, and cascade-based liquefaction technologies were introduced with typical examples. An additional category of hybrid processes was also proposed to describe those processes with more than one element of the above technologies. Qyyum et al. (2017) considered only MR-based and N_2-expander-based processes in this early framework, and discussed optimization techniques for such NGLPs with a comprehensive table of state-of-the-art optimization algorithms. Most recently, He et al. (2018) focused on progress on the design and optimization of onshore and offshore NGLPs. From their point of view, current onshore NGLPs included the three categories in the early framework, while offshore NGLPs were dominated by single MR processes and N_2 expander processes. For offshore processes, in addition to the goal of minimizing energy consumption, deck space and sensitivity to platform waving should be taken into consideration.

Due to the inconsistent classification bases of the early framework, problems inevitably arose as a variety of NGLPs were developed. For example, the widely used C_3H_8 precooled mixed refrigerant (C3MR) process usually fell into the mixed refrigerant process category in the early framework, but showed the features of cascade processes. Therefore, some new classification ideas were proposed to offer better descriptions of NGLPs. Barclay and Shukri (2000) classified NGLPs into single-cycle, two-cycle, three-cycle processes, etc., considering the number of refrigeration cycles used for precooling, liquefaction, and subcooling of NG as the key parameter of different liquefaction processes. Corresponding refrigerant combinations should be selected according to the number of cycles. Mazyan et al. (2016) presented a review on the procedures involved in the NG industry, including extraction, transportation, storage, and treatment. As a key step in the preparation for transport, the liquefaction procedure was considered based on the type of refrigerant used, including PR, MR, and a combination of the two. The classifications of Barclay and Shukri (2000) and Mazyan et al. (2016) initially performed well, but further classifications were not offered. Chang (2015) focused on the structure and efficiency of the refrigeration cycles in NGLPs. Sixteen typical processes were evaluated theoretically by their figures of merit (FOMs) with the corresponding optimal conditions, in which thermodynamic analyses were based on ideal refrigeration cycles. A new nomenclature was proposed to identify the structures of cycles clearly by abbreviations, in which three different expansion processes (JT expansion, adiabatic expansion, and a combination of the two) were introduced as one of the criteria, as well as the types of refrigerants used in the refrigeration cycles and the number of refrigeration cycles. However, the number of phase separators in the MR cycles, as an important structural feature related to the system performance, was confused with the number of evaporating pressure stages in the nomenclature.

Looking back upon the development of NGLPs, MRs have been increasingly adopted not only in JT expansion cycles, but also in isentropic expansion cycles. In recent decades, a variety of natural gas liquefaction processes using mixed refrigerants (MR-NGLPs) have been developed, which have greatly enriched the family of NGLPs. Therefore, in this paper our attention is focused on all NGLPs that adopted MRs as working fluids, and which went beyond the traditional concepts of MRCs in the early framework. Previous reviews have already covered several aspects, such as process design techniques, optimization algorithms, and a comparison of onshore and offshore applications. However, the various process configurations of MR-NGLPs have not been explored in detail, and so were the priority of this study.

2 A proposed classification framework of natural gas liquefaction processes using mixed refrigerants

Evidently, the overall performance of MR-NGLPs is largely determined by their configurations and refrigerant combinations. Hence, firstly, a clear classification would contribute to a better understanding of the configurative features and suitable choices for practical applications among various NGLPs. Secondly, the selection of MR components and the optimization of MR composition and other operation parameters would serve to improve the energy efficiency of the selected process. Similar to Chang's nomenclature (Chang, 2015), in this paper we propose the establishment of a modified comprehensive classification framework for MR-NGLPs, focusing mainly on configurations and performance. Featured commercial processes and patented designs are organized chronologically in each category, in which their process configurations are first introduced. Parameters such as operating pressures, refrigeration temperature in each stage, evaporating pressure levels, and MR composition are elaborated in detail, and the specific power consumption (SPC) is considered as the major performance indicator. This review aims to clarify the development of MR-NGLPs from a configurative perspective, and to provide a reference for future thermodynamic performance improvements.

Similar to the relation between liquefaction processes and basic refrigeration cycles, MR-NGLPs were structured on specific refrigeration cycles operating with MRs. The proposed classification framework was elaborated as follows.

Optimizing the cascade of refrigeration cycles is a traditional way to improve performance. As shown in Fig. 1, MR-NGLPs were first classified into the following two classes according to whether the liquefaction cycle (the liquefaction stage) was cascaded with other refrigeration cycles: (1) single-cycle processes and (2) multi-cycle processes. Multi-cycle processes refer to those adopting two or more refrigeration cycles as the cold sources by coupled heat exchangers (HEXs), with one cycle in the liquefaction stage and others in the precooling or subcooling stage.

Component separation has an important impact on the performance of MR-NGLPs, and is realized mainly by gas-liquid separators or rectifying units in the refrigeration cycle. Therefore, according to the number of component separations, the single-cycle processes were further classified into two types: (1) MR0 processes and (2) MRx processes, in which x denotes the number of MR component separations and 0 denotes the absence of MR component separation. In open type single-cycle liquefaction processes where a portion of the NG itself serves as the refrigerant, MR separators are sometimes shared with LNG product separators. In such cases, the above classification standard should be modified as follows, for both the closed and open type processes: when the refrigerant composition at the hottest point (e.g. the outlet of the final compressor) and the coldest point (e.g. the outlet of the final expansion unit) of the refrigeration cycle stays the same, a process is classified as an MR0 process; otherwise, it is an MRx process.

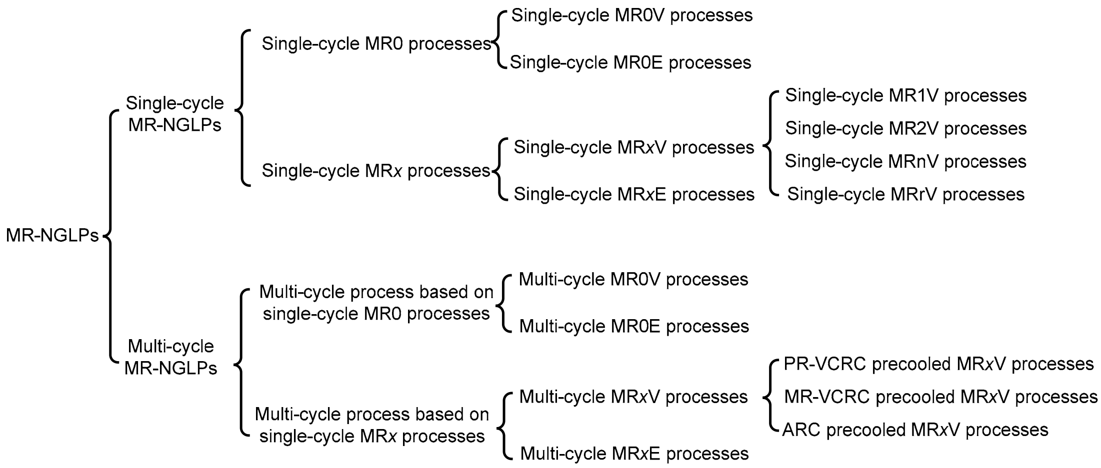

Fig. 1 Classification framework proposed for MR-NGLPs
VCRC: vapor compression refrigeration cycle; ARC: absorption refrigeration cycle

In addition to component separation, the expansion method also has an important impact on the performance of MR-NGLPs. Therefore, single-cycle MR0 and MR*x* processes are further classified into the following two kinds by the expansion methods used in the refrigerant cycles, respectively: (1) MR0V and MR*x*V processes and (2) MR0E and MR*x*E processes, in which V denotes involving only JT expansion (namely employing JT expansion units such as expansion valves and capillary tubes), while E denotes involving other types of expansion rather than only JT expansion (namely employing non-JT expansion units such as expanders, vortex tubes, and ejectors, as well as combinations of JT and non-JT expansion units). A further criterion, the number of phase separators, is proposed for single-cycle MR*x*V processes.

Numerous multi-cycle processes can be constructed when the single-cycle processes are cascaded with other refrigeration cycles. Therefore, multi-cycle processes are classified into four types on the basis of the single-cycle processes used in the liquefaction stage: (1) multi-cycle MR0V processes, (2) multi-cycle MR0E processes, (3) multi-cycle MR*x*V processes, and (4) multi-cycle MR*x*E processes. The form of precooling cycles serves as a further criterion for multi-cycle MR*x*V processes.

In summary, MR-NGLPs are classified by three main criteria successively in the proposed framework (Fig. 1): employing a single refrigeration cycle or cascaded cycles, using phase separators for component separation or not, and using only JT expansion or other expansion methods, all of which will be introduced in the following sections.

3 Single-cycle natural gas liquefaction processes using mixed refrigerants

The configurations of single-cycle NGLPs are relatively simple. In closed type single-cycle processes, there is only one refrigeration loop, while in open type single-cycle processes, the cooling capacity is provided only by the expansion of the NG feed or a mixture of NG and other added components.

3.1 Single-cycle processes without component separation (single-cycle MR0 processes)

In late 1890s, von Linde (1895) and Hampson (1896) independently proposed constantly running air liquefiers which can also be used as a closed type refrigerator. Since the 1960s, the Linde-Hampson refrigeration cycle has undergone considerable development due to the adoption of N_2-HC mixtures. Over decades, it had evolved from an open system to a closed system and from multi-stage oil-free compression to single-stage oil-lubricated compression. Alfeev et al. (1973) and Little (1978a, 1978b) conducted studies on the performance of the open systems with N_2-HC mixtures as the multi-component working fluids. Later, Little (1988, 1990) studied the performance of closed systems, adopting multi-stage oil-free compressors and reversible gas purification systems. Longsworth (1994) introduced a single-stage oil-lubricated hermetic compressor to the closed system, and further improved its thermodynamic efficiency (Boyarsky et al., 1995; Longsworth et al., 1995, 1996).

The Siemens refrigeration cycle proposed by Siemens (1857) was first used to cool or liquefy gases with a piston expansion engine. This cycle was also called the reverse Brayton cycle. At first, pure N_2 was adopted in the Siemens refrigeration cycle to liquefy NG, but its power consumption was too high. Although proposed before the Linde-Hampson cycle, the use of MRs in the Siemens refrigeration cycle to liquefy NG was adopted much later due to two-phase expansion problems at low temperatures.

As mentioned above, MR-NGLPs were structured on basic refrigeration cycles operating with MRs. Hence, from a configurative point of view, the liquefaction processes without component separation (MR0 processes) could be regarded as being developed from the Linde-Hampson refrigeration cycle (von Linde, 1895; Hampson, 1896) or the Siemens refrigeration cycle (Siemens, 1857) (or the reverse Brayton cycle). Single-cycle MR0V and MR0E will be discussed in detail below.

3.1.1 Single-cycle MR0 processes with only JT expansion (single-cycle MR0V processes)

Maher and Sudduth (1975) patented a closed type single-cycle MR0V process (Fig. 2). The MR runs between a high pressure of 2.07–4.48 MPa and a low pressure of 0.28–1.03 MPa, and consists mainly of CH_4 and C_3H_8 (advisably 40%–60% mole percent of CH_4, 40%–60% mole percent of C_3H_8, and 0–10% mole percent of N_2 and other HCs, where the sum of CH_4 and C_3H_8 exceeded 90% mole percent). The flow rates are regulated such that every 3 mol of refrigerant can liquefy 1 mol of NG. After being liquefied in HEX (Fig. 2, item 3), the NG is depressurized and stored in a liquid state, during which boil-off gas (BOG) is inevitably generated. The structure of the process requires little investment and is considered the simplest form of an MR0V process. It is also known in the literature as the SMR (single mixed refrigerant) process.

Swenson (1977) from the Black & Veatch (Pritchard) Company proposed a single MR0V process operating at one evaporating pressure level (Fig. 3), also known as the poly refrigerant integrated cycle operation (the PRICO process). Though essentially similar to the process in Fig. 2, it is better suited to industrial applications. One of the modifications lay in the gas-liquid separation after partial condensation of the single MR in a refrigerant drum (Fig. 3, item 3). The liquid phase is then pumped to join the gaseous phase at the same hot refrigerant inlet of the HEX (item 6). Though a gas-liquid separation process takes place here, the mixing of the two phases restores the same composition of the compressed refrigerant before heat exchange, which serves the purpose of avoiding maldistribution. According to the original patent, the MR loop operates between 2.04 MPa and 0.41 MPa to liquefy 4 MPa NG, with the expected MR mole fractions of 0–12% N_2, 20%–36% CH_4, 20%–40% C_2H_4 (C_2H_6), 2%–12% C_3H_6 (C_3H_8), 6%–24% i-C_4H_{10} (n-C_4H_{10}), and 2%–14% i-C_5H_{12} (n-C_5H_{12}). When cooled to about −5 °C and −32 °C, the NG is extracted twice from the HEX using the sensible heat of BOG, to remove it from the heavy components.

The PRICO process was commercialized successfully and first applied in the Skikda LNG plant in Algeria (Geist, 1983). It requires relatively less equipment and investment, has a lower operation cost, is reliable and flexible, and has a fast start-up. By 2015, 21 sets of LNG facilities had adopted the PRICO process, 13 of which had been put into production in China (Luo et al., 2015). The PRICO process is suitable for small and medium scale NG liquefaction operations, where the capacity is generally 50–2000 t/d.

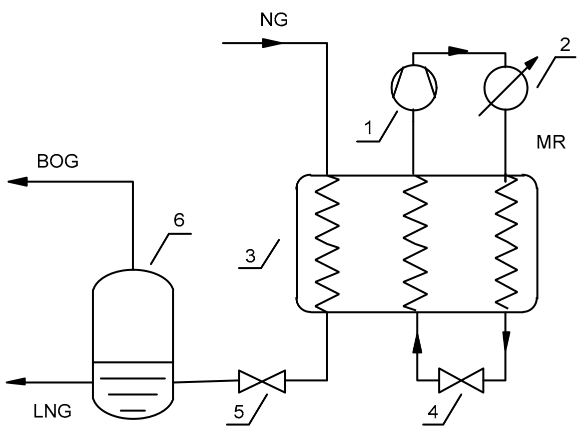

Fig. 2 A single-cycle MR0V process, adapted from Maher and Sudduth (1975)

1: compressor; 2: condenser; 3: HEX; 4, 5: expansion valves; 6: storage tank

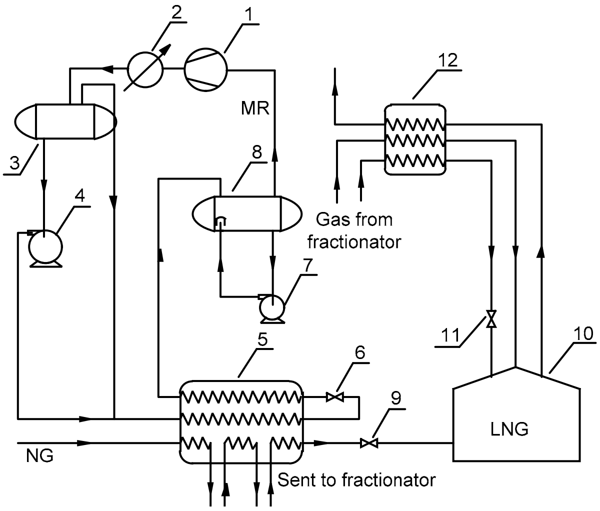

Fig. 3 A single-cycle MR0V process adapted from Swenson (1977)

1: compressor; 2: condenser; 3, 8: MR drums (separators); 4, 7: pumps; 5, 12: HEXs; 6, 9: expansion valves; 10: storage tank; 11: back pressure valve

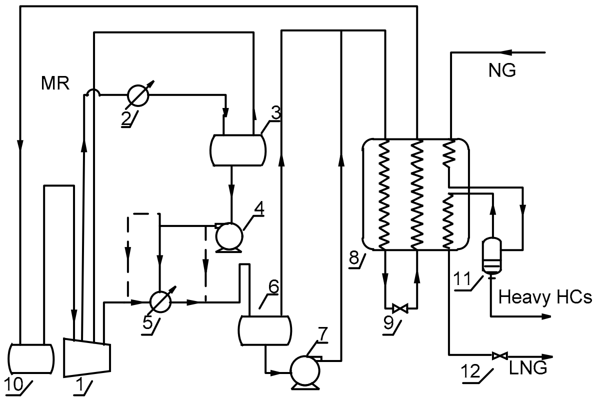

Fig. 4 A single-cycle MR0V process adapted from Price (1997)

1: two-stage compressor; 2, 5: condensers; 3, 6: MR separators; 4, 7: pumps; 8: HEX; 9, 12: expansion valves; 10: suction drum; 11: NG separator

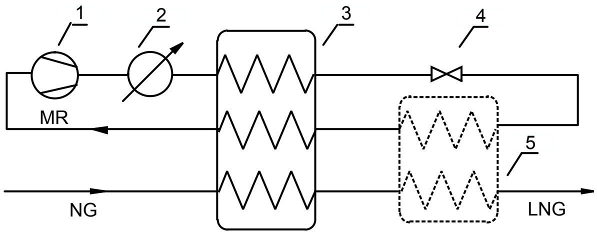

Fig. 5 A single-cycle MR0V process adapted from Gong et al. (2004)

1: compressor; 2: condenser; 3: HEX; 4: expansion valve; 5: optional evaporator

Further revisions were made to Swenson (1977)'s invention by Price (1997), as shown in Fig. 4. A two-stage compressor (Fig. 4, item 1) and an MR separator (item 3) between the first and second compression stages are adopted to remove a portion of MR, so as to reduce the amount of refrigerant to be compressed in the second stage and therefore decrease the power consumption. The pressure ratios of the two compressors were also reduced, also to reduce compression power consumption. The separator used here serves a similar purpose of avoiding refrigerant maldistribution as in Swenson's design, and is also used to reduce the refrigerant flow rate in the second compression stage.

Gong et al. (2004) suggested that the configuration of the single-cycle MR0V process (Fig. 2) was suitable for supercritical NG, because there was no latent heat load in the low temperature section. However, their theoretical analyses showed that an evaporator (Fig. 5, item 5) was needed in the low temperature section in addition to the main HEX (Fig. 5, item 3) for subcritical NG, because the latent heat of NG was more than half of the total heat load. An SPC of 0.42 kW·h/kg for liquefying 6 MPa NG was reached in their simulation, but experiments gave only 1.35 kW·h/kg for 5 MPa CH_4 and 1.81 kW·h/kg for 0.1 MPa CH_4.

With the extensive application of single-cycle MR0V processes, their thermodynamic performance became a widespread concern, where energy and exergy analyses served as excellent approaches. Remeljej and Hoadley (2006) conducted exergy analyses on the PRICO process similar to that shown in Fig. 3 (the special compression process considered, heavy component removal process neglected) with given inlet temperature, inlet pressure, NG composition, pressure losses, and ambient temperature. Results showed that an SPC of 0.355 kW·h/kg was achieved when 5.5 MPa NG was liquefied to −157 °C. Two thirds of the exergy loss was caused by the compression and after-cooling, and the remainder by the temperature differences in the HEX. Exergoeconomic and exergoenvironmental analyses were introduced to the optimization of a single-cycle MR0V process similar to that shown in Fig. 2 by Morosuk et al. (2015). Aspen Plus was used as the simulation tool, where 6.7 MPa NG was cooled from 38 °C to −159 °C by the MR loop operating at 0.3–2.2 MPa. The compositions of NG and MR were obtained from Mokhatab and Economides (2006) and Jensen and Skogestad (2009a). Results showed a coefficient of performance (COP) of 0.44 and an SPC of 0.507 kW·h/kg (1824 kJ/kg LNG). According to the exergy analysis, the exergy efficiency of the whole system was 22.7%. The main HEX accounted for 58% of total exergy destruction, and the compression process for 22%. When the exergy destruction was considered with the capital investment and operating and maintenance expenses, the exergyeconomic efficiency of the main HEX was the worst among all components, making it a priority for further improvement. Considered with the environmental analysis, the worst environmental impact was still closely related to the large exergy destruction of the HEX. These new analytical methods combined with economic and environmental analyses were also instructive in the optimization of other processes.

Apart from analyses on steady operation, the variation in performance of single-cycle MR0V processes under different conditions was also a focus. Jensen and Skogestad (2009a) discussed single-cycle MR0V process (Fig. 2) cases under various constraints and tried to find the highest LNG production under specified compressor conditions. They found that LNG production was little affected by changes in some constraints, like the degree of superheating of MR at the compressor inlet, but other factors strongly affected the optimal solution. For example, a higher exhaust pressure (5.04 MPa) and a higher pressure ratio (22) resulted in higher LNG production and required a lower refrigerant flow rate. Also, in consideration of NG feed load fluctuation or gas well depletion, the designs of single-cycle MR0V processes for load variation were discussed in several studies. Sun and Ding (2014) discussed the use of a variable-frequency MR compressor in the PRICO process (Fig. 3) under part-load conditions, and found it satisfactory to use the frequency conversion method combined with MR composition optimization for the MR loop to match different NG loads. Lee et al. (2018) also presented a design approach for the PRICO process considering gas well depletion. This approach first determined the MR composition, the overall heat transfer coefficient (UA value) of HEXs, and the pressure ratio of compressors at the maximum production rate, and then determined other variables (such as the MR flow rate and pressure) with fixed parameters in the first step to obtain minimum operating costs per year according to the NG load reduction curve. Although the approach seemed complicated, it guaranteed the normal operation of the process and achieved better economic efficiency.

To increase the thermodynamic competitiveness of a single-cycle MR0V process, it is necessary to find out the optimal design variables. Due to the highly nonlinear interactions of these variables, the optimization essentially involves searching for the minimum or maximum of the objective functions under certain constraints. Various mathematical methods have been proven efficient and have been adopted in the optimization of MR-NGLPs, especially single-cycle MR0V processes. In turn, single-cycle MR0V processes with simple structures have become increasingly popular choices when a new optimization method has been introduced to such a nonlinear application. On the one hand, deterministic algorithms such as sequential quadratic programming (SQP) (Lee et al., 2002; Venkatarathnam, 2008; Khan et al., 2012; Wahl et al., 2013; Lee and Moon, 2016), the interior-point algorithm (Jacobsen and Skogestad, 2013; Rao and Karimi, 2017; Watson et al., 2018), and the modified coordinate descent (MCD) algorithm (Qyyum et al., 2018a, 2018c) have been commonly applied because of their rigorous calculating procedures and repeatable results. On the other hand, stochastic algorithms have been gradually gaining attention in this field, as they incorporate some random elements and do not require good initial estimates. Many stochastic algorithms have been proven effective in the optimization of single-cycle MR0V processes, such as a method combining Tabu search (TS) and the Nelder-Mead downhill simplex (NMDS) (Aspelund et al., 2010), simulated annealing (SA) algorithm (Austbø et al., 2013), particle swarm optimization (PSO) algorithm (Khan and Lee, 2013; Park et al., 2016), vortex search optimization (VSO) algorithm (Ali et al., 2018), and genetic algorithm (GA) (Shirazi and Mowla, 2010; Castillo and Dorao, 2012; Xu et al., 2013, 2014; Cao et al., 2016; Ali et al., 2019).

Available operating parameters of single-cycle MR0V processes in the abovementioned studies are listed in Table 1 for reference.

Table 1 Available operating parameters from studies of single-cycle MR0V processes

Reference	Process	Study type	NG feed conditions, [p_{NG} (MPa), T_{NG} (°C)][a]	MR pressures, [p_{low}, $p_{interstage}$, p_{high}][b] (MPa)	MR temperatures, [MITA, $T_{liquefaction}$][c] (°C)	Numbers of [evaporating pressure level, separation stage]	Mole percent of MR (%)	SPC (kW·h/kg)
Gong et al., 2004	Closed type single-cycle MR0V	E	[0.1/5, N.F.]	N.F.	[N.F.[d], −163]	[1, N.A.[e]]	[N_2, C1, C2, C3, i-C4]=[22.8, 31.4, 21.5, 12.5, 11.8]	1.35/1.81
Remeljej and Hoadley, 2006		S	[5.5, 25]	[0.37, 4]	[2, −157]	[1, N.A.]	N.F.	0.355
Morosuk et al., 2015		S	[6.7, 38]	[0.3, 0.8, 2.2]	[3, −159]	[1, N.A.]	[N_2, C1, C2, n-C4] =[14.97, 30.05, 30, 24.98]	0.507
Jensen and Skogestad, 2009a[f]		S	[4, N.F.]	[0.4, 2.2]	[2, −156]	[1, N.A.]	Optimized [N_2, C1, C2, n-C4]=[9.9, 32.3, 33.2, 24.6]	0.516
Sun and Ding, 2014[g]		S	[4.5, 45]	[0.28, 1.548, 3.403]	[2, −157.6]	[1, N.A.]	[N_2, C1, C2=, C3, C5]=[10.8, 20.79, 36.21, 12.63, 19.58]	0.368
Lee et al., 2018		S	[5, 32]	[0.34, 4.11]	[3, −160]	[1, N.A.]	Optimized [N_2, C1, C2, C3, n-C4]= [12.4, 24.1, 36.1, 5.6, 21.8]	N.F.
Lee et al., 2002		S	[5.5, 25]	[0.37, 4]	[1, −163]	[1, N.A.]	Optimized [N_2, C1, C2, C3, C4]= [13.9, 18.5, 47, 0.01, 20.6]	0.325
Venkatarathnam, 2008		S	[4, 27]	[0.3, N.F., 2.4]	[3, −160]	[1, N.A.]	Optimized [N_2, C1, C2, C3, n-C4, i-C5] =[11.6, 28.4, 30.7, 14, 5.7, 9.5]	0.353
Khan et al., 2012		S	[5, 32]	[0.13, N.F., 4.785]	[3, −149.6]	[1, N.A.]	Optimized [N_2, C1, C2, C3]=[7.81, 23.14, 19.13, 49.92]	0.424
Wahl et al., 2013[h]		S	[6, 20]	[0.23, 4.47]	[2.6, −163.8]	[1, N.A.]	Optimized [N_2, C1, C2, n-C4]=[13.23, 27.93, 36.03, 22.81]	0.397
Lee and Moon, 2016		S	[5, 37]	[0.285, 0.69, 1.683, 3.5]	[3, −163.5]	[1, N.A.]	Optimized [N_2, C1, C2, C3, i-C4, n-C4]=[23.39, 36.42, 0.05, 0.13, 25.92, 14.09]	0.332
Rao and Karimi, 2017		S	[5.5, 25]	[0.301, 2.337]	[1.2, −155]	[1, N.A.]	Optimized [N_2, C1, C2, C3, n-C4]= [7.85, 24.87, 37.99, 0.01, 29.28]	0.299
Watson et al., 2018		S	[5.5, 22]	[0.1, 3.734]	[2.73, −163]	[1, N.A.]	Optimized [N_2, C1, C2, C3, n-C4]= [6.33, 29.59, 27.82, 8.80, 27.47]	0.385

To be continued

Table 1

Reference	Process	Study type	NG feed conditions, [p_{NG} (MPa), T_{NG} (°C)][a]	MR pressures, [p_{low}, $p_{interstage}$, p_{high}][b] (MPa)	MR temperatures, [MITA, $T_{liquefaction}$][c] (°C)	Numbers of [evaporating pressure level, separation stage]	Mole percent of MR (%)	SPC (kW·h/kg)
Qyyum et al., 2018c	Closed type single-cycle MR0V	S	[5, 32]	[0.213, N.F., 4.997]	[3, N.F.]	[1, N.A.]	Optimized [N_2, C1, C2, C3]=[8.02, 25.1, 22.15, 44.73]	0.373
Qyyum et al., 2018a		S	[8, 32]	[0.25, N.F., 3.9]	[3, N.F.]	[1, N.A.]	Optimized [N_2, C1, C2, C3, i-C5]=[7.06, 29.42, 23.98, 19.8, 19.74]	0.256
Aspelund et al., 2010[i]		S	[6, 20]	[0.323, 5.237]	[2.93, −163.7]	[1, N.A.]	Optimized [N_2, C1, C2, C3, C4]=[15.5, 28.8, 34.5, 2.2, 19]	0.401
Austbø et al., 2013		S	[6, 20]	[0.409, 2.28]	[0.1, N.F.]	[1, N.A.]	Optimized [N_2, C1, C2, n-C4]=[9.78, 26.09, 40.38, 23.75]	0.295
Khan and Lee, 2013		S	[5, 32]	[0.1, 0.261, 0.682, 4.65]	[3, −149.7]	[1, N.A.]	Optimized [N_2, C1, C2, C3]=[6.76, 24.64, 15.94, 52.66]	0.381
Park et al., 2016		S	[6, 40]	[0.339, 2.858]	[1.4, −163.65]	[1, N.A.]	[N_2, C1, C2, C3, n-C4]=[9, 12.5, 34.7, 0.1, 43.6]	0.361
Ali et al., 2018		S	[8, 32]	[0.38, N.F., 5.2]	[3, N.F.]	[1, N.A.]	Optimized [N_2, C1, C2, C3, i-C5]= [10.64, 28.81, 28.62, 14.16, 17.77]	0.2681
Shirazi and Mowla, 2010		S	[5.5, 25]	[0.446, 1.451, 3.95]	[1.5, −163.2]	[1, N.A.]	Optimized [N_2, C1, C2, C3, i-C4, n-C4] =[14.2, 29.7, 22.6, 13.6, 13.2, 6.7]	0.303
Xu et al., 2013[j]		S	[5, N.F.]	[0.25, 1, 4]	[3, −160]	[1, N.A.]	Optimized [N_2, C1, C2=, C3, i-C4]= [14.59, 20.21, 32.94, 18, 14.25]	0.282
Xu et al., 2014[k]		S	[5, N.F.]	[0.34, N.F., 2.68]	[3, −160]	[1, N.A.]	Optimized [N_2, C1, C2=, C3, i-C4]= [12.88, 21.33, 32.43, 17.22, 16.14]	0.279
Cao et al., 2016		S	[8, 32]	[0.38, N.F., 3.5,]	[3, −155]	[1, N.A.]	Optimized [N_2, C1, C2=, C3, i-C5]= [13.16, 21.9, 31.69, 15.18, 18.08]	0.297
Ali et al., 2019		S	[5, 32]	[0.23, N.F., 4.557]	[2.64, −158.42]	[1, N.A.]	Optimized [N_2, C1, C2, C3]=[5.79, 12.24, 12.57, 69.38]	0.4056

[a]: p_{NG} is the pressure of the NG feed, and T_{NG} is the temperature of the NG feed; [b]: p_{low} and p_{high} are the lowest and highest operating pressures of the MR loop, respectively, and $p_{interstage}$ is the inter-stage pressure levels in cases of multi-stage compression or expansion; [c]: MITA is the minimum internal temperature approach, and $T_{liquefaction}$ is the liquefaction temperature, i.e. the outlet temperature of the HEX; [d]: N.F. indicates 'not found'; [e]: N.A. indicates 'not applicable'; [f]: design results of case 2, constraints on the liquefaction rate; [g]: design results under 100% load; [h]: results of case 2 corresponding to Aspelund's case 2 with fixed HEX area for lean gas; [i]: results of case 2, fixed HEX area for lean gas (with a calculated MITA of 2.93 °C of comparative value); [j]: specified MR operating pressures; [k]: optimized MR operating pressures. E and S in the study type indicate experiment and simulation, respectively

3.1.2 Single-cycle MR0 processes with not only JT expansion (single-cycle MR0E processes)

According to the expansion devices of MRs, closed type single-cycle MR0E processes can be roughly divided into those with both JT and non-JT expansion units, and those with only non-JT expansion units. Among the former, non-JT units, especially expanders, usually deal with the gaseous MR expansion in warmer sections, while the two-phase MR expansion in colder sections is left for JT units.

A typical example of a single-cycle MR0E process with both JT and non-JT expansion units is shown in Fig. 6. This process was proposed and simulated by Cao et al. (2006) for skid-mounted LNG packages, with a mixture of 55% N_2 and 44% CH_4 (mole fraction) as the working fluid. A portion of the MR stream is extracted after the first HEX (Fig. 6, item 5) for expansion in the expander (item 6), while the other portion is further cooled in the second HEX (item 7) before being expanded in an expansion valve (item 8) rather than an expander, because of its low dryness. From a configurative perspective, this process can be considered a modified single-cycle MR0V process by adding a bypass in the MR loop. Simulation results gave an SPC as large as 1.317 kW·h/kg for the liquefaction of 5 MPa NG. This might be attributed to the unoptimized temperature profiles, where the temperature approaches in the two HEXs were higher than 15 °C.

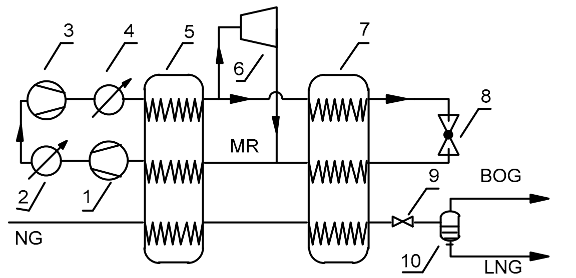

Fig. 6 A single-cycle MR0E process adapted from Cao et al. (2006)

1, 3: compressors; 2, 4: condensers; 5, 7: HEXs; 6: expander; 8, 9: expansion valves; 10: NG separator. Reprinted from (Cao et al., 2006), Copyright 2006, with permission from Elsevier

Some modifications were made to this typical single-cycle MR0E process by Wang K et al. (2014), with more HEXs employed and an extra compression stage for MR driven by the work recovered from the MR expander. A second HEX (Fig. 7, item 9) was added between the high pressure and low pressure sides of the MR expander (item 10), and another two-channel HEX (item 12) was added at the cold end for further cooling of NG. After optimization with a coordinate alternation method, a liquefaction ratio of 93.82% was obtained when the mole fraction of N_2 was 40%, the expander outlet pressure was 700 kPa, and the NG temperature before expansion was −155 °C. The low and high pressures of MR were specified as 0.7 MPa and 4.5 MPa, respectively.

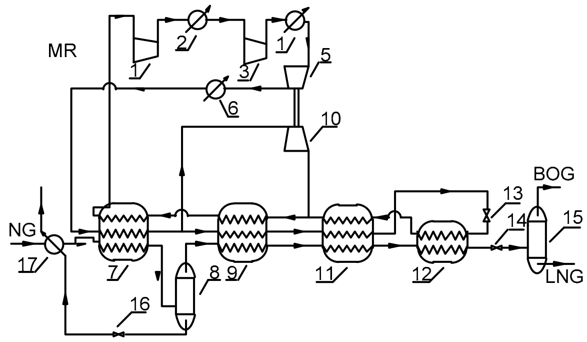

Fig. 7 A single-cycle MR0E process adapted from Wang K et al. (2014)

1, 3: compressors; 2, 4, 6: condensers; 5: booster compressor; 7, 9, 11, 12, 17: HEXs; 8, 15: NG separators; 10: expander; 13, 14, 16: expansion valves. Reprinted from (Wang K et al., 2014), Copyright 2014, with permission from Editorial Board of *Natural Gas Chemistry Industry* (China)

Pu et al. (2007, 2008) proposed two similar single-cycle MR0E processes, both operating with two-stage expansion and N_2-CH_4 as working fluids. In the first configuration, the expanders are in serial connection (Fig. 8), in which the high pressure MR after the first HEX (Fig. 8, item 10) is expanded to an intermediate pressure in the first expander (item 7). Then, only a portion of refrigerant after the third HEX (item 12) is extracted to the second expander (item 8) with its pressure reduced to the low pressure, and is then mixed with the low pressure refrigerant at the inlet of the same HEX. The other portion is subcooled in the following two HEXs (items 13 and 14), expanded in an expansion valve (item 9), and sent back as low pressure refrigerant. The second configuration shares the same equipment as the first, but the two expanders are in parallel connections from the high pressure inlets of the second HEX (item 11) and the fourth HEX (item 13) to the low pressure inlets of the same respective heat exchanges. In the thermodynamic analyses for both connections, the mole fractions of N_2 and CH_4 were fixed as 50%, and the high, intermediate, and low pressure levels of the serial configuration were 8.00, 3.88, and 0.55 MPa, respectively, while the two pressure levels of the parallel configuration were 3.88 and 0.55 MPa. Results showed that the SPCs of the series and parallel connections were 0.786 kW·h/kg and 0.833 kW·h/kg, respectively.

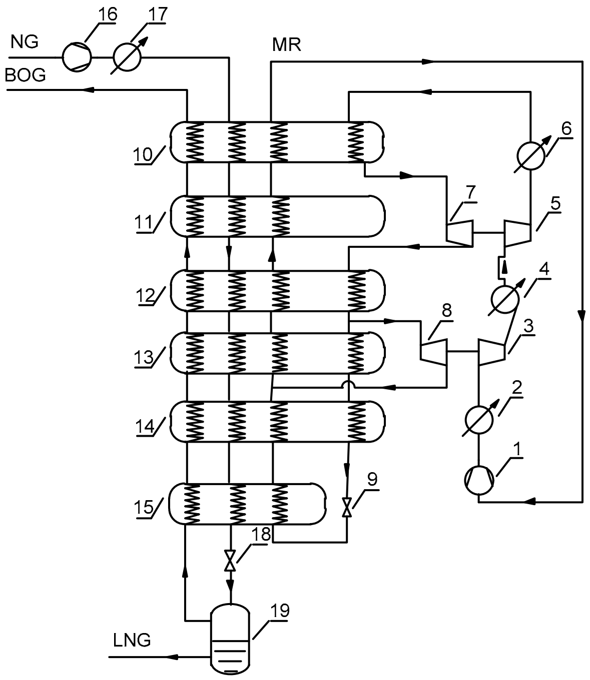

Fig. 8 A single-cycle MR0E process adapted from Pu et al. (2008)

1, 16: compressors; 2, 4, 6, 17: water coolers; 3, 5: booster compressors; 7, 8: expanders; 9, 18: expansion valves; 10, 11, 12, 13, 14, 15: HEXs; 19: storage tank. Reprinted from (Pu et al., 2008), Copyright 2008, with permission from Editorial Board of *Chemical Engineering* (China)

There are fewer closed type single-cycle MR0E processes with only non-JT expansion units, possibly because they are usually limited to gas expansion.

Taking the most common non-JT expansion unit, expanders, as an example, they may function feasibly in the coldest section when a mixture of N_2-CH_4 serves as the working fluid, but this has rarely been the case. The only closed type single-cycle MR0E process operating with only non-JT expansion units and an N_2-CH_4 mixture found in our literature survey was the study of Moein et al. (2016). The original purpose of that study was to discuss the effect of CH_4 addition on a dual N_2 expander NGLP (Fig. 9), which could be regarded from a configurative perspective as an MR composition optimization of a single-cycle MR0E process with two expanders. The GA method was used to minimize the net power consumption, and gave an optimum CH_4 mole fraction of 26%.

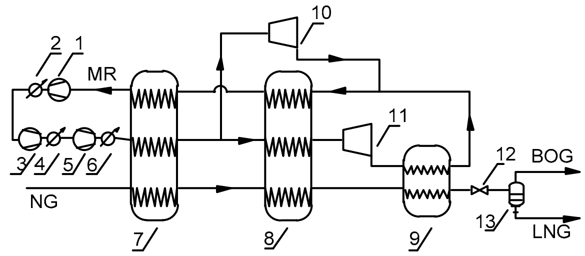

Fig. 9 A single-cycle MR0E process adapted from Moein et al. (2016)

1, 3, 5: compressors; 2, 4, 6: condensers; 7, 8, 9: HEXs; 10, 11: expanders; 12: expansion valve; 13: NG separator. Reprinted from (Moein et al., 2016), Copyright 2016, with permission from Elsevier

However, when MRs consisting of HCs heavier than CH_4 are used in MR-NGLPs, they often enter the two-phase or liquid region, in which most non-JT expansion units, such as gas expanders, vortex tubes, and ejectors, are not feasible. As a result, researchers turned to an alternative, the hydraulic turbine. As early as 1980s, there appeared a design of a single-cycle MR0E process operating with MR consisting of at least one HC. In this process patented by Paradowski (1982), two-stage compression (Fig. 10, item 1) and two hydraulic turbines (items 4 and 6) are employed. A hydraulic turbine can expand the MR stream monophasically to above its saturation pressure, and the further expansion is dealt with by an additional valve. Due to the replacement of hydraulic turbines, the energy loss is greatly reduced compared with single-cycle MR0V processes. Besides, the expansion work of the hydraulic turbines can be used by compressors, which is beneficial for further reducing the liquefaction power consumption.

As reported by Liu et al. (2015), hydraulic turbines can reach an efficiency higher than 90%, which gives them a thermodynamic advantage over JT expansion units in MR-NGLPs. Qyyum et al. considered the replacement of hydraulic turbines (Qyyum et al., 2018b) and two-phase expanders (Qyyum et al., 2018d) in basically the same single-cycle MR0E process as shown in Fig. 10 (with more compression stages). They reported 14.86% and 46.4% relative energy savings compared to a single-cycle MR0V process and a conventional N_2 single expander process, respectively.

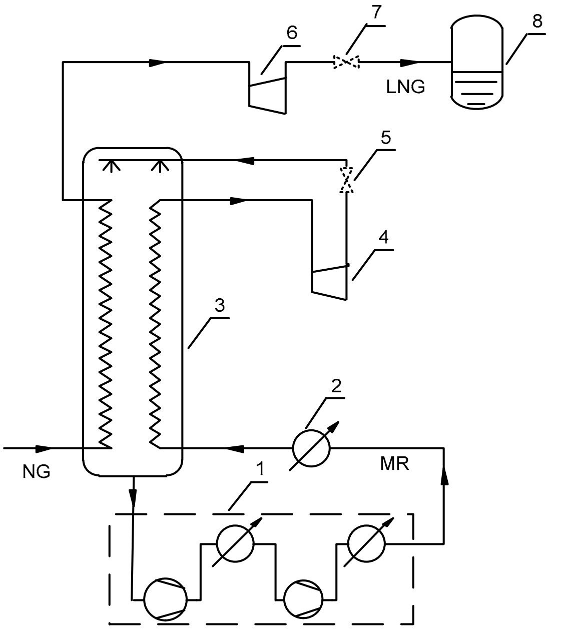

Fig. 10 A single-cycle MR0E process adapted from Paradowski (1982)

1: two-stage compressor and after-cooler; 2: condenser; 3: HEX; 4, 6: cryogenic hydraulic expansion turbines; 5, 7: additional expansion valves; 8: storage tank

Besides the closed type single-cycle MR0E processes discussed above, there were also some featured open types, which usually use the expansion of NG itself as the cooling source.

As shown in Fig. 11, the open type single-cycle MR0E process proposed by Johanson (1965) uses expanded NG out from the expander (Fig. 11, item 9) to cool against the other portion in a CH_4 liquefier (item 10). The other portion is partly liquefied in the liquefier (item 10) and undergoes expansions and gas-liquid separations twice in successive valves (items 11 and 13) and NG separators (items 12 and 14). The final liquid phase is the LNG product for storage, while the gaseous phase is sent back to the HEXs (items 4 and 6) for refrigeration recovery. However, as pointed out in the patent, the amount of NG that can be liquefied is very small (6% of the total NG flow).

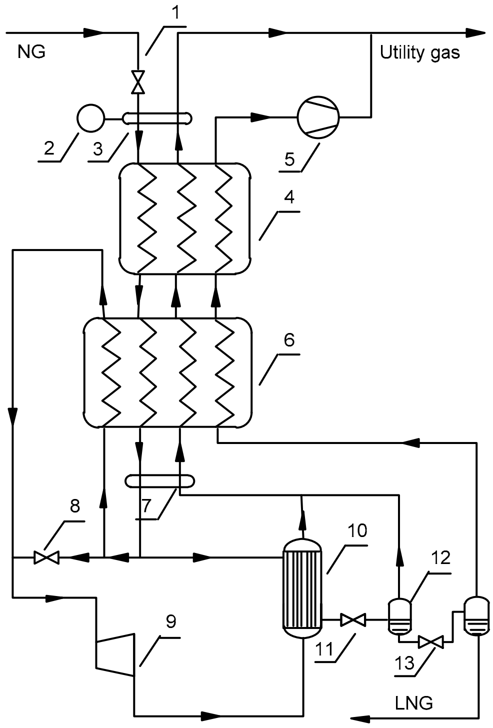

Fig. 11 A single-cycle MR0E process adapted from Johanson (1965)

1: reducing valve; 2: valve motor; 3: reversing valve; 4, 6: reversing HEXs; 5: compressor; 7: check valve; 8: valve; 9: expander; 10: CH_4 liquefier; 11, 13: expansion valves; 12, 14: NG separators

Hanson and Kun (1988) also proposed an open type single-cycle MR0E process to liquefy critical or supercritical NG (Fig. 12). This process is similar to that proposed by Pu et al. (2007, 2008), but uses NG itself as the refrigerant instead of an N_2-CH_4 mixture. NG is compressed and cooled in successive HEXs (Fig. 12, items 11–14). The first and second portions of NG are extracted at the high pressure outlet of the first HEX (item 11) and the third HEX (item 13), respectively, to obtain the same intermediate pressure streams at different temperatures. These two low pressure streams are sent to the low pressure inlets of the second HEX (item 12) and the fourth HEX (item 14) to provide cooling capacity. The remaining portion of NG is further liquefied and expanded as product. Specifically, the expansion work is recovered to elevate the pressures of both refrigerant NG and product NG beyond the critical point.

Open type MR0E processes are also suitable for the recovery of pressure energy in urban NG pipeline networks, where NG must be depressurized before entering the user pipelines. He and Ju (2013) studied an MR0E process similar to that of Hanson and Kun (1988) for a pipeline scenario in which two expanders are used (Fig. 13). In their process, 4 MPa NG from the pipeline is divided into two portions before entering the successive HEXs (Fig. 13, items 4, 5, 7, and 9). The larger portion, which serves as the refrigerant, is divided into two streams again after being cooled in the HEX (item 4). One stream is extracted to the expander (item 8) and sent to a sub-high pressure network (1.7 MPa) after providing cooling capacity for the HEXs (items 7, 5, and 4), while the other one is further cooled in the HEX (item 7), then expanded in a parallel expander (item 10) to 0.4 MPa, and returned through the four HEXs. The smaller portion, to be liquefied, goes through these successive HEXs and is finally expanded in an expansion valve (item 11) to produce LNG, where the cold energy of flash gas is also recovered. Simulation results indicated a very small SPC of 0.052 kW·h/kg, because the expansion work is used for the pressure elevation of only a portion of the NG, and the NG pipeline pressure is already as high as 4 MPa.

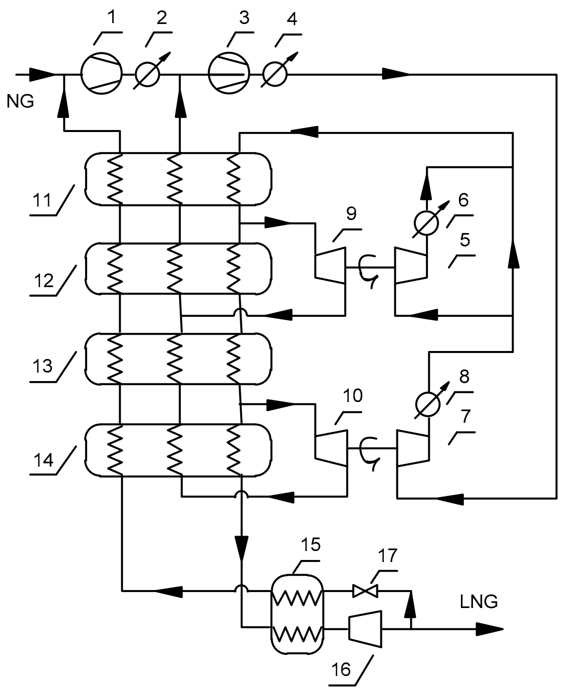

Fig. 12 A single-cycle MR0E process adapted from Hanson and Kun (1988)
1, 3: compressors; 2, 4, 6, 8: condensers; 5, 7: booster compressors; 9, 10: expanders; 11, 12, 13, 14, 15: HEXs; 16: expansion unit (turbine or expander); 17: expansion valve

Another non-JT expansion unit, the vortex tube, was reported to have been adopted in the open type MR0E process in Russian urban gas distributing stations (Сердюков, 2000; Xu, 2005), as shown in Fig. 14. A portion of high pressure NG is extracted from the pipeline and divided to four streams. Two streams enter two HEXs I (items 5 and 6), and the other two enter two vortex tubes (items 11 and 12). NG from the hot ends of the two vortex tubes is sent to the user pipeline, while NG from the cold ends provides precooling for the two NG streams entering the HEXs I. The precooled NG streams are then

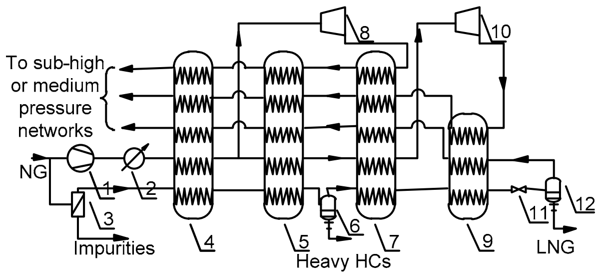

Fig. 13 A single-cycle MR0E process adapted from He and Ju (2013)
1: compressor; 2: condenser; 3: pretreatment process; 4, 5, 7, 9: HEXs; 6, 12: NG (MR) separators; 8, 10: expanders; 11: expansion valve. Reprinted from (He and Ju, 2013), Copyright 2013, with permission from Elsevier

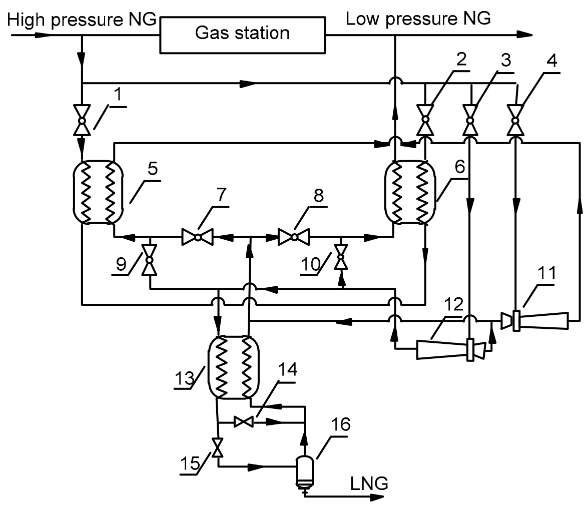

Fig. 14 Vortex tubes used for liquefaction in Russian gas distribution stations adapted from Xu (2005)
1, 2, 3, 4, 7, 8, 9, 10: valves; 5, 6: HEXs I; 11, 12: vortex tubes; 13: HEX II; 14, 15: expansion valves; 16: LNG separator. Reprinted from (Xu, 2005), Copyright 2005, with permission from Editorial Board of *Chemical Engineering of Oil & Gas* (China)

partially liquefied in HEX II (item 13) and expanded in an expansion valve (item 15) to be exported as the LNG product. These small-scale vortex tube liquefiers using their pressure energy without any other energy input and component separation have been built for many years and have undergone continuous improvement.

Available operating parameters from the above-mentioned studies of single-cycle MR0E processes are listed in Table 2.

3.1.3 Discussion

The single-cycle MR0V and MR0E processes were introduced in Sections 3.1.1 and 3.1.2.

From Table 1, single-cycle MR0V processes (33 references) have usually adopted N_2 and HCs from CH_4 to C_4H_{10}/C_5H_{12} as the MR components. Analysis of the optimized compositions in Table 1 shows that the most volatile components, N_2 and CH_4, generally accounted for 30%–45% (in mole) to ensure low enough liquefaction temperatures. The least volatile components C_4H_{10} and C_5H_{12} accounted for 14%–30%. The optimized simulated SPCs ranged roughly from about 0.27 to 0.40 kW·h/kg. Compared to the conventional PR cascade liquefaction process, there was no significant reduction in the power consumption of single-cycle MR0V processes because small temperature differences could not be achieved along the whole temperature range in the HEXs with just a single set of MR. However, the equipment and process configurations of the single-cycle MR0V processes are greatly simplified, which is suitable for small-scale NG liquefaction applications as well as medium-scale applications insensitive to power consumption.

Expanders served as the dominant non-JT expansion units in single-cycle MR0E processes (13 references). From Table 2, an N_2-CH_4 mixture was used mainly in closed type single-cycle MR0E processes to meet the dryness requirement of common expanders, but heavier HCs could also be adopted in the presence of hydraulic turbines or two-phase expanders. Unfortunately, there were no adequate theoretical or experimental studies of single-cycle MR0E

Table 2 Available operating parameters from studies of single-cycle MR0E processes

Reference	Process	Study type	NG feed conditions, [p_{NG} (MPa), T_{NG} (°C)]	MR expansion pressures, [p_{low}, p_{high}] (MPa)	MR temperatures, [MITA, $T_{liquefaction}$] (°C)	Numbers of [evaporating pressure level, separation stage]	Mole percent of MR (%)	SPC (kW·h/kg)
Cao et al., 2006	Closed type MR0E (expander+valve)	S	[5, 32]	[0.6, 4.4]	[N.F., −140[a]]	[1, N.A.]	[N_2, CH_4]=[56, 44]	1.317
Wang K et al., 2014[b]		S	[4.8, 35]	[0.7, 4.5]	[2, −155]	[1, N.A.]	[N_2, CH_4]=[40, 60]	0.639
Pu et al., 2007, 2008[c]		S	[5.1, 30]	[0.55, 3.88] and [3.72, 8]	[3, N.F.]	[1, N.A.]	[N_2, CH_4]=[50, 50]	0.786
Pu et al., 2007, 2008[d]		S	[5.1, 30]	[0.55, 3.88]	[3, N.F.]	[1, N.A.]	[N_2, CH_4]=[50, 50]	0.833
Moein et al., 2016[e]	Closed type MR0E (expander)	S	[6.29, 40]	[0.59, 4.75]	[2, −155]	[1, N.A.]	[N_2, CH_4]=[74, 26]	0.567
Qyyum et al., 2018b	Closed type MR0E (hydraulic turbine)	S	[5, 32]	[1.69, 7.99]	[3, −147[a]]	[1, N.A.]	Optimized [N_2, C1, C2, C3]=[1.87, 31.17, 21.92, 45.04]	0.318
Qyyum et al., 2018d	Closed type MR0E (two-pahse expander)	S	[5, 30]	[0.49, 7.9]	[3, −146]	[1, N.A.]	Optimized [N_2, C3]=[63.86, 36.14]	0.3989
He and Ju, 2013	Open type MR0E (expander)	S	[4, 15]	[0.45, 6.3] and [1.75, 6.3]	[3–7, N.F.]	[N.A., N.A.]	NG	0.052[f]

[a]: value obtained from the heat flow–temperature profile; [b]: results with the lowest power consumption; [c]: two expanders in series connection; [d]: two expanders in parallel connection; [e]: results obtained from the figures at the condition of the lowest power consumption; [f]: SPC converted from 0.03975 kW·h/Nm^3

processes; therefore, we are unable to summarize the optimum MR composition range. According to our literature survey, N_2 was found to account for 40%–74% (in mole) in N_2-CH_4 mixtures, while N_2 or N_2+CH_4 made up more than 35% when heavier HCs were added. Due to the lack of optimization of these processes, big differences (0.318–1.317 kW·h/kg) exist among the simulated SPCs derived from different studies. Single-cycle MR0E processes operating with N_2-CH_4 had obviously larger SPCs than single-cycle MR0V processes, but those operating with common N_2-HCs had an SPC level similar to that of single-cycle MR0V processes. This indicates that MRs with a heavier HC might have an advantage over an N_2-CH_4 mixture if the expansion units are capable of handling two-phase working fluids, because better heat transfer might be obtained in low temperature sections when such MRs enter their two-phase zones. However, proposals and studies related to the use of hydraulic turbines and common N_2-HCs considered the process performance only at steady states. It remains to be tested whether they could function normally during start-up or under conditions with dramatic dryness changes. In open type single-cycle MR0E processes, NG itself is usually extracted to serve as the MR. Such processes could be used for pipeline pressure energy utilization, but the liquefaction rate might be low. As for other non-JT expansion units, only one case was found to use vortex tubes, while the use of ejectors was not found in the literature of this section.

3.2 Single-cycle processes with component separation (single-cycle MR*x* processes)

The most prominent feature of single-cycle MR*x* processes is the presence of separated MR streams that keep their respective composition during heat transfer. This differs from the use of separators in the PRICO process (Figs. 3 and 4), where the separated MR streams mix again before the HEX inlet. The single-cycle MR*x* processes are regarded as having been developed from the auto-cascade refrigeration cycle. The concept of the auto-cascade refrigeration cycle was proposed by Podbielniak (1936) and validated by Kleemenko (1959). In recent decades, it has evolved from using one separator to using multiple separators, then to self-cleaning systems. The compression process has also gradually developed from multi-stage compression free of lubricating oil to oil-lubricated single-stage compression.

To avoid oil block in the low temperature section in small-scale refrigerators, an auto-cascade refrigeration cycle with multiple gas-liquid separators was developed by Missimer (1972) in the 1970s to condense the lubricating oil entrained in MR streams as much as possible before it entered the low temperature section. Later, Little (1997) and Little and Sapozhnikov (1997) proposed the concept of a self-cleaning auto-cascade refrigeration cycle, by adding a fractionator to the separator to clean the residual oil and other contaminants in the MR. This method of using rectifying units was further developed by Chen et al. (2000), Zhang et al. (2001), and Wu et al. (2002, 2003). They used a rectifying column or fractional condensation separator to provide a better separation effect for the volatile and less volatile MR components, and to prevent entrained oil from entering the low temperature sections and blocking the expansion units. This development promoted the application of low-cost and reliable oil-lubricated compressors in low temperature refrigeration systems.

Various auto-cascade refrigeration cycles promoted the development of single-cycle MR*x* processes, and the feature of MR separation was the major reason for the diversity of single-cycle MR*x* processes, which will be discussed in detail below.

3.2.1 Single-cycle MR*x* processes with only JT expansion (single-cycle MR*x*V processes)

Similar to the single-cycle MR0V processes, expansion valves are commonly adopted as the expansion units for MRs in MR*x* processes. Single-cycle MR*x*V processes are further classified by the number of the separators adopted in the MR loop.

3.2.1.1 Single-cycle MR*x*V processes with one phase separator (single-cycle MR1V processes)

Streich (1973) put forward a single-cycle MR1V process with two-stage compression and two evaporating pressure levels (Fig. 15). Compressed and condensed MR goes through one MR separator (Fig. 15, item 3) and is separated into gaseous and liquid phases. The liquid phase rich in less volatile components is expanded to an intermediate pressure of 0.5–1.0 MPa to provide cooling capacity and then returned to the compressor (item 1), while the gaseous phase rich in volatile components is further cooled and expanded to a low pressure of 0.1–0.5 MPa, also to provide cooling capacity. Meanwhile, 2 MPa NG is cooled, freed from heavy HCs at −100 °C, and partially liquefied to −120 °C. Then, it is sent into an N_2 rectification column (item 14) to remove enriched N_2.

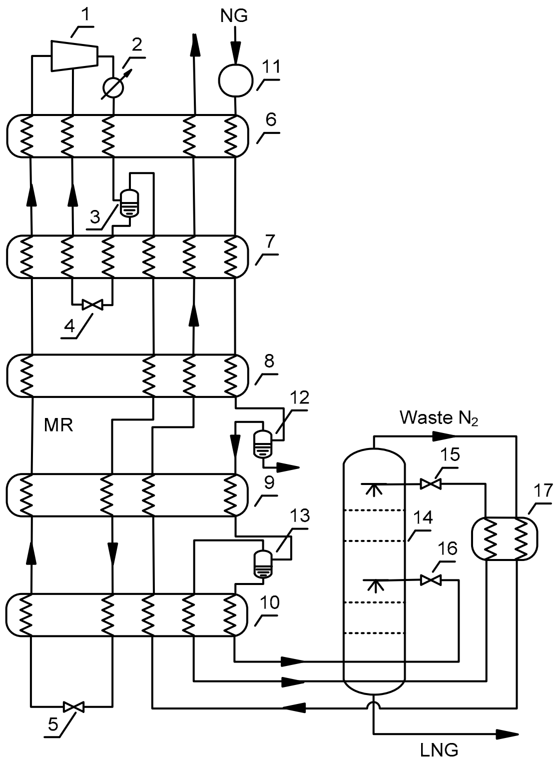

Fig. 15 A single-cycle MR1V process adapted from Streich (1973)

1: compressor; 2: condenser; 3: MR separator; 4, 5, 15, 16: expansion valves; 6, 7, 8, 9, 10, 17: HEXs; 11: purification unit; 12, 13: NG separators; 14: N_2 rectification column

Later, a single-cycle MR1V process with only one evaporating pressure level (Fig. 16) was proposed by Coers and Sudduth (1976) based on the proposal of the MR0V process shown in Fig. 2 (Maher and Sudduth, 1975). NG is fed at 24 °C and 4 MPa, and cooled and liquefied through the HEX. The operating pressures of this system fall between 0.17 and 3.1 MPa. Multi-stage compression might be used with the pressure ratio as high as 18, though this was not mentioned in the original patent. The most obvious difference between the MR loops in Figs. 15 and 16 lies in the mixing position of the separated MR streams, which influences the number of evaporating pressure levels and the temperature profiles in the HEXs. In later optimizations, this process could reach an SPC of 0.411 kW·h/kg and an exergy efficiency of 49.96% as reported by He et al. (2019), which is an improvement thermodynamically over the parallel N_2 expansion process.

Nelson and Garcia (1991) also put forward a single-cycle MR1V process with an MR loop similar to that in Fig. 16. This process features an NG treatment loop, in which the vapor produced in NG expansion and the BOG are gathered for cold energy recovery, and then mixed with NG feed after the multi-stage compression (Fig. 17). In this way, N_2 is enriched in the vapor without residing in the LNG product, and the power consumption to remove N_2 is also reduced. The heavy components isolated from the NG during the cooling process are also recycled to an intermediate compression stage.

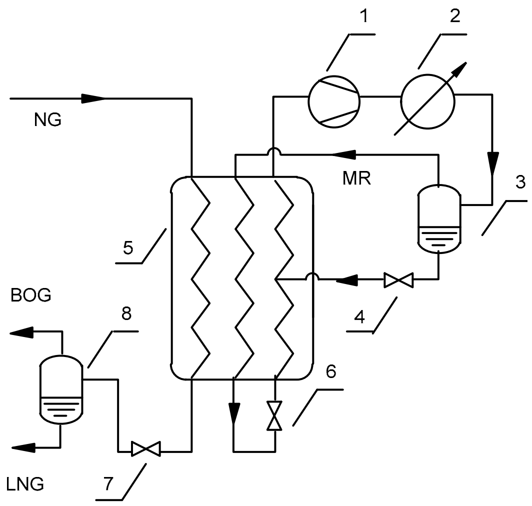

Fig. 16 A single-cycle MR1V process adapted from Coers and Sudduth (1976)

1: compressor; 2: condenser; 3: MR separator; 4, 6, 7: expansion valves; 5: HEX; 8: storage tank

Air Products and Chemicals Incorporated (APCI) has been committed to the development of MR*x*V processes for many years. A single-cycle MR1V process proposed by Roberts et al. (2002b) is shown in Fig. 18. Compared to Streich's design in Fig. 15 (Streich, 1973), multi-stage compression and two evaporating pressure levels are also used, but these two MR1V processes can be distinguished by the states of the MR streams before separation and before compression. In Roberts et al. (2002b)'s MR1V process (Fig. 18), MR separation takes place after ambient cooling rather than after precooling. In addition, the MR stream (rich in volatile components) at the lowest evaporating pressure is returned to the compressor without heat exchange with warm NG and high pressure MR. This results in a much lower suction temperature (<0 °C), which is beneficial for reducing the specific volume and volume flow rate to further reduce the size of the HEXs and the power of compressors. The inventors called this configuration 'cold compression'.

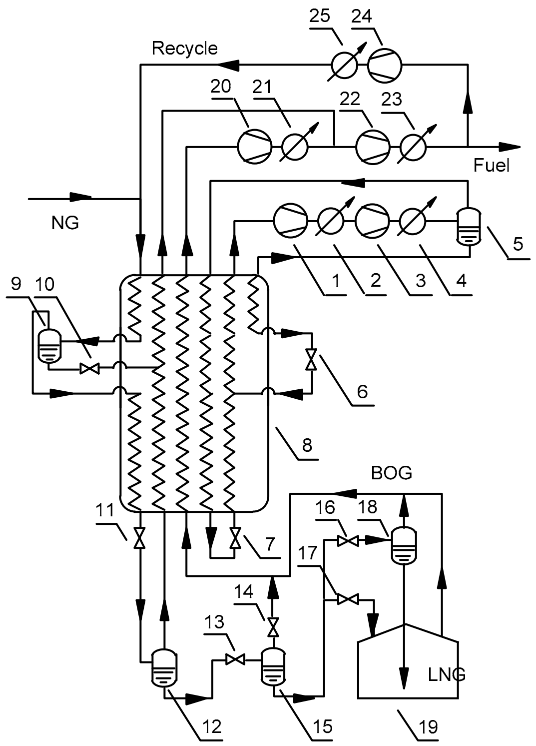

Fig. 17 A single-cycle MR1V process adapted from Nelson and Garcia (1991)

1, 3, 20, 22, 24: compressors; 2, 4, 21, 23, 25: condensers; 5: MR separator; 9, 12, 15, 18: NG separators; 6, 7, 10, 11, 13, 14, 16, 17: expansion valves; 8: HEX; 19: storage tank

Single-cycle MR1V processes with a single evaporating pressure (Fig. 16) or double evaporating pressures (Fig. 18) were also simulated and analyzed by Venkatarathnam (2008), who simplified the compression process by using three compressors without pumps. Similar to his analyses of the PRICO process, the optimization aimed to maximize the exergy efficiency of the 'cold box' including the separators, recuperative HEXs, and expansion valves. The MR1V process with single evaporating pressure (Fig. 16) reached an optimum SPC of 0.321 kW·h/kg with an overall exergy efficiency of 36.7%, close to that of the PRICO process in his simulation (37.3%). As for the MR1V process with double evaporating pressures (Fig. 18), results showed a reduced compression power consumption due to the increase of evaporating pressure levels, as well as an increase in overall exergy efficiency by about 3%. However, the detailed operation parameters were not elaborated. A similar optimization of a single-cycle MR1V process was also found in (Na et al., 2017).

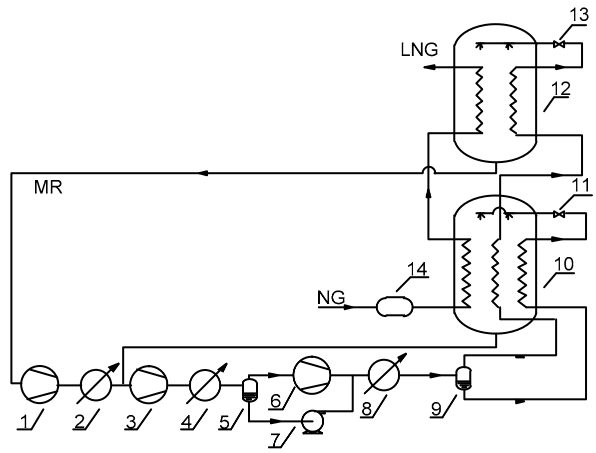

Fig. 18 A single-cycle MR1V process adapted from Roberts et al. (2002b)

1, 3, 6: compressors; 2, 4, 8: condensers; 5, 9: MR separators; 7: pump; 10, 12: HEXs; 11, 13: expansion valves; 14: NG pretreatment section

3.2.1.2 Single-cycle MR*x*V processes with two-phase separators (single-cycle MR2V processes)

Increasing the number of separators is one way to optimize a process. Kleemenko (1959) implemented two separators in a single-cycle MR2V process (Fig. 19). The increase in the number of separators improved separation of the volatile and less volatile MR components, which in turn improved refrigeration performance. In this process, on the one hand, an open type MR loop can be used for liquefying NG with a higher content of heavy HCs, in which NG itself is used as the working fluid. Heavy HC components can be gradually removed in two separators (Fig. 19, items 5 and 8), while light components consisting mainly of CH_4 are gradually liquefied and expanded to produce the refrigerating vapor and the product LNG. On the other hand, a closed type MR loop can be used for the liquefaction of air or NG with a very low content of heavy HCs by a control valve switch. The gas to be liquefied is cooled in the dotted A-B pipeline. This process, when operated in a closed loop, is now well known as the Kleemenko process. It was optimized and analyzed by Venkatarathnam (2008) using the method described previously. The results showed an optimum MR composition of 7.52% N_2, 28.43% CH_4, 43.9% C_2H_6, 5.01% C_3H_8, 4.34% n-C_4H_{10}, and 10.81% n-C_5H_{12} with an SPC of 0.243 kW·h/kg and an overall exergy efficiency of 48.5%. Compared to the MR1V process described in Section 3.2.1.1, the increase in the simulated SPC and overall exergy efficiency in this MR2V process might be related to the compression process in the simulation, where pumps in parallel with the compressors (similar to the PRICO process) were used between the compression stages.

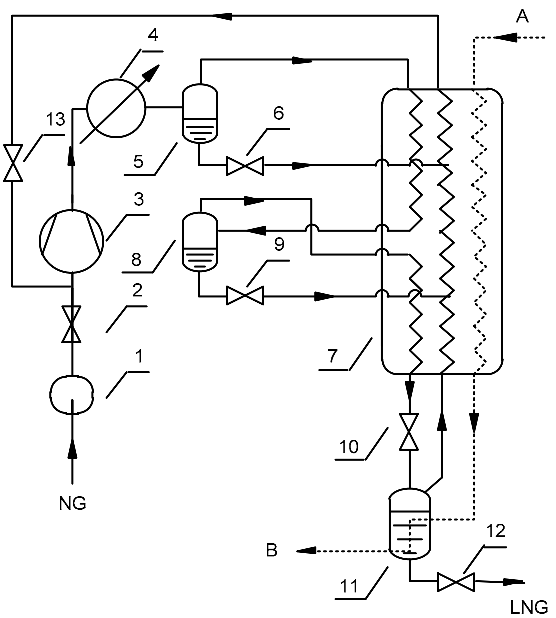

Fig. 19 A single-cycle MR2V process adapted from Kleemenko (1959)

1: gas dehydration unit; 2, 12, 13: control valves; 3: compressor; 4: condenser; 5, 8: MR separators; 6, 9, 10: expansion valves; 7: HEX; 11: receiver

Modifications were made to the Kleemenko process by Neeraas and Brendeng (2004) from SINTEF (Stiftelsen for Industriell og Teknisk Forskning), Norway. In the SINTEF concept (Fig. 20), two two-channel plate HEXs are used in place of a three-channel HEX. One is used for cooling the high pressure MR and the other for cooling the NG feed. The key part of this process is the method for distributing the returned low pressure refrigerant. Two ejector-shaped distributors combined with four temperature sensors are used to overcome the pressure losses in the mixing sections for better performance. In simulation, an SPC of 0.6–0.9 kW·h/kg was obtained when liquefying 5 MPa NG to −150 °C (Nekså and Brendeng, 2007). An experimental prototype with production of 1 t/d was built and has been operating with an SPC of 0.63 kW·h/kg in the SINTEF-NTNU lab since 2003. The prototype uses oil-lubricated screw compressors, and an ejector is used to gain a pressure lift in the MR coming from the lowest pair of HEXs (Nekså and Brendeng, 2007). In applications requiring compactness, this MR2V process could be easily simplified to an MR1V process by eliminating a separator and several plate HEXs, as proposed by Brendeng and Neksa (2010).

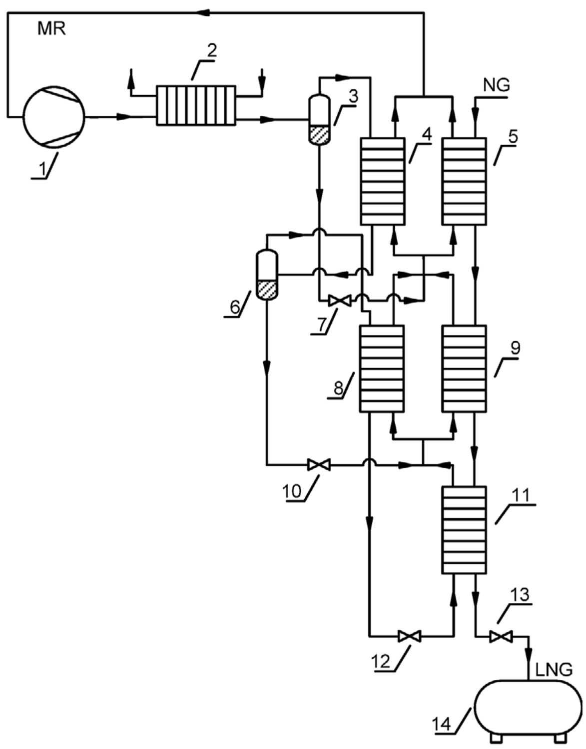

Fig. 20 A single-cycle MR2V process adapted from Neeraas and Brendeng (2004)

1: compressor; 2: condenser; 3, 6: MR separators; 4, 5, 8, 9, 11: plate HEXs; 7, 10, 12, 13: expansion valves; 14: storage tank

3.2.1.3 Single-cycle MR*x*V processes with multiple phase separators (single-cycle MRnV processes)

A single-cycle MR3V process was put forward by Charles (1968), in which three separation stages and two evaporating pressure levels were adopted (Fig. 21). After the second MR separator (Fig. 21, item 6), the liquid phase is divided into two steams to cool the MR and NG, respectively. The liquid phase separated in the third MR separator (item 9) functions in a similar way. Therefore, NG and the high pressure MR are cooled in different HEXs with different pressure levels in Charles's process, rather than being cooled together by the same cold MR stream.

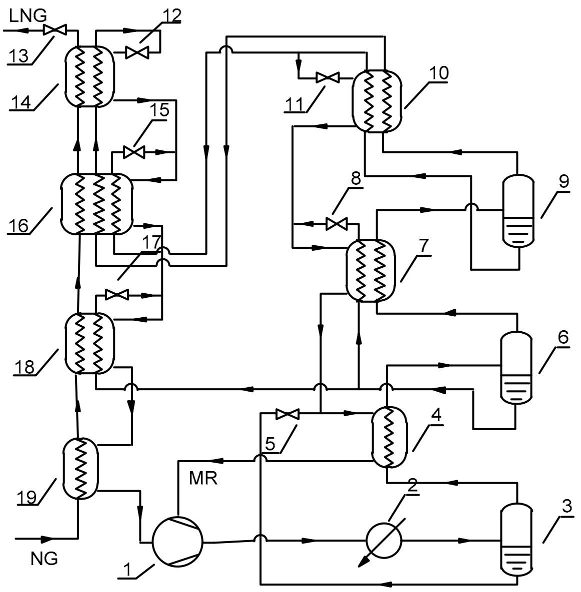

Fig. 21 A single-cycle MR3V process adapted from Charles (1968)
1: compressor; 2: condenser; 3, 6, 9: MR separators; 4, 7, 10, 14, 16, 18, 19: HEXs; 5, 8, 11, 12, 13, 15, 17: expansion valves

Darredeau (1973) from Air Liquide modified a single-cycle MR3V process based on the Kleemenko process. Two-stage compression and three-stage separation are used in the MR loop, but there is only one evaporating pressure level (Fig. 22). The major modification was the addition of an expansion valve (Fig. 22, item 6) and a second separator (item 7) between the second stage compressor (item 3) and the first separator (item 5). The separated liquid MR stream from the separator (item 5) is expanded to an intermediate pressure and undergoes a second separation. Afterwards, the separated vapor from the separator (item 7) is recycled to the second stage compressor, while the separated liquid is cooled in the first HEX. Thus, the heavy MR components are enriched twice in the separated liquid from the separator (item 7), resulting in a higher boiling point in this process compared to the Kleemenko process. Correspondingly, it has a smaller temperature difference in the warmer HEX so as to reduce power consumption without increasing the heat exchange area.

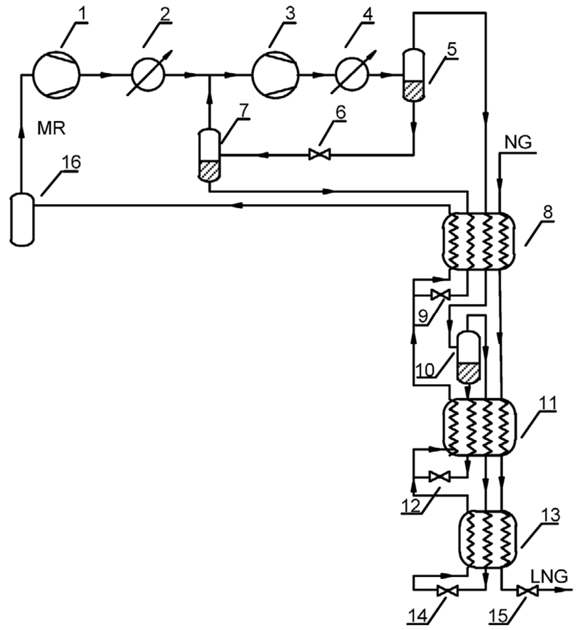

Fig. 22 A single-cycle MR3V process adapted from Darredeau (1973)
1, 3: compressors; 2, 4: condensers; 5, 7, 10: MR separators; 6, 9, 12, 14, 15: expansion valves; 8, 11, 13: HEXs; 16: suction drum

Gaumer Jr and Newton (1971, 1972) from APCI put forward two single-cycle MR4V processes with complicated NG pretreatments. One is shown in Fig. 23. The novelty of this design is the configuration of the multi-stage separator (Fig. 23, item 7) and the integral HEX (item 12). Unlike the individual separators in other MRnV processes, the multi-stage separator seems more like a distillation column without trays, which improves compactness. In the other process (not shown), the vapor and liquid streams from the separators are both cooled in the HEX before expansion. The vertically placed multi-zone HEX, with the warm end as its lower end and the cold end as its upper end, uses spray headers for distributing the returned low pressure streams. It also has the advantages of low cost and ease of fabrication over a series connection of individual HEXs. However, this integral HEX is suitable only for processes with one evaporating pressure.

Another configurative modification involved the addition of a buffer volume to an MR4V process design, as proposed by Simon et al. (1974). They considered that the liquid refrigerants would gradually evaporate in a closed type MR*x*V system after plant shutdown, which would increase the system pressure. Not only gasholders, but also tube-and-shell HEXs with longer shell sides than tube sides can serve as the buffer volume. This method suits not only MR4V processes, but all kinds of MR-NGLPs, and must be taken into consideration before industrialization.

Similar to the open type MR2V process designed by Kleemenko, several open type MRnV processes have been designed for NG liquefaction.

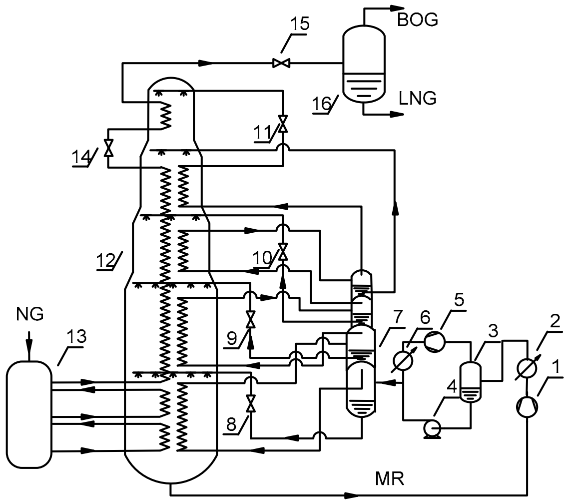

Fig. 23 A single-cycle MR4V process adapted from Gaumer Jr and Newton (1971)

1, 5: compressors; 2, 6: condensers; 3: MR separator; 4: pump; 7: integrated MR separator; 8, 9, 10, 11, 14, 15: expansion valves; 12: integral HEX; 13: NG treatment; 16: NG separator

An open type single-cycle MR3V process was put forward by Streich (1971) (Fig. 24). Some existing components in NG (especially heavier HCs) are premixed with the NG feed to produce enough liquid in separators and provide enough cooling capacity for the warmer HEXs. After successive cooling and separation, the final separated vapor is sent to a distillation column for further denitrogenation. The separated liquids in the first two separators (Fig. 24, items 5 and 8) are expanded respectively to the intermediate pressure (0.5–1.0 MPa) and the low pressure (about 0.1 MPa), while the liquid from the third separator (item 11) is subcooled and sent to the N_2 column (item 16) as intermediate feed. The final LNG product comes from the bottom product of the distillation column and a very small portion of the liquid from the separator (item 5), to ensure a similar composition of LNG and the NG feed, and to keep the composition of the working fluid stable. Such open type MRnV processes and the closed types essentially share the same recuperative heat exchange and separation procedures, except that the open types aim to separate the premixed components appropriately without altering the LNG composition significantly.

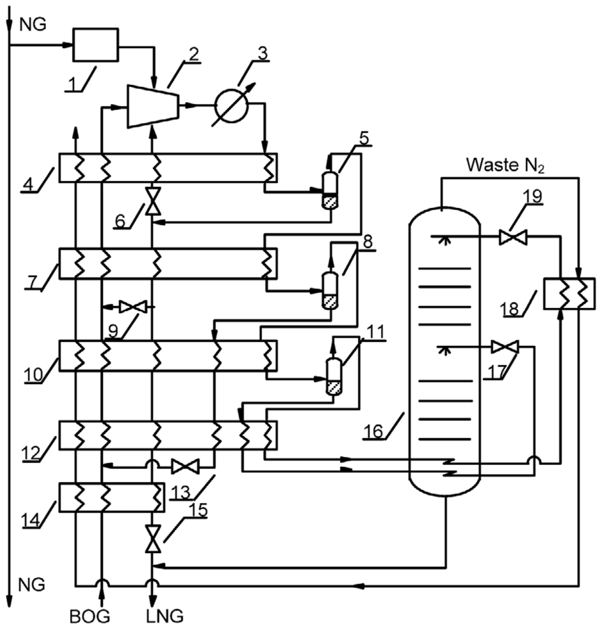

Fig. 24 A single-cycle MR3V process adapted from Streich (1971)

1: purification unit; 2: compressor; 3: condenser; 4, 7, 10, 12, 14, 18: HEXs; 5, 8, 11: MR (NG) separator; 6, 9, 13, 15, 17, 19: expansion valves; 16: N_2 column

Another example is an open type MR6V process (Fig. 25) proposed by Etzbach and Förg (1972). According to its inventors, increasing the heavy components in the working fluid brings a higher latent heat of vaporization and an increase in the refrigeration capacity, but many heavy components remain in the gaseous phase after separation, which results in a higher refrigeration temperature. Therefore, as many as 6 MR (NG) separators (Fig. 25, items 3, 6, 10, 14, 17, and 19) are adopted in the process. NG is mixed with the cycle media vapor from the first separator (item 3) at an intermediate pressure, and goes through another stage of compression together to 3.5 MPa before multiple phase separations and condensations. The partial condensation after the first compression is helpful in reducing the heavy components entering the low temperature sections, thus reducing their influence on the refrigeration temperature and refrigeration capacity.

The number of MR separators is an optimization parameter. More separators are more beneficial for the temperature matching in HEXs, but definitely increase the complexity of the system. Generally speaking, as Finn et al. (1999) pointed out, three separation stages can be considered as a balancing point between power consumption and complexity.

3.2.1.4 Single-cycle MR*x*V processes with rectifying units (single-cycle MRrV processes)

As mentioned in Section 3.2, rectifying units have been used in auto-cascade refrigeration cycles to provide a better separation effect without increasing systematic complexity (Chen et al., 2000; Zhang et al., 2001; Wu et al., 2002, 2003). Zhang et al. (2008) first introduced the proposal of Chen et al. (2000) to the field of NG liquefaction. This single-cycle MRrV process (Fig. 26) uses the low pressure MR backflow as the cooling source for the rectifying column top condenser. Thus, the separated vapor is further cooled and a portion of entrained less volatile components is condensed and brought downwards by the reflux, which gives an overhead stream richer in volatile components and a bottom stream richer in less volatile components than those from flash separation. Preliminary experiments were conducted with a six-component MR, and succeeded in cooling N_2 from ambient to −157.6 °C. Later, some modifications were made to increase system efficiency, such as optimization of the mixing position of the separated MR streams, and the addition of a variable composition module to improve the startup procedure (Wang Q et al., 2012a, 2012b), which resulted in variants of this MRrV process. Design variables such as operating pressures, MR composition, and the mixing position of the MR streams were studied theoretically and experimentally with different configurations (Wang Q et al., 2012c, 2013, 2019a, 2019b; Liu, 2013; Ren

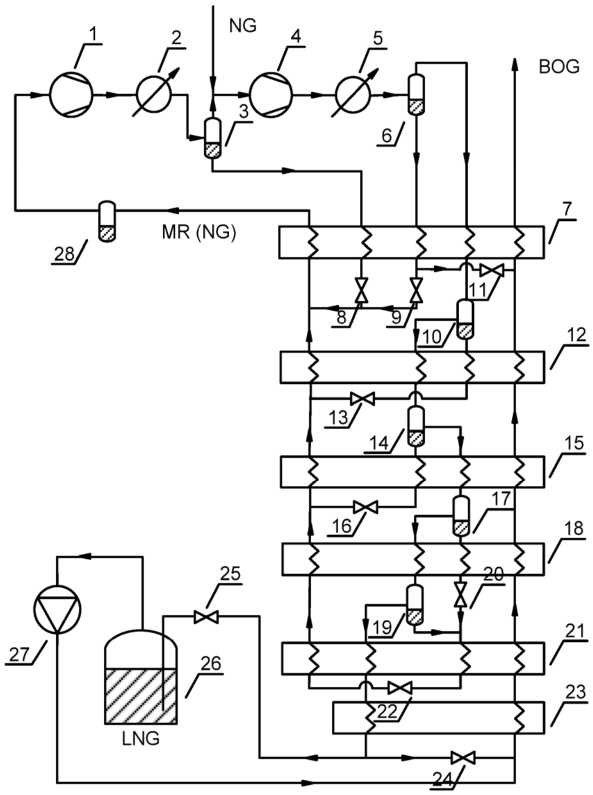

Fig. 25 A single-cycle MR6V process adapted from Etzbach and Förg (1972)

1, 4: compressors; 2, 5: condensers; 3, 6, 10, 14, 17, 19: MR (NG) separators; 7, 12, 15, 18, 21, 23: HEXs; 8, 9, 11, 13, 16, 20, 22, 24, 25: expansion valves; 26: storage tank; 27: BOG blower; 28: liquid trap

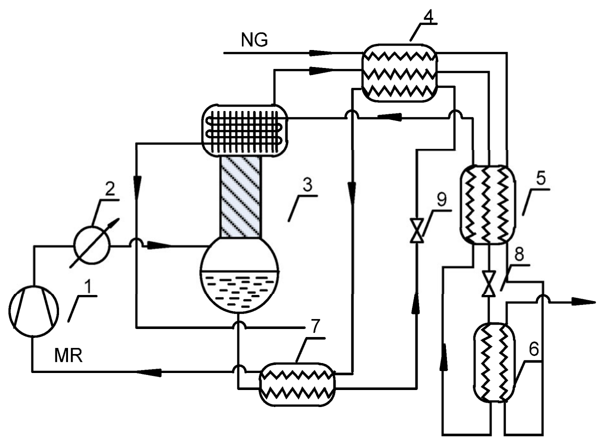

Fig. 26 A single-cycle MRrV process adapted from Zhang et al. (2008)

1: compressor; 2: condenser; 3: rectifying column; 4, 5, 6, 7: HEXs; 8, 9: expansion valves. Reprinted from (Zhang et al., 2008), Copyright 2008, with permission from Editorial Board of *Journal of Zhejiang University (Engineering Science)* (China) et al., 2014; Wang H et al., 2015). For the configuration in Fig. 26, an experimental apparatus reached an LNG production range of 0.61–1.68 kg/h with a 3 kW oil-lubricated scroll compressor, and the optimized experimental results showed an SPC range of 4.49–1.29 kW·h/kg for 0.1–0.7 MPa NG (Wang Q et al., 2019b).

Only a few operating parameters from the abovementioned studies on single-cycle MR*x*V processes discussed in Section 3.2.1 could be found. They are listed in Table 3.

3.2.2 Single-cycle MR*x* processes with not only JT expansion (single-cycle MR*x*E processes)

Similar to MR0E processes, non-JT expansion units are also used in single-cycle MR*x* processes.

Besides the single-cycle MR0E process mentioned in Section 3.1.2, Paradowski (1982) also proposed another embodiment operating with a separator and two hydraulic turbines (Fig. 27). The two hydraulic turbines (Fig. 27, items 5 and 7) deal with the expansion of separated MR streams respectively, with

Table 3 Available operating parameters from studies of single-cycle MR*x*V processes

Reference	Process		Study type	NG feed conditions, [p_{NG} (MPa), T_{NG} (°C)]	Compression/expansion stage pressures, [p_{low}, $p_{interstage}$, p_{high}] (MPa)	MR temperatures, [MITA, $T_{liquefaction}$] (°C)	Numbers of [evaporating pressure level, separation stage]	Mole percent of MR (%)	SPC (kW·h/kg)
He et al., 2019[a]	Closed type single-cycle	MR1V	S	[0.7, 25]	[0.251, N.F., 2.080]	[3, −159]	[1, 1]	Optimized [N_2, C1, C2, C3, n-C5]=[7.61, 15.62, 33.61, 22.4, 20.76]	0.411
He et al., 2019[b]		MR1V	S	[0.7, 25]	[0.298, N.F., 2.784]	[3, −159]	[1, 1]	Optimized [N_2, C1, C2, C3, n-C5]=[8.82, 16.49, 36.15, 19.95, 18.59]	N.F.
Venkatarathnam, 2008		MR1V	S	[6.5, 27]	[0.3, 0.75, 1.875, 4.675]	[3, −160]	[1, 1]	Optimized [N_2, C1, C2, C3, n-C4]=[8.59, 25.97, 25.42, 39.11, 0.92]	0.321
Na et al., 2017		MR1V	S	[6.5, 27]	[0.312, 0.75, 1.875, 4.675]	[2.85/3, N.F.]	[1, 1]	Optimized [N_2, C1, C2, C3, n-C4]=[8.58, 25.78, 30.68, 15.64, 19.32]	0.254
Venkatarathnam, 2008		MR2V	S	[6.5, 27]	[0.49, 1.25, 2.48, 4.27]	[3, −160]	[1, 2]	Optimized [N_2, C1, C2, C3, n-C4, n-C5]=[7.52, 28.42, 43.9, 5.01, 4.34, 10.81]	0.243
Nekså and Brendeng, 2007		MR2V	E	N.F.	N.F.	[N.F., −140]	[1, 2]	N.F.	0.65
Zhang et al., 2008[c]		MRrV	E	[0.14, 27]	[0.29, N.F., 1.54]	[N.F., −157.6]	[1, N.A.]	N.F.	0.69
Wang Q et al., 2019a		MRrV	S	[0.5, 25]	[0.3, N.F., 1.8]	[2, −140]	[1, N.A.]	Optimized [N_2, C1, C2=, C3, i-C4]=[9, 33, 18, 13, 27]	0.846
Wang Q et al., 2019b		MRrV	E	[0.5, N.F.]	[0.23, N.F., 1.59]	[N.F., −138.8]	[1, N.A.]	Optimized [N_2, C1, C2=, C3, i-C4]=[16.2, 23.8, 15.2, 12.6, 32.2]	1.61

[a]: minimum SPC as the objective function; [b]: minimum total investment as the objective function; [c]: converted from the experimental results by cooling 0.54 g/s N_2 to −157.6 °C

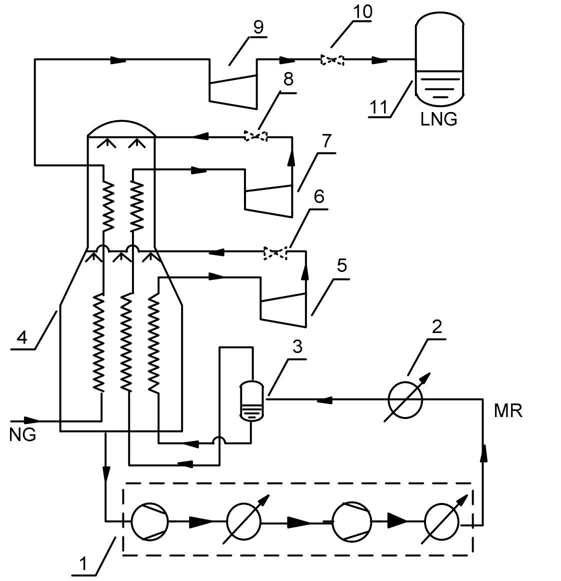

Fig. 27 A single-cycle MR1E process adapted from Paradowski (1982)

1: two-stage compressor and after-cooler; 2: condenser; 3: MR separator; 4: HEX; 5, 7, 9: cryogenic hydraulic expansion turbines; 6, 8, 10: additional expansion valves; 11: LNG storage tank

the expansion work recovered to reduce the total power consumption in the usual manner.

Based on a single-cycle MR2V process, Baek et al. (2010) substituted an expander for the MR expansion valve at the coldest point with the aim of reducing irreversibility caused by valves. To meet the dryness requirement at the expander inlet, the MR contains only N_2, CH_4, and C_3H_8, and the MR vapor from the second separator (Fig. 28, item 10) is superheated by NG alone in the HEX (item 6), rather than being further cooled in the HEX (item 7) as in general MR2V processes. Because of the modified arrangement of the HEX (item 6), the heat exchange between the vapor from the first separator (item 3) and the low pressure MR stream takes place independently in a newly added two-channel HEX (item 9). Simulation results gave a higher FOM in the new MR2E process than in the original MR2V process under respective appropriate MR compositions, which indicates a higher exergy efficiency was obtained by the substitution of the expander. However, without global optimization, the simulated SPC was still as high as 1.029 kW·h/kg. This was a worthwhile attempt to combine a gas expander and an MR containing heavier HCs in a system, in which C_3H_8 was beneficial for improving the temperature profile in the warmer temperature section and was separated as much as possible to avoid liquid expansion.

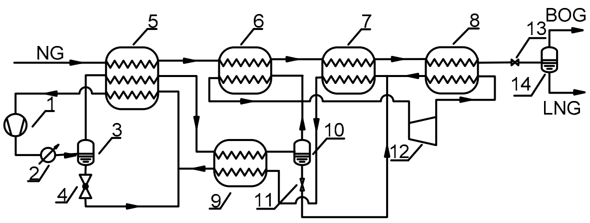

Fig. 28 A single-cycle MR1E process adapted from Baek et al. (2010)

1: compressor; 2: condenser; 3, 10: MR separators; 4, 11, 13: expansion valves; 5, 6, 7, 8, 9: HEXs; 12: expander; 14: NG separator. Reprinted from (Baek et al., 2010), Copyright 2010, with permission from American Institute of Physics

Besides expanders, ejectors have been used in MR*x*E processes, mainly for the expansion of liquid streams from separators. As in the single-cycle MR2E process (Fig. 29) proposed by Lu et al. (2009), two expansion valves for separated liquid streams are replaced with ejectors (items 7 and 11), while the expansion valve for the separated vapor stream at the coldest point remains. With the use of ejectors, throttling losses can be reduced, and the suction pressure of the compressor elevated.

Available operating parameters from the above-mentioned studies of single-cycle MR*x*E processes discussed in Section 3.2.2 are listed in Table 4.

3.2.3 Discussion

Single-cycle MR*x*V and MR*x*E processes were introduced in Sections 3.2.1 and 3.2.2.

In the single-cycle MR*x*V processes, separation units included one gas-liquid separator (7 references), two gas-liquid separators (4 references), multiple gas-liquid separators (7 references), and rectifying units (10 references). From Table 3, the simulated SPCs of single-cycle MR1V and MR2V processes ranged from 0.243 to 0.411 kW·h/kg, but those of single-cycle MRrV processes were much higher. Experimental SPCs were far higher. The MRs used in these processes are usually mixtures of N_2 and HCs from CH_4 to C_4H_{10}/C_5H_{12}, because a two-phase state is the necessary condition for MR component separation. The reported composition of most volatile components (N_2 and CH_4) was usually about

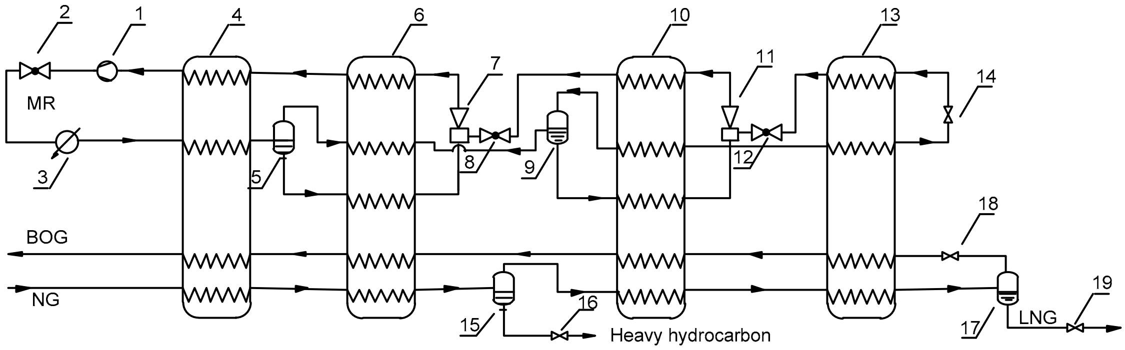

Fig. 29 A single-cycle MR1E process adapted from Lu et al. (2009)
1: compressor; 2, 8, 12: check valves; 3: condenser; 4, 6, 10, 13: HEXs; 5, 9: MR separators; 7, 11: ejectors; 14, 16, 18, 19: expansion valves; 15, 17: NG separators

Table 4 Available operating parameters from studies of single-cycle MR*x*E processes

Reference	Process	Study type	NG feed conditions, [p_{NG} (MPa), T_{NG} (°C)]	Compression/ expansion stage pressures, [p_{low}, p_{high}] (MPa)	MR temperatures, [MITA, $T_{liquefaction}$] (°C)	Numbers of [evaporating pressure level, separation stage]	Mole percent of MR (%)	SPC (kW·h/ kg)
Baek et al., 2010	Closed type single-cycle MR*x*E	S	[6, 27]	[0.2, 3]	[2.5/10, −143]	[1, 2]	[N_2, C1, C3]= [20, 35, 45]	1.029

35%–40% (in mole), which could be used as a reference. Among the single-cycle MR*x*V processes, multi-stage compression and multiple evaporating pressures were commonly adopted, which provided extra degrees of freedom for process optimization by adding intermediate pressure levels. Similar to cascaded cycles, the different evaporating temperatures on multiple pressures facilitate improvement of the match between hot and cold streams in different temperature ranges of HEXs, but the complexity and cost of the system might be increased. Therefore, the adoption of multiple evaporating pressures should be determined case by case. There were far fewer open type single-cycle MR*x*V processes than closed ones, which might be attributed to the difficulties in composing the required working fluids mixed with NG.

There were far fewer studies of single-cycle MR*x*E processes (3 references), most of which were patented designs. Furthermore, they were basically closed type processes modified from MR*x*V processes. Only one theoretical study was found (Table 3). In that study, the power consumption level was not as good as that in single-cycle MR*x*V processes. Therefore, it is hard to recommend operation stated, and two-phase states of MRs are necessary for component separation, which might limit the use of gas expanders and N_2-CH_4 mixtures. If well designed and operated, gas expanders could deal with appropriate MRs or the separated vapor stream, as in the proposal of Baek et al. (2010). Hydraulic turbines introduced in single-cycle MR0E processes also seem usable in MR*x*E processes, but we could find no relevant reports.

Therefore, expansion valves, rather than expanders, are still the dominant expansion units in single-cycle MR*x* processes. Although the use of vortex tubes and ejectors was rarely seen, further studies on the possibility of their use in MR*x* processes would be worthwhile.

4 Multi-cycle natural gas liquefaction processes using mixed refrigerants

The single-cycle MR0V and MR*x*V processes had reduced the variety of equipment used in the PR cascade liquefaction processes, but the hope of minimizing the temperature differences of the hot and cold streams in HEXs had not been completely fulfilled. After all, it was difficult to find a set of MRs to match the hot and the cold composite temperature curves perfectly in such a wide temperature range, from 30 °C to −162 °C.

A cascade of refrigeration cycles is necessary to obtain a low temperature, and has been widely applied in the field of NG liquefaction. Therefore, the NG feed, or the MR in the liquefaction stage (liquefaction cycle), or both, are cooled by one or more independent refrigerant cycles to increase system efficiency or LNG production. Various refrigeration cycles can be used in the precooling stage, such as vapor compression refrigeration cycles operating with PRs (PR-VCRCs) or with MRs (MR-VCRCs, including basic, Linde-Hampson, and auto-cascade refrigeration cycles operating with MRs) and absorption refrigeration cycles (ARCs). When an MR-VCRC occupies the precooling stage, the MR-NGLP is often called the dual mixed refrigerant (DMR) process. In this process, the temperature difference in the precooling stage is further reduced compared to the zigzag temperature curves of the PR precooling. The ‘high-level’ and ‘low-level’ cycles often refer to the refrigeration cycles used in the precooling and liquefaction stages, respectively, in DMR processes. A few MR-NGLPs use VCRCs or N_2 expansion cycles (NECs) in the subcooling stage. These include the mixed fluids cascade (MFC) and AP-X processes, which will be described in the following sections.

In summary, multi-cycle processes are regarded as single-cycle processes coupled with precooling or subcooling cycles in a cascade manner. Hence, they are classified based on, and named in accordance with, the single-cycle processes discussed in the above sections. Particularly, multi-cycle MR*x*V processes are categorized into three subclasses according to the precooling cycles, considering the greater number and diversity of applications of precooling cycles than subcooling cycles found in the literature. The only two examples of the use of a subcooling cycle, the MFC process and the AP-X process, are considered more as modifications of existing multi-cycle MR0V and MR*x*V processes, respectively, and hence are not considered as separate subclasses.

To avoid confusion, note that the term ‘main (precooling/subcooling) cycle’ refers to the independent refrigeration cycle in the liquefaction (precooling/subcooling) stage of an MR-NGLP, while ‘process’ refers to the entirety of an MR-NGLP, including all the coupled MR loops and the NG loop.

4.1 Multi-cycle processes based on single-cycle MR0 processes (multi-cycle MR0 processes)

4.1.1 Multi-cycle MR0 processes with only JT expansion in the liquefaction stage (multi-cycle MR0V processes)

PR-VCRCs operating with HCs or halogenated HCs are the simplest solution to provide precooling from ambient to about −40 °C. Gong et al. (2012) designed and established an MR0V system precooled by pure R22 (Fig. 30), in which an aluminum four-channel plate-fin HEX serves as the core of the cold box. Experiments were conducted with CH_4 in place of NG. Oil-lubricated screw compressors are used in both the precooling R22 system and the main refrigerant system, with an ordinary oil separator for the R22 system and an enhanced oil separator for the main refrigerant system. This system has a capacity of 10 000–15 000 Nm^3/d, with a minimum SPC of about 0.77 kW·h/kg. Based on this system, skid-mounted LNG liquefaction packages with larger capacities of 15 000–100 000 Nm^3/d were developed and manufactured from 2011 to 2014 (Gong et al., 2015).

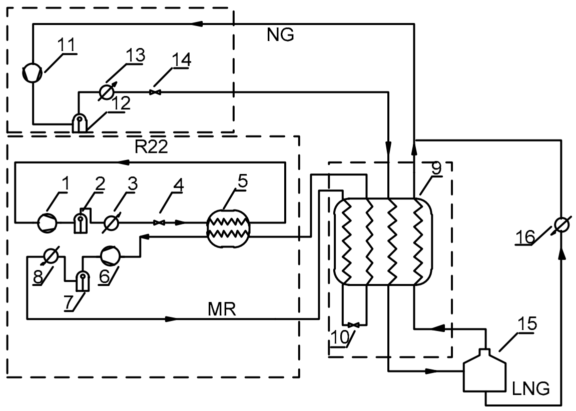

Fig. 30 A schematic diagram of the R22 precooled MR0V process adapted from Gong et al. (2012)

1, 6, 11: compressors; 2, 7, 12: oil separators; 3, 8, 13: air-cooling condensers; 4, 10, 14: expansion valves; 5, 9: HEXs; 15: LNG storage tank; 16: LNG vaporizer. Reprinted from (Gong et al., 2012), Copyright 2012, with permission from Elsevier

However, MR-VCRCs are more frequently found in the precooling stages of multi-cycle MR0V processes. As already stated, such a configuration forms one main kind of DMR process. An MR-VCRC precooled MR0V process (Fig. 31) was proposed by

Shell Internationale Research Maatschappij NV (1962). A set of MRs (C_2H_6, C_3H_8, and C_4H_{10}) is circulated in the high-level cycle from 0.07 to 3.5 MPa to provide most of the cooling capacity in the HEX (Fig. 31, item 11), while another set (CH_4 and C_2H_6) is circulated in the low-level cycle from 0.1 to 4.0 MPa to ensure the subcooling of the NG. After cooling in the two HEXs, the NG is expanded and the cooling capacity of the gaseous phase is recovered.

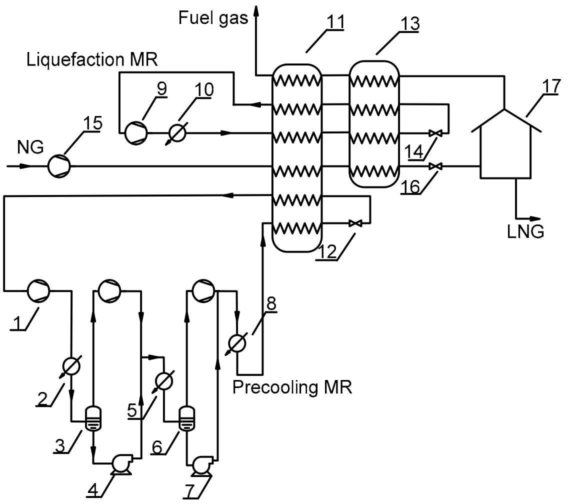

Fig. 31 A multi-cycle MR0V process adapted from Shell Internationale Research Maatschappij NV (1962)
1, 9, 15: compressors; 2, 5, 8, 10: condensers; 3, 6: MR separators; 4, 7: pumps; 11, 13: HEXs; 12, 14, 16: expansion valves; 17: storage tank

The process proposed by Fischer et al. (2004) (Fig. 32), known as the LIQUEFIN process, is another example of an MR-VCRC precooled MR0V process. In the high-level cycle, a first set of MRs consisting of C_2H_6, C_3H_8, and C_4H_{10} is divided into three streams evaporating at different pressure levels to cool both the low-level MR and NG. If operated under appropriate pressures and precooling temperature, the second set of refrigerants consisting of N_2, CH_4, C_2H_6, and C_3H_8 at the outlet of the precooling stage HEX (Fig. 32, item 9) can be totally condensed. Therefore, unlike in the PRICO process, there is no need to use a separator to avoid maldistribution. The LNG stream out from the HEX (item 10) is twice expanded to produce gaseous and liquid phases which serve as the fuel and LNG product, respectively.

Several studies of their optimum thermodynamic performance have been conducted based on a simplified version of the multi-cycle MR0V process shown in Fig. 31, neglecting the cold energy recovery of BOG. Energy and exergy analyses by Venkatarathnam (2008) gave a minimum SPC of 0.296 kW·h/kg and an overall exergy efficiency of 45% with specified precooling and liquefaction temperatures of −28 °C and −160 °C, respectively. Husnil and Lee (2014) correlated the flow rate of high-level MR and the total compressor duty under fixed NG and LNG parameters on an operational map, in search of feasible operating condition boundaries. Several lines of constant variables, such as MR flow rates and temperature differences at the hot ends of the HEXs, were also plotted. Analyses indicated two promising variables worth optimizing (the flow rate ratio of the two sets of MRs and the hot end temperature difference in the precooling HEX), which, if kept constant, would keep the process operating in the feasible area with a 1% deviation from the optimum efficiency value. Khan et al. (2016) searched for optimized flow rates and pressures to minimize the power consumption under ambient temperatures of 25 and 38 °C. Results showed that the lower ambient temperature led to a lower SPC of 0.34 kW·h/kg for such a DMR process, which indicated that the arctic region was beneficial for the DMR process. Available operating parameters from the abovementioned studies on DMR processes are summarized in Table 5.

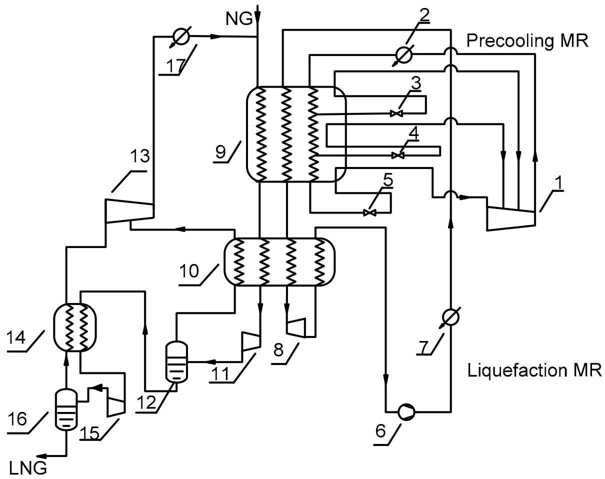

Fig. 32 A multi-cycle MR0V process (the LIQUEFIN process) adapted from Fischer et al. (2004)
1, 6, 13: compressors; 2, 7, 17: condensers; 3, 4, 5: expansion valves; 8, 11, 15: expansion units; 9, 10, 14: HEXs; 12, 16: NG separators

Table 5 Available operating parameters from studies of multi-cycle MR0V processes

Reference	Process		Study type	NG feed conditions, [p_{NG} (MPa), T_{NG} (°C)]	Compression stage pressures, [p_{low}, $p_{interstage}$, p_{high}][b] (MPa)	MR temperatures, [MITA, $T_{eachstage}$][a] (°C)	Numbers of [evaporating pressure level, separation stage]	Mole percent of MR (%)	SPC (kW·h/kg)
Venkatarathnam, 2008	Two-cycle	MR precooled MR0V (DMR)	S	[4, 32]	Precooling: [0.31, 0.71, 1.96] Liquefaction: [0.3, 1.44, 1.96, 2.4]	Precooling: [3, −28] Liquefaction: [3, −160]	Precooling: [1, N.A.] Liquefaction: [1, N.A.]	Precooling: optimized [C2=, C3, n-C4]=[31.15, 36.02, 32.83] Liquefaction: optimized [N_2, C1, C2, C3]=[10.88, 30.52, 43.57, 15.03]	0.296
Gong et al., 2012		R22 precooled MR0V	E	[0.8–1.4, N.F.]	Precooling: N.F. Liquefaction: [0.45, 2]	Precooling: [N.F., 5/−15] Liquefaction: [2 (design), −125]		Precooling: [R22]=[100] Liquefaction: N.F.	0.753[b]
Husnil and Lee, 2014		MR precooled MR0V (DMR)	S	[5.2, 38]	Precooling: [0.355, N.F., 2.978] Liquefaction: [0.331, N.F., 5.145]	Precooling: N.F. Liquefaction: N.F.	Precooling: [1, N.A.] Liquefaction: [1, N.A.]	Precooling: [C1, C2, C3, i-C4, n-C4]=[8, 49.2, 6.5, 15.9, 27.6] Liquefaction: [N_2, C1, C2, C3]=[13.7, 35.6, 40.9, 9.8]	N.F.
Khan et al., 2016[c]		MR precooled MR0V (DMR)	S	[5.5, 25]	Precooling: [0.13, N.F., 2.4] Liquefaction: [0.325, N.F., 5.5]	Precooling: [17, N.F.] Liquefaction: [3.2, N.F.]	Precooling: [1, N.A.] Liquefaction: [1, N.A.]	Precooling: optimized [C1, C2, C3, i-C4, n-C4]= [3.68, 18.67, 26.8, 25.42, 25.42] Liquefaction: [N_2, C1, C2, C3]=[11.48, 26.94, 25.51, 36.07]	0.3399
Venkatarathnam, 2008	Three-cycle	MFC	S	[6.5, 27]	Precooling: [0.3, 0.67, 1.69] Liquefaction: [0.31, N.F., 2.79] Subcooling: [0.35, N.F., 3.39]	Precooling: [3, −25] Liquefaction: [3, −86] Subcooling: [3, −160]	Precooling: [2, N.A.] Liquefaction: [1, N.A.] Subcooling: [1, N.A.]	Precooling: optimized [C2, C2=, C3, n-C4]=[0.01, 11.29, 73.56, 15.13] Liquefaction: optimized [C1, C2, C2=, C3]=[12.65, 32.92, 27.77, 26.65] Subcooling: optimized [N_2, C1, C2=]=[17.31, 42.45, 40.24]	0.234
Jensen and Skogestad, 2006		MFC	S	[6.15, 11]	Precooling: [0.2, 0.645, 1.5] Liquefaction: [0.2, 2.058] Subcooling: [0.2, 2.838, 5.699]	Precooling: [N.F., 0.34] Liquefaction: [N.F., −77] Subcooling: [N.F., −155]	Precooling: [2, N.A.] Liquefaction: [1, N.A.] Subcooling: [1, N.A.]	Precooing: optimized [C2, C3]=[37.7, 62.3] Liquefaction: optimized [C1, C2, C3]=[4.02, 82.96, 13.02] Subcooling: optimized [N_2, C1, C2]=[4.55, 52.99, 42.45]	0.169

To be continued

Table 5

Reference	Process	Study type	NG feed conditions, [p_{NG} (MPa), T_{NG} (°C)]	Compression stage pressures, [p_{low}, $p_{interstage}$, p_{high}][b] (MPa)	MR temperatures, [MITA, $T_{eachstage}$][a] (°C)	Numbers of [evaporating pressure level, separation stage]	Mole percent of MR (%)	SPC (kW·h/kg)
Vatani et al., 2014	Three-cycle MFC	S	[6, 13]	Precooling: [N.F., N.F., 1.59] Liquefaction: [N.F., N.F., 2.79] Subcooling: N.F.	Precooling: N.F. Liquefaction: [N.F., −81.5] Subcooling: [N.F., −162]	Precooling: [2, N.A.] Liquefaction: [1, N.A.] Subcooling: [1, N.A.]	Precooling: N.F. Liquefaction: N.F. Subcooling: N.F.	0.255
Nawaz et al., 2019	MFC	S	[5, 30]	Precooling: [0.251, 0.985] Liquefaction: [0.288, 2.79] Subcooling: [0.312, 3.40]	Precooling: [3, −27.76] Liquefaction: [3, −88.9] Subcooling: [3, −147.1]	Precooling: [1, N.A.] Liquefaction: [1, N.A.] Subcooling: [1, N.A.]	Precooling: optimized [C2, C3, n-C4]=[23.55, 14.07, 62.37] Liquefaction: optimized [C1, C2, C3] =[13.38, 72.45, 14.17] Subcooling: optimized [N_2, C1, C2] =[9.99, 59.24, 30.77]	0.220
Ding et al., 2017	MFC	S	[5, 30]	Precooling: [0.153, 0.389, 1.316] Liquefaction: [0.372, 1, 2.033] Subcooling: [0.419, 1, 4.089]	Precooling: [3, −40] Liquefaction: [3, −92] Subcooling: [3, −150]	Precooling: [1, N.A.] Liquefaction: [1, N.A.] Subcooling: [1, N.A.]	Precooling: optimized [C2=, C3, n-C4]=[7.26, 77.43, 15.31] Liquefaction: optimized [C1, C2=, C3]=[10.55, 78.29, 11.16] Subcooling: optimized [N_2, C1, C2=]=[9.62, 69.28, 21.09]	0.266
Castillo et al., 2013	MFC	S	N.F.	Precooling: N.F. Liquefaction: [0.2, N.F., 2.06] Subcooling: [0.2, N.F., 5.7]	Precooling: [N.F., −50] Liquefaction: N.F. Subcooling: [N.F., −160]	Precooling: [2, N.A.] Liquefaction: [1, N.A.] Subcooling: [1, N.A.]	Precooling: optimized [C2, C3]= [30, 70] (warm)/[37.7, 62.3] (cold) Liquefaction: optimized [C1, C2, C3] =[4.02, 82.96, 13.02] Subcooling: optimzied [N_2, C1, C2] =[4.55, 52.99, 42.45]	N.F.
Mehrpooya et al., 2016	Modified MFC	S	[6.5, 26.85]	Precooling: N.A. Liquefaction: [0.31, 2.79] Subcooling: [0.32, 3.39]	Precooling: [4.3, −25] Liquefaction: [3, −86] Subcooling: [3, −160]	Precooling: [1, N.A.] Liquefaction: [1, N.A.] Subcooling: [1, N.A.]	Precooling: N.A. Liquefaction: [C1, C2, C2=, C3]= [12.7, 32.9, 27.8, 26.7] Subcooling: [N_2, C1, C2=]= [17.3, 42.5, 40.2]	0.17

[a]: $T_{eachstage}$: the temperatures of hot MR or NG streams out from the HEXs in the precooling, liquefaction, or subcooling stages; [b]: the minimum SPC with 1.4 MPa CH_4, converted from 0.54 kW·h/Nm^3; [c]: results of case 3 with NG feed at 25 °C and intercooled at 30 °C

The MR-VCRC precooled MR0V processes did not seem to outperform the single-cycle MR0V processes strongly in terms of simulated SPC, and lost the advantage of a simple structure. If the factor of simplicity was put aside, would a third coupled VCRC on the existing precooled MR0V processes result in more competitive SPCs? Inspired by the conventional PR cascade process, the MFC process was put forward by the Statoil Linde LNG Technology Alliance as a competitor, especially in large-scale applications (Bach, 2002). Three MR-VCRCs are used to precool, liquefy, and subcool the NG feed (Fig. 33). Generally speaking, a mixture of C_2H_6 (or C_2H_4), C_3H_8, and C_4H_{10} is used in the first stage refrigeration cycle to reach −35–−55 °C. Similarly, a mixture of CH_4, C_2H_6 (or C_2H_4), and C_3H_8, and a mixture of N_2, CH_4, and C_2H_6 (or C_2H_4) are used in the second and third stages to reach −40–−100 °C and −85–−160 °C, respectively (Stockmann et al., 2001).

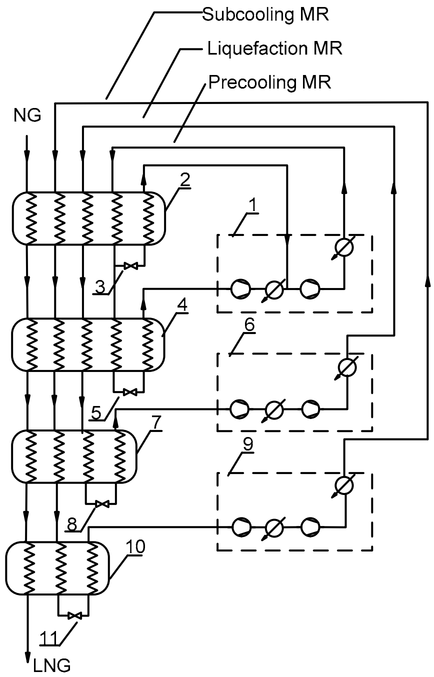

Fig. 33 A multi-cycle MR0V process adapted from Stockmann et al. (2001)

1, 6, 9: multi-stage compressors and after-coolers; 2, 4, 7, 10: HEXs; 3, 5, 8, 11: expansion valves

However, the size of the third HEX and its corresponding equipment is generally smaller than those of the two warmer HEXs in the MFC process. Because the size of equipment would increase with increased LNG production, the sizes of high temperature parts would reach their maximum earlier. To increase LNG production, a modified MFC process was proposed by Roberts (2006), in which the subcooling stage MR is only partially evaporated in the subcooling HEX (Fig. 34, item 17) and is self-refrigerated. No coupling of the precooling and liquefaction stages helps to reduce the heat load and the equipment size of these two warmer stages.

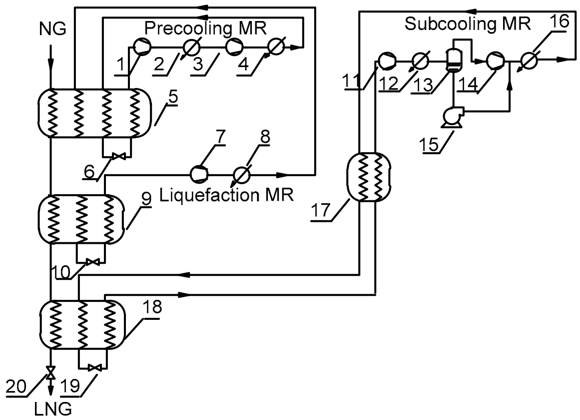

Fig. 34 A modified MFC process adapted from Roberts (2006)

1, 3, 7, 11, 14: compressors; 2, 4, 8, 12, 16: after coolers; 5, 9, 17, 18: HEXs; 6, 10, 19, 20: expansion valves; 13: MR separator; 15: pump

Regarding the MFC process, theoretical analyses were usually based on the configuration in Fig. 33. Jensen and Skogestad (2006, 2009b) discussed the potential maximum degrees of freedom (DOFs) and found 13 variables critical in the search for optimum operation of a specific MFC plant. These variables involved nine manipulating the composition of four-component MRs in three stages, and another four brought by precooling/liquefaction temperatures and intermediate pressure. With these DOFs used optimally, an excellent SPC of 0.169 kW·h/kg was achieved. The thermodynamic analyses conducted by Vatani et al. (2014) showed the MFC process could reach an SPC as low as 0.2545 kW·h/kg and an overall exergy efficiency of 52% for the liquefaction of 6 MPa NG, with respective exergy efficiencies of 45.7%, 62.5%, and 42.9% for the three stages. Venkatarathnam (2008) estimated a similar overall exergy efficiency of 52.1%, which is larger than that of the MR-VCRC precooled MR0V process shown in

Fig. 31 (45%). Nawaz et al. (2019) further lifted its exergy efficiency to 64.09% with the help of the Coggins step-up approach, which presented a set of satisfactory working conditions for the MFC process and verified the effectiveness of this novel optimization method.

Some studies discussed the differences brought about by modifications. Ding et al. (2017) investigated the influence of evaporating pressure level in each stage, and suggested that the most efficient and optimal configuration for an MFC process should be three pressure levels in the precooling stage, and one in both the liquefaction stage and subcooling stage, which achieved an SPC of 0.240 kW·h/kg (4.205 kW·h/kmol). Castillo et al. (2013) considered replacing the precooling MR (C_2H_6-C_3H_8 mixture) in the MFC process with pure C_3H_8 with three evaporating pressure levels. The substitution led to an increased precooling temperature from −50 °C to −36 °C, resulting in less heat load in the precooling stage, but more in the liquefaction stage. Compared with the original process, the modified one was more competitive with a lower SPC no matter whether under warm or cold climate conditions. However, increased heat loads in the liquefaction and subcooling stages after the substitution would result in an increase in total costs, because the capital cost of equipment in these two stages is larger than that in the precooling stage. Mehrpooya et al. (2016) even considered replacing the VCRC in the precooling stage with an NH_3-H_2O ARC. An ARC could use available waste heat in the LNG plant to supply a part of the cooling capacity at about −30 °C. In this way, electrical power consumption could be reduced. Simulation results gave an SPC of 0.172 kW·h/kg with 31% power savings, and cost savings from a smaller HEX area. These savings could compensate for the increased fixed costs of ARC equipment (pump, generator, absorber, etc.), making this substitution attractive in large-scale LNG plants. Available operating parameters from the abovementioned studies on MFC processes are summarized in Table 5.

4.1.2 Multi-cycle MR0 processes with not only JT expansion in the liquefaction stage (multi-cycle MR0E processes)

In Section 4.1.1, the LIQUEFIN process (Fischer et al., 2004) was briefly introduced. As mentioned in the patent, the expansion units in the liquefaction MR loop and NG recovery loop can be expansion valves, expanders, or a combination of both. When expanders are used in the liquefaction stage, it is an MR-VCRC precooled Siemens cycle (or precooled reverse Brayton cycle) operating with MRs, thus falling into the category of a multi-cycle MR0E process in this paper.

Pu et al. (2007, 2008) proposed and analyzed a C_3H_8 precooled MR0E process with one expander. Except for the precooling cycle, it had a configuration similar to that of the single-cycle MR0E process mentioned in Fig. 8, except that the first stage expander was removed. The added precooling system cooled both the high pressure MR and the NG. Operated at 3.88–0.55 MPa, this multi-cycle MR0E process reached an SPC of 0.744 kW·h/kg, lower than that of the other two single-cycle MR0E processes (the serial configuration and parallel configuration), which indicates the usefulness of precooling.

As shown in Fig. 35, Ding et al. (2016) added C_3H_8 precooling to a single-cycle MR0E process with a configuration similar to that of Paradowski's design shown in Fig. 10 (Paradowski, 1982). With N_2-CH_4 mixture as the working fluid, a two-stage expander was adopted instead of a hydraulic turbine. A simulated SPC of 0.392 kW·h/kg was obtained with the MR expanded twice from 4.40 to 0.24 MPa for the liquefaction of 5 MPa NG. This was also a lower SPC than those of closed type single-cycle MR0E

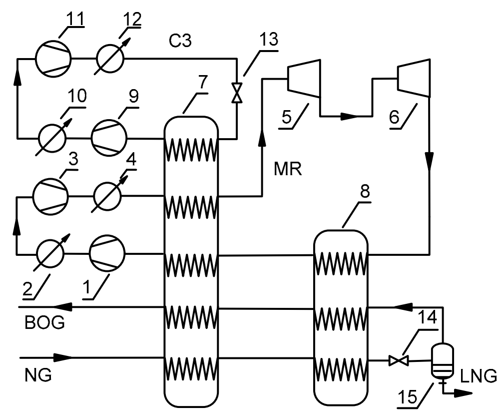

Fig. 35 A multi-cycle MR0E process adapted from Ding et al. (2016)

1, 3, 9, 11: compressors; 2, 4, 10, 12: condensers; 5, 6: expanders; 7, 8: HEXs; 13, 14: expansion valves; 15: NG separator. Reprinted from (Ding et al., 2016), Copyright 2016, with permission from Elsevier processes as listed in Table 2. CO_2 could serve as an alternative precooling refrigerant in similar processes (Sanaye and Ghoreishi, 2019).

Available operating parameters from the above-mentioned studies are summarized in Table 6.

4.1.3 Discussion

The multi-cycle MR0V and MR0E processes were introduced in Sections 4.1.1 and 4.1.2.

The multi-cycle MR0V processes discussed included mainly two-cycle processes (the precooled MR0V process, 7 references) and three-cycle processes (the MFC process, 11 references). In this category, PR precooling was less often seen than MR precooling. Precooling MRs generally contained HCs from C_2H_4/C_2H_6 to C_4H_{10}. C_2H_4/C_2H_6 and C_3H_8 usually made up 50%–60% (in mole) in two-cycle processes, and over 80% in three-cycle ones. CH_4 is not necessary in the precooling MRs of three-cycle MR0V processes, but a small percentage could sometimes be found in those of two-cycle processes. The liquefaction MRs usually required 40%–50% of N_2+CH_4 in two-cycle MR0V processes, but only 5%–10% of CH_4 and over 60% of C_2H_4/C_2H_6 in three-cycle ones. N_2 is not necessary in the liquefaction MRs of three-cycle MR0V processes because their liquefaction temperatures are higher than those of two-cycle processes. As for the subcooling stage in three-cycle MR0V processes, over 60% of N_2+CH_4 is necessary to ensure the lowest temperature. The simulated SPCs of this category usually lay in the range of 0.169–0.340 kW·h/kg, indicating reduced power consumption to some extent by the addition of precooling or subcooling, compared to single-cycle MR0V processes. However, the SPCs of two-cycle MR0V processes were not as good as those of three-cycle ones, and might even lose the merits of a simple structure and low cost compared to the single-cycle types. This might explain why there have been relatively few studies of two-cycle MR0V processes. Besides, multiple evaporating pressures were also adopted in the precooling stages of multi-cycle MR0V processes, such as the LIQUEFIN process (Fig. 32) and MFC process (Fig. 33), which were not seen in the single-cycle MR0V processes.

There were relatively few studies of multi-cycle MR0E processes (5 references), which probably reflects the small number of single-cycle MR0E

Table 6 Available operating parameters from studies of multi-cycle MR0V processes

Reference	Process	Study type	NG feed conditions, [p_{NG} (MPa), T_{NG} (°C)]	Compression/ expansion stage pressures, [p_{low}, $p_{interstage}$, p_{high}] (MPa)	MR temperatures, [MITA, $T_{eachstage}$] (°C)	Numbers of [evaporating pressure level, separation stage]	Mole percent of MR (%)	SPC (kW·h/ kg)
Pu et al., 2007, 2008	C_3H_8 pre-cooled MR0E	S	[5.1, 30]	Precooling: N.F. Liquefaction: [0.55, N.F., 3.88]	Precooling: N.F. Liquefaction: [3, N.F.]	Precooling: [N.F., N.A.] Liquefaction: [1, N.A.]	Precooling: [C3]=[100] Liquefaction: [N_2, C1]=[50, 50]	0.774
Ding et al., 2016[a]	C_3H_8 pre-cooled MR0E	S	[5, 30]	Precooling: N.F. Liquefaction: [0.24, N.F., 4.44]	Precooling: [N.F., −33] Liquefaction: [3, −148.1]	Precooling: [1, N.A.] Liquefaction: [1, N.A.]	Precooling: [C3]=[100] Liquefaction: [N_2, C1]=[13.95, 86.05]	0.389
Ding et al., 2016[b]	C_3H_8 pre-cooled MR0E	S	[5, 30]	Precooling: [0.153, 0.42, 1.5] Liquefaction: [0.24, 2, 4.389]	Precooling: [N.F., −30] Liquefaction: [3, −148.1]	Precooling: [1, N.A.] Liquefaction: [1, N.A.]	Precooling: [C3]=[100] Liquefaction: [N_2, C1]=[16.01, 83.99]	0.369
Sanaye and Ghoreoshi, 2019	CO_2 pre-cooled MR0E	S	[5, 30]	Precooling: [1.5, 2.924, 5.724] Liquefaction: [2.403, 1.05, 4.55]	Precooling: [2, −30] Liquefaction: [2, −147.6]	Precooling: [1, N.A.] Liquefaction: [1, N.A.]	Precooling: [CO_2]=[100] Liquefaction: [N_2, C1]=[N.F.]	0.482

[a]: results obtained by the novel method introduced by Ding et al. (2016); [b]: results obtained by the GA method of Ding et al. (2016)

processes. From limited simulation results, the SPCs of the multi-cycle MR0E processes lay in a broad range of 0.220–0.774 kW·h/kg, higher than those of the multi-cycle MR0V processes. In the multi-cycle MR0E processes discussed, pure C_3H_8 was usually used in the precooling stage, while an N_2-CH_4 mixture was still widely adopted in the liquefaction stage. There was only one study concerning composition optimization, indicating a 14%–16% of N_2 in the optimum N_2-CH_4 mixture.

From the literature survey, open type processes were not found in multi-cycle MR0V or MR0E processes. Among the single-cycle MR0 processes mentioned before, open types were seen only in single-cycle MR0E processes. It might weaken the merit of simplicity if single-cycle MR0 processes were cascaded with another refrigeration cycle.

4.2 Multi-cycle processes based on single-cycle MR*x* processes (multi-cycle MR*x* processes)

4.2.1 Multi-cycle MR*x* processes with only JT expansion in the liquefaction stage (multi-cycle MR*x*V processes)

Efforts have been made to improve the performance of single-cycle MR*x*V processes by coupling with other refrigeration cycles. As presented in single-cycle MR*x*V processes, the number of MR separators serves as a classification criterion. However, in multi-cycle MR*x*V processes structurally developed from single-cycle ones, there are usually one or two separators in the liquefaction cycle (liquefaction stage), which makes the number of MR separators a less critical parameter. Given the diversity of refrigeration cycles that could be used in the precooling stage, we further classified multi-cycle MR*x*V processes based on the types of precooling cycles, namely PR-VCRC precooled MR*x*V processes, MR-VCRC precooled MR*x*V processes, and ARC precooled MR*x*V processes.

4.2.1.1 Multi-cycle MR*x*V processes with PR-VCRC precooling (PR-VCRC precooled MR*x*V processes)

Gaumer Jr and Newton (1973) proposed a new multi-cycle process as an alternative approach to obtain a better temperature match in HEXs (Fig. 36), besides the two MR4V processes proposed by Gaumer Jr and Newton (1971, 1972). This process, cascaded by a PR-VCRC without separators and an auto-cascade refrigeration cycle with one separator, could be considered, from a configurative perspective, as being constructed by adding a PR-VCRC to a single-cycle MR1V process. The PR provides precooling for both the NG and liquefaction stage MR. Integral HEXs, similar to those in Gaumer Jr and Newton's former design (Fig. 23), were used, greatly simplifying the structure of the system and improving the economy. According to the inventor, among the pure HCs mentioned above, C_3H_8 achieves optimum temperatures at ideal pressures when serving as a precooling stage refrigerant. Therefore, the C_3H_8 VCRC precooled multi-cycle MR1V process, also well-known as the C3MR process, has become a popular choice in LNG industries. Apart from the configuration in Fig. 36 in which C_3H_8 is split into precool NG and MR, the process could also be used for only one of them, as in the proposal by Sarsten (1977a, 1977b), in which C_3H_8 precools only the NG feed at two evaporating pressures for water and heavy HC removal. After the removal process, NG is sent into HEX at about −40 °C. In this way, the structural complexity of the C_3H_8 VCRC and the hot section area of the MR HEX are reduced.

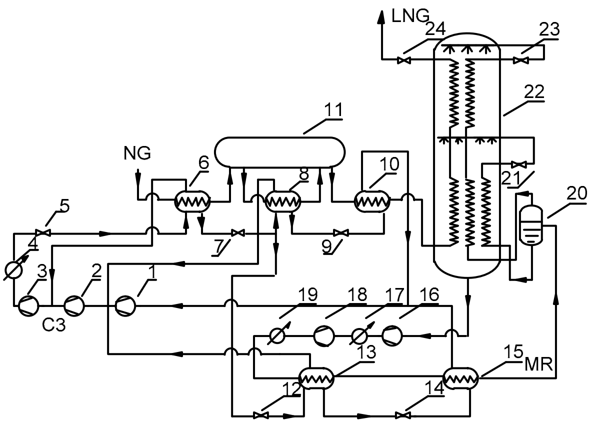

Fig. 36 A multi-cycle MR1V process adapted from Gaumer Jr and Newton (1973)

1, 2, 3, 16, 18: compressors; 4, 17, 19: condensers; 5, 7, 9, 12, 14, 21, 23, 24: expansion valves; 6, 8, 10, 13, 15, 22: HEXs; 11: NG treatment unit; 20: MR separator

Generally speaking, the C_3H_8 in the C3MR process evaporates at three pressures in cold climates and at four pressures in warm climates (Venkatarathnam, 2008). There are usually no more than two MR separators in the liquefaction stage of the C3MR process, in consideration of simplicity and low investment. Therefore, the well-known C3MR process generally includes the C_3H_8 VCRC precooled MR1V and MR2V processes according to the framework proposed in this paper.

The C3MR process developed rapidly in recent decades, and has now become the mainstream for large-scale LNG plants. Hence, attention has been paid to its thermodynamic performance (Venkatarathnam, 2008; Nezhad et al., 2012; Ghorbani et al., 2016; Mehrpooya et al., 2018), as well as comparisons of its performance with that of other processes (Vink and Nagelvoort, 1998; Yoon et al., 2009; Castillo and Dorao, 2013; Castillo et al., 2013; Pereira and Lequisiga, 2014; Vatani et al., 2014). Compared to single-cycle processes, the addition of the precooling stage resulted in more DOFs in multi-cycle MR*x*V processes. On the one hand, this brought more variables worthy of optimization, while on the other hand, it inevitably increased the difficulty of searching for optimum working conditions. Effort was put into studies of the optimization of important parameters such as the operating pressures of C_3H_8 and MR (including pressure ratios), the liquefaction temperature that MR provided, and the MR components and composition. Various deterministic or heuristic algorithms introduced in Section 3.1.1 were proven to be applicable to the C3MR process (Venkatarathnam, 2008; Helgestad, 2009; Alabdulkarem et al., 2011; Wang MQ et al., 2011, 2012; Khan et al., 2013; Lee et al., 2013, 2015; Ghorbani et al., 2016; Sanavandi and Ziabasharhagh, 2016; Song et al., 2019). These optimization results were of great value to upcoming researchers and relevant engineering technicians. Moreover, these studies showed that the power consumption related parameters (e.g. total or specific power consumption) were the most commonly selected objective functions, followed by exergy related parameters (e.g. exergy efficiencies of a part, of the whole, or of the process). There have been several studies comparing different objective functions (Hatcher et al., 2012; Wang MY et al., 2013, 2014), which considered more thermodynamic and economic variables. Available operating parameters from the abovementioned studies are summarized in Table 7 for reference.

Generally, the production of the C3MR process is limited to 5 MTPA (million tonnes per annum). The upscaling of LNG production brought difficulties in the manufacture of large-scale HEXs and compressors. To increase the production of a single LNG plant, Roberts and Agrawal (2001b) from APCI considered the use of pure gas expansion to bear heat loads in the low temperature section. These designs were the embryonic forms of the now well-known AP-X process. Designed for large-scale LNG plants in Qatar's tropical desert climate (Air Products and Chemicals, Inc, 2005), the AP-X process can be regarded from a configurative perspective as being constructed based on a multi-cycle MR*x*V process (usually the C3MR process) with an additional single stage N_2 expander cycle (NEC) for subcooling (Fig. 37). After the NG is cooled to about −120 °C by C_3H_8 and MR successively, it enters the HEX (Fig. 37, item 14) of the NEC and is further cooled. The NEC reduces the heat loads of the former two stages, which can reduce the flow rates of both C_3H_8 and the MR, and also make it possible for existing equipment to deal with a larger quantity of NG. This modification sacrifices the simplicity of the system to some extent, but the LNG production can be increased easily to 7–10 MTPA (Roberts et al., 2002a, 2004; Bukowski et al., 2011).

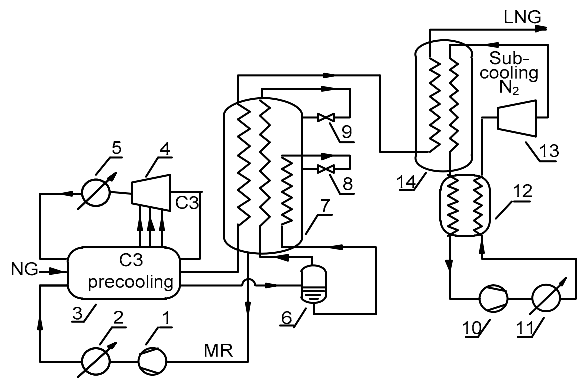

Fig. 37 A multi-cycle MR1V process adapted from Roberts and Agrawal (2001b)

1, 4, 10: compressors; 2, 5, 11: condensers; 3: C_3H_8 evaporators; 6: MR separator; 7, 12, 14: HEXs; 8, 9: expansion valves; 13: expander

Until now, except for reports from the APCI Company (Roberts et al., 2002a, 2004; Air Products and Chemicals, Inc, 2005; Bukowski et al., 2011), there have been only a few comprehensive analyses of the AP-X process. Bin Omar et al. (2012) presented an SPC as low as 0.14 kW·h/kg and an overall exergy efficiency of 15% for the AP-X process shown in

Table 7 Available operating parameters from studies of multi-cycle MRxV processes

Reference	Process	Study type	NG feed conditions, [p_{NG} (MPa), T_{NG} (°C)]	Compression/ expansion stage pressures, [p_{low}, $p_{interstage}$, p_{high}] (MPa)	Temperatures, [MITA, T_{stage1}, …, T_{stagen}][a] (°C)	Numbers of [evaporating pressure level, separation stage]	Mole percent of MR (%)	SPC (kW·h/ kg)
Venkatarathnam, 2008	PR-VCRC precooled MR1V	S	[6.5, 27]	Precooling: [0.13, 0.25, 0.51, 0.72, 1.43] Liquefaction: [0.3, N.F.,⋯, 4.86]	Precooling: [3, 17.6, 5.8, −16.2, −33] Liquefaction: [3, N.F., −160]	Precooling: [4, N.A.] Liquefaction: [1, 1]	Precooling: [C3]=[100] Liquefaction: optimized [N_2, C1, C2, C3]=[7, 41.8, 29.9, 21.3]	N.F.
Nezhad et al., 2012		S	[4.5, 35]	Precooling: [N.F., N.F., 0.87, 2] Liquefaction: [0.44, 1.41, 4.5, 5.2]	Precooling: [N.F., N.F., …, −40] Liquefaction: [N.G, N.F., −140]	Precooling: [4, N.A.] Liquefaction: [1, 1]	Precooling: [C3]=[100] Liquefaction: [N_2, C1, C2, C3] =[7, 38, 41, 14]	0.234
Ghorbani et al., 2016		S	[6.5, 27]	Precooling: [0.13, 0.25, 0.51, 0.72, 1.43] Liquefaction: [0.3, 2.1, 4.86]	Precooling: [≈3, 17.6, 5.8, −16.2, −35.5] Liquefaction: [≈3, −128.3, −160]	Precooling: [4, N.A.] Liquefaction: [1, 1]	Precooling: [C3]=[100] Liquefaction: [N_2, C1, C2, C3] =[7, 41.81, 29.89, 21.31]	0.2594
Mehrpooya et al., 2018		S	[1.379, 25]	Precooling: [0.25, N.F.,⋯, N.F.] Liquefaction: N.F.	Precooling: [0.37/0.41/4.89, −19, −25, −60] Liquefaction: [1.02/2, −119, −165]	Precooling: [3, N.A.] Liquefaction: [1, 1]	Precooling: [C3]=[100] Liquefaction: [N_2, C1, C2, C3] =[25.66, 33.41, 23.9, 17.03]	0.796
Yoon et al., 2009		S	[5, 32]	Precooling: N.F. Liquefaction: N.F.	Precooling: [N.F., N.F., …, −35] Liquefaction: [N.F., N.F., …, −160]	Precooling: [3, N.A.] Liquefaction: [1, 1]	Precooling: [C3]=[100] Liquefaction: [N_2, C1, C2, C3] =[2, 44, 39, 15]	0.26
Castillo and Dorao, 2013		S	[4, N.F.]	Precooling: N.F. Liquefaction: [0.54, N.F.,⋯, 4.8]	Precooling: [1, N.F., …, −36] Liquefaction: [1, N.F., …, −154.4]	Precooling: [3, N.A.] Liquefaction: [1, 1]	Precooling: [C3]=[100] Liquefaction: [N_2, C1, C2, C3] =[8, 45, 45, 2]	N.F.
Pereira and Lequisiga, 2014		S	[4, 30]	Precooling: N.F. Liquefaction: N.F.	Precooling: [N.F., N.F., …, −35] Liquefaction: [N.G, N.F., −160]	Precooling: [3, N.A.] Liquefaction: [1, 1]	Precooling: [C3]=[100] Liquefaction: N.F.	0.276[b]
Helgestad, 2009		S	[4, 30]	Precooling: [0.126, 0.257, 0.483, N.F.] Liquefaction: [0.54, 2.296, 3.383, 4.8]	Precooling: [0.5, N.F., …, −36] Liquefaction: [0.5, N.F., −156.9]	Precooling: [3, N.A.] Liquefaction: [1, 1]	Precooling: [C3]=[100] Liquefaction: [N_2, C1, C2, C3] =[8, 45, 45, 2]	0.307

To be continued

Table 7

Reference	Process	Study type	NG feed conditions, [p_{NG} (MPa), T_{NG} (°C)]	Compression/ expansion stage pressures, [p_{low}, $p_{interstage}$, p_{high}] (MPa)	Temperatures, [MITA, T_{stage1}, …, T_{stagen}][a] (°C)	Numbers of [evaporating pressure level, separation stage]	Mole percent of MR (%)	SPC (kW·h/kg)
Alabdulkarem et al., 2011	PR-VCRC precooled MR1V	S	N.F.	Precooling: [0.253, 0.406, 0.618, 0.882, 1.54] Liquefaction: [0.451, 2.346, 4.137]	Precooling: [3, 22, 9, −5, −19, −33] Liquefaction: [3, N.F., −160]	Precooling: [4, N.A.] Liquefaction: [1, 1]	Precooling: [C3]=[100] Liquefaction: [N_2, C1, C2, C3] =[8, 45, 45, 2]	0.283
Wang MQ et al., 2012		S	N.F.	Precooling: N.F. Liquefaction: [0.1, 0.35, 1.026, 2.962, 5.5]	Precooling: [N.F., N.F., …, −40] Liquefaction: [2/7.28, −128.7, −160]	Precooling: [3, N.A.] Liquefaction: [1, 1]	Precooling: [C3]=[100] Liquefaction: [N_2, C1, C2]= [8, 46, 46]	N.F.
Khan et al., 2013		S	[5, 32]	Precooling: N.F. Liquefaction: [0.16, N.F., 4.65]	Precooling: [N.F., 12.45, −12.59, −33.34] Liquefaction: [3, −137.1]	Precooling: [3, N.A.] Liquefaction: [1, 1]	Precooling: [C3]=[100] Liquefaction: optimized [N_2, C1, C2, C3]= [21.8, 40.75, 33.22, 23.86]	0.278
Lee et al., 2015		S	[6.26, 15]	Precooling: [0.13, 0.234, 0.376, 0.646, 1.36] Liquefaction: [0.39, 0.957, 1.725, 2.968, 5.06]	Precooling: [3, N.F., …, −33.34] Liquefaction: [3, −137.1]	Precooling: [3/4, N.A.] Liquefaction: [1, 1]	Precooling: [C3]=[100] Liquefaction: [N_2, C1, C2, C3] =[5.86, 46.93, 33.93, 13.28]	0.273
Sanavandi and Ziabasharhagh, 2016		S	[5.5, 25]	Precooling: N.F. Liquefaction: [N.F., …, 4]	Precooling: [N.F., −1.5, −22.5, −42] Liquefaction: N.F.	Precooling: [3, N.A.] Liquefaction: [1, 1]	Precooling: [C3]=[100] Liquefaction: optimized [N_2, C1, C2, C3, i-C4, n-C4]= [7.6, 38.4, 46.74, 4.77, 1.8, 7]	0.259
Song et al., 2019		S	[6.5, 27]	Precooling: N.F. Liquefaction: [0.3, …, 4.86]	Precooling: [N.F., N.F., …, −33] Liquefaction: [3, N.F., −160]	Precooling: [N.F., N.A.] Liquefaction: [1, 1]	Precooling: [C3]=[100] Liquefaction: optimized [N_2, C1, C2, C3]= [7.14, 41.20, 31.21, 20.45]	0.252
Hatcher, 2012[c]	PR-VCRC precooled MR2V (C3MR)	S	[4.2, 38]	Precooling: N.F. Liquefaction: [≈0.526, 2.578, 2.689]	Precooling: N.F. Liquefaction: [N.F., −99.2, −136.6, N.F.]	Precooling: [3, N.A.] Liquefaction: [1, 2]	Precooling: [C3]=[100] Liquefaction: optimized [N_2, C1, C2, i-C4]=[7.3, 36.1, 48.8, 7.7]	N.F.

To be continued

Table 7

Reference	Process	Study type	NG feed conditions, [p_{NG} (MPa), T_{NG} (°C)]	Compression/ expansion stage pressures, [p_{low}, $p_{interstage}$, p_{high}] (MPa)	Temperatures, [MITA, T_{stage1}, …, T_{stagen}]^a (°C)	Numbers of [evaporating pressure level, separation stage]	Mole percent of MR (%)	SPC (kW·h/ kg)
Wang MY et al., 2013[d]	PR-VCRC precooled MR2V (C3MR)	S	[5, 25]	Precooling: [N.F., …, 1.098] Liquefaction: [N.F., …, 2.633]	Precooling: [N.F., N.F., …, −35] Liquefaction: [5, N.F., …, N.F.]	Precooling: [3, N.A.] Liquefaction: [1, 2]	Precooling: [C3]=[100] Liquefaction: optimized [N_2, C1, C2, C3, i-C4] =[7.31, 35.81, 49.02, 0.03, 7.84]	0.408
Wang MY et al., 2014[c]		S	[5, 25]	Precooling: [N.G., …, 1.086] Liquefaction: [N.F., …, 2.547]	Precooling: [N.F., N.F., …,−35] Liquefaction: [N.F., −98.6, −144.3, N.F.]	Precooling: [3, N.A.] Liquefaction: [1, 2]	Precooling: [C3]=[100] Liquefaction: optimized [N_2, C1, C2, C3, i-C4] =[7.42, 47.98, 35.64, 8.65, 0.32]	0.358
Bin Omar et al., 2012	AP-X	S	[2, N.F.]	Precooling: N.F. Liquefaction: [1, 2.1, 3.8] Subcooling: [1.1, 6.7]	Precooling: [N.F., N.F., …, −30] Liquefaction: [0.3/6.4, −99.2, −136.6, N.F.] Subcooling: [2.1/17.7, −166]	Precooling: N.F. Liquefaction: [1, 1] Subcooling: [1, N.A.]	Precooling: [C3]=[100] Liquefaction: [N_2, C1, C2, C3, i-C4, n-C4]=[1.4, 34.3, 39.5, 0.6, 9.1, 15.1] Subcooling: [N_2]=[100]	N.F.
Sun et al., 2016		S	[5, 30]	Precooling: [N.F., 0.311, 0.582, 1.2] Liquefaction: [0.433, N.F., 3.009] Subcooling: [1.904, 6.76]	Precooling: [3, N.F., …, −30] Liquefaction: [3, −105] Subcooling: [3, −151]	Precooling: [3, N.A.] Liquefaction: [1, 0] Subcooling: [1, N.A.]	Precooling: [C3]=[100] Liquefaction: optimized [C1, C2=, C3]=[20.01, 63.25, 16.74] Subcooling: [N_2]=[100]	0.248
Venkata-rathnam, 2008[e]	MR-VCRC precooled MR1V (DMR)	S	[6.5, 27]	Precooling: [0.37, 0.67, 2.18] Liquefaction: [0.3, N.F., …, 4.86]	Precooling: [3, −33] Liquefaction: [3, −160]	Precooling: [1, N.A.] Liquefaction: [1, 1]	Precooling: optimized [C2, C3, n-C4]= [45.47, 4.94, 49.59] Liquefaction: optimized [N_2, C1, C2, C3]=[7, 41.8, 29.9, 21.3]	N.F.
Venkata-rathnam, 2008[f]		S	[6.5, 27]	Precooling: [0.28, 0.76, 1.92] Liquefaction: [0.3, N.F., …, 4.86]	Precooling: [3, 0, −33] Liquefaction: [3, −160]	Precooling: [2, N.A.] Liquefaction: [1, 1]	Precooling: optimized [C2, C3, n-C4]= [24.82, 64.16, 11.03] Liquefaction: optimized [N_2, C1, C2, C3]=[7, 41.8, 29.9, 21.3]	0.248[g]

To be continued

Table 7

Reference	Process	Study type	NG feed conditions, [p_{NG} (MPa), T_{NG} (°C)]	Compression/ expansion stage pressures, [p_{low}, $p_{interstage}$, p_{high}] (MPa)	Temperatures, [MITA, T_{stage1}, …, T_{stagen}][a] (°C)	Numbers of [evaporating pressure level, separation stage]	Mole percent of MR (%)	SPC (kW·h/ kg)
Gou et al., 2015	MR-VCRC precooled MR1V (DMR)	S	[5, 25]	Precooling: [0.15, N.F., 1.8] Liquefaction: [0.165, N.F., 2.4]	Precooling: [N.F., −51] Liquefaction: N.F.	Precooling: [1, N.A.] Liquefaction: [1, 1]	Precooling: optimized [C2, C3, n-C4, i-C5]=[29, 51, 16, 3] Liquefaction: optimized [N_2, C1, C2, C3]=[5, 38, 40, 17]	0.357
Ansarinasab and Mehr-pooya, 2017b		S	[6.3, 37]	Precooling: [0.3, 0.76, 1.92] Liquefaction: [0.3, N.F., …, 4.86]	Precooling: [0.5, 3, −33] Liquefaction: [0.5, −128, −160.1]	Precooling: [2, 1] Liquefaction: [1, 1]	Precooling: N.F. Liquefaction: N.F.	0.375
Hwang et al., 2013		S	[6.5, 27]	Precooling: [0.285, 0.77, 1.92] Liquefaction: [0.3, N.F., …, 4.86]	Precooling: [3, N.F., −23] Liquefaction: [3, N.F., −160]	Precooling: [2, N.A.] Liquefaction: [1, 1]	Precooling: optimized [C2, C3, n-C4]= [22.02, 65.3, 12.68] Liquefaction: optimized [N_2, C1, C2, C3]= [6.5, 42.5, 29.8, 21.2]	0.245
Wang MY et al., 2014[c]		S	[5, 25]	Precooling: [N.F., …, 1.283] Liquefaction: [N.F., …, 3.386]	Precooling: [N.F., −33] Liquefaction: [N.F., −115.9, N.F.]	Precooling: [1, N.A.] Liquefaction: [1, 1]	Precooling: optimized [N_2, C1, C2, C3, i-C4, n-C4]=[0.4, 2.07, 33.85, 24.08, 1.61, 37.99] Liquefaction: optimized [N_2, C1, C2, C3, i-C4] =[7.29, 42.44, 44.35, 0.1, 5.81]	0.313
Ghorbani et al., 2017	ACR precooled MR1V process	S	[6.31, 37]	Precooling: N.A. Liquefaction: [0.2, 2.2, 3.8]	Precooling: [1.7, −33] Liquefaction: [2.4/2, −119, −165]	Precooling: [1, N.A.] Liquefaction: [1, 1]	Precooling: N.A. Liquefaction: [N_2, C1, C2, C3]=[25.6, 33.4, 23.9, 17.1]	0.257
Ansarinasab and Mehr-pooya, 2017a		S	[6.5, 26.85]	Precooling: N.A. Liquefaction: [0.3, 2.5, 4.86]	Precooling: [3.18, −26.37] Liquefaction: [6.22/3.69, −128.45, −160.15]	Precooling: [1, N.A.] Liquefaction: [1, 1]	Precooling: N.A. Liquefaction: [N_2, C1, C2, C3]=[7, 41.8, 29.9, 21.3]	0.207

[a]: T_{stagen}: the temperature of the hot MR or NG stream out from the *n*th HEX in the precooling, liquefaction, or subcooling stages; [b]: SPC converted from 5.83 kW·h/MMBTU-LNG, taking 1 MMBTU-LNG≈27 Nm^3; [c]: results with the total shaft work as the objective function; [d]: results with the new exergy efficiency expression as the objective function; [e]: single evaporating pressure in the precooling stage; [f]: double evaporating pressures in the precooling stage; [g]: SPC obtained from Hwang et al. (2013)

Fig. 37, in which the exergy destruction was related mainly to the HEXs and multi-stage compression of the liquefaction cycle. Sun et al. (2016) minimized the power consumption of the AP-X process using the GA method based on a simplified configuration (ignoring the separator in the MR loop). In their optimizations, they considered not only the MR composition, but also the choice of refrigerant in the expander cycle. Results showed that pure N_2 remained a better choice than an N_2-CH_4 mixture. The optimum SPC reached 0.247 kW·h/kg, which was 15.62% lower than that of a typical C3MR (C_3H_8 precooled MR1V) process. Detailed operating parameters are listed in Table 7.

4.2.1.2 Multi-cycle MR*x*V processes with MR-VCRC precooling (MR-VCRC precooled MR*x*V processes)

PR-VCRV precooled MR*x*V processes had performed better when the temperature differences were reduced from ambient to about −30 °C. However, because of the property of pure C_3H_8, their temperature profile was actually a zigzag in this section, as a result of the multiple evaporating pressures. Here came the chance for MR to improve the temperature match in the precooling section. Similar to the MR-VCRC precooled MR0V processes discussed in Section 4.1.1, MR-VCRV precooled MR*x*V processes make up another kind of DMR process. The use of MR precooling leads not only to a better temperature match, but also to more abundant precooling cycle configurations. Note that there are usually fewer than two MR separators in the liquefaction stage of this kind of DMR process.

Krieger (1978) came up with an MR-VCRC precooled MR2V process (Fig. 38), which is cascaded by a basic refrigeration cycle operating with MR and an auto-cascade refrigeration cycle with two separators. Though a separator is used in the precooling cycle, it separates the gaseous and liquid phases for further pressure elevation. The separated phases mix again to restore the original composition before entering the precooling HEX, as in the PRICO process. NG and low-level MR are both cooled in the precooling HEX. The Linde-Hampson refrigeration cycle with MRs and a single evaporating pressure were also seen in the precooling stage of processes developed by Garier and Paradowski (1981) and Caetani and Paradowski (1982), except that the high-level MR dealt only with the heat load of the low-level MR.

Auto-cascade refrigeration cycles have also been applied in the precooling stage (Förg, 1978; Liu and Pervier, 1985; Newton, 1985; Liu and Newton, 1988). Taking the proposal of Newton (1985) in Fig. 39 as an example, an auto-cascade refrigeration cycle with one separator and three evaporating pressure levels provides precooling for the low-level MR, while another auto-cascade refrigeration cycle with one separator and a single pressure level provides refrigeration for the NG. The BOG from the LNG tank is reheated by a portion of the separated vapor in the liquefaction stage to serve as fuel. Thus, the cold energy of the BOG is recovered to reduce the total energy consumption.

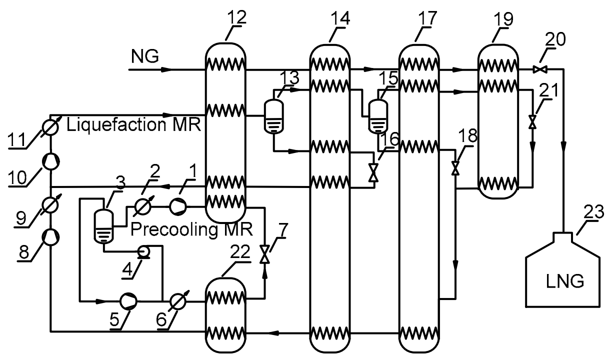

Fig. 38 A multi-cycle MR*x*V process adapted from Krieger (1978)

1, 5, 8, 10: compressors; 2, 6, 9, 11: condensers; 3: precooling MR separator; 4: pump; 7, 16, 18, 20, 21: expansion valves; 12, 14, 17, 19, 22: HEXs; 13, 15: liquefaction MR separators; 23: storage tank

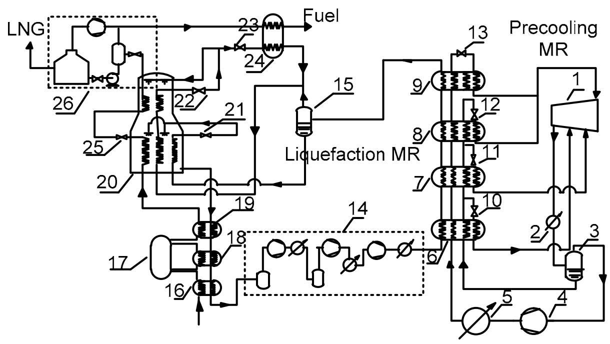

Fig. 39 A multi-cycle MR*x*V process adapted from Newton (1985)

1, 4, 14: compressors (and after-coolers); 2, 5: condensers; 3: precooling MR separator; 6, 7, 8, 9, 16, 18, 19, 20, 24: HEXs; 10, 11, 12, 13, 21, 22, 23, 25: expansion valves; 15: liquefaction MR separator; 17: purifying units; 26: LNG storage and relevant components

From the above configurations, we found that there were several factors to be considered in the construction of an MR-VCRC precooled MR*x*V process, such as the number of evaporating pressure levels in both the precooling and liquefaction stages, the use of component separation in the precooling cycle, and the part of the heat load that the precooling cycle should deal with. Roberts and Agrawal (2001a) considered it better when NG and the low-level MR were both precooled by the high-level MR in the same HEX, as in Fig. 38. If NG exchanged heat only with the low-level MR, additional HEXs would be required, like the series of HEXs (Fig. 39, items 16, 18, and 19). Regarding the number of evaporating pressure levels, Roberts and Agrawal (2001a) considered that a single pressure was preferable, because the mixing of non-equilibrium MR streams of different composition in the compression stages would cause thermodynamic irreversibility if a multi-pressure arrangement was adopted. However, an exergy analysis by Venkatarathnam (2008) indicated that a double pressure arrangement would actually reach a higher exergy efficiency of the precooling cycle than a single pressure one. There have been few comparisons of configurative selections in the literature, and this aspect is worthy of further investigation.

Similarly, studies of MR-VCRC precooled MR*x*V processes have centered on performance analyses and comparisons (Nibbelke et al., 2002; Gou et al., 2015; Ansarinasab and Mehrpooya, 2017b), as well as attempts to find optimum operating parameters (Venkatarathnam, 2008; Hwang et al., 2013; Wang MY et al., 2014; Gou et al., 2015). Available operating parameters from the abovementioned studies are summarized in Table 7.

Similar to the C3MR process, the DMR process also encountered a bottleneck of LNG production in large-scale applications. To break through the limitations originating from key equipment fabrication, APCI came up with the AP-X process by adding a subcooling stage to a C3MR process, while Nagelvoort (2002) from Shell put forward an alternative solution. He considered adding another liquefaction stage in parallel connection with the original in either the C3MR or DMR process. The DMR process was preferred due to its flexibility in MR composition and proven better efficiency (Buijs et al., 2005). The precooling refrigerant is evaporated in HEXs (Fig. 40, items 4a, 4b, and 4c) to cool the two streams of liquefaction MRs and NG. Precooled NG is divided into two streams in a distributor (item 5), and then enters two liquefaction stage HEXs (items 9a and 9b) to be liquefied.

Shell's solution was developed and is now known as the parallel mixed refrigerant (PMR) process. The precooling liquefaction temperatures are usually designed as −25 and −150 °C (Pek et al., 2004). Three well-proven GE Frame 7 gas turbines were selected as the driving force for MR compressors, increasing the LNG production to 8 MTPA. The mature technologies used in the PMR process are helpful in providing robustness and high liquefaction efficiency in large-scale LNG systems, as well as high reliability of continuous operation where the LNG production is expected to be 60% during the failure of one liquefaction stage (Pek et al., 2004; Buijs et al., 2005, 2006). The Shell PMR process was first applied industrially in the Pluto LNG plant in Australia. However, there have been few published analyses of the performance of this process.

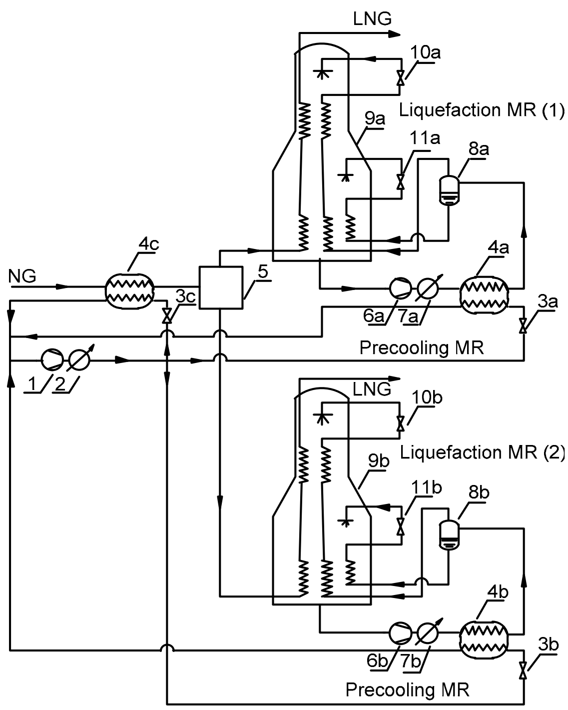

Fig. 40 A PMR process adapted from Nagelvoort (2002)
1, 6a, 6b: compressors; 2, 7a, 7b: condensers; 3a, 3b, 3c, 10a, 10b, 11a, 11b: expansion valves; 4a, 4b, 4c: precooling stage evaporators; 5: distributor; 8a, 8b: liquefaction stage MR separator; 9a, 9b: HEXs

4.2.1.3 Multi-cycle MR*x*V processes with ARC precooling (ARC precooled MR*x*V processes)

In pursuit of better thermodynamic performance of MR*x*V processes, PR-VCRC and MR-VCRC precooling provided solutions by reducing the temperature differences in warmer temperature zones, but they still consumed only electrical power. Recently, there has been a growing trend for using ARCs in the precooling stages of NGLPs, which can be driven by low-grade waste heat. Hence, a part or all of the precooling capacities come from the heat of exhaust gases from the turbines, which drive the MR compressors. The use of ARC in a modified MFC process (multi-cycle MR0V process) was briefly introduced in Section 4.1.1, and can be more widely seen in multi-cycle MR*x*V processes, especially C3MR processes.

In our literature survey, such an idea could be traced back to the proposal by Davis and Newton (1990), which involved adding an NH_3-H_2O ARC to an MR-VCRC precooled MR1V process (Fig. 41). The ARC is driven by ducting the turbine exhaust gas to the generator, and produces refrigeration for NG before purification, and for both high-level and low-level MRs after each condensation. After the deep flash system (Fig. 41, item 19), a portion of the BOG is recycled and cooled again, while the remainder serves as fuel for driving the MR compressors. A preliminary

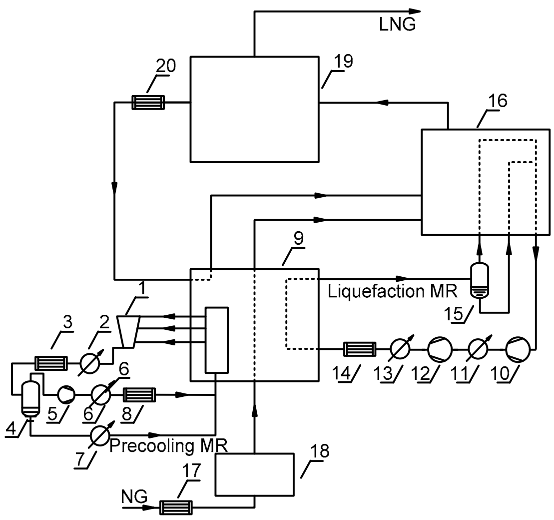

Fig. 41 A multi-cycle MR1V process adapted from Davis and Newton (1990)
1, 5, 10, 12: compressors; 2, 6, 7, 11, 13: condensers; 3, 8, 14, 17, 20: ARC evaporators; 4: precooling stage MR separator; 9, 16: HEXs; 15: liquefaction stage MR separator; 18: drying and Hg removal unit; 19: deep flash system

simulation showed that the new cycle brought about a 16.4% energy efficiency lift compared with the original multi-cycle MR1V process.

Recent studies have focused on the optimum ways of coupling ARCs. Kalinowski et al. (2009) compared a double-lift NH_3-H_2O ARC and two serially connected single-effect NH_3-H_2O ARCs in an attempt to replace the C_3H_8 VCRCs in a C3MR process at 18 °C and −42 °C. Simulation results showed that the two single-effect cycles could provide enough cooling loads at both temperatures with a total COP of 0.41, while the double-lift cycle, though having a higher COP of 0.47, could provide enough cooling loads only at 18 °C, and only part of the cooling loads at −42 °C. Mortazavi et al. (2008) summarized typical waste heat sources and their possible applications in LNG plants, and put forward two strategies for waste heat use of turbine exhaust gases based on the C_3H_8 VCRC precooled MR1V process (APCI C3MR process). The first strategy involves subcooling C_3H_8 after the condenser, as introduced by Davis and Newton (1990), while the second is an indirect way to reduce the C_3H_8 condensing pressure by precooling the cooling water. These two strategies were further studied by Rodgers et al. (2012). Simulations showed respective increases of 13% and 63% in the COPs of C_3H_8 VCRCs enhanced by each strategy. They also evaluated the cooling capacities of single-effect, double-effect, and cascaded single- and double-effect LiBr-H_2O ARCs, and presented their availability in the enhanced precooling cycles under both part-load and full-load conditions. Mortazavi et al. (2010) further compared eight different options for APCI C3MR process enhancement with a double-effect LiBr-H_2O ARC working at 22 °C and 9 °C. The options included replacing the original C_3H_8 evaporators or providing refrigeration at some points in C_3H_8 or MR loops. They found the largest reduction in fuel consumption was obtained when the ARC evaporators were used to replace both C_3H_8 evaporators at 22 °C and 9 °C, and to provide additional cooling after the C_3H_8 condensers and after inter-stage MR compression at the same time. Though it is a very complex enhancement strategy, a small efficiency improvement in large-scale plants would result in a considerable energy-saving. The overall performance of ARC precooled MR*x*V processes was evaluated in a few studies. Ghorbani et al. (2017) reported the replacement of ARC in a DMR process helped it reach an SPC of 0.25 kW·h/kg, representing a 24.2% reduction compared to the original DMR process. However, the exergy efficiency of the modified DMR process was not improved, because the ARC provided precooling only at a fixed temperature, resulting in larger gaps between the hot and cold composite curves in the precooling section. Using conventional and advanced exergoeconomic analyses, Ansarinasab and Mehrpooya (2017a) presented a complicated evaluation of the ARC precooled MR1V process, and commented on future improvement from thermodynamic and economic perspectives.

Subject to the configurations of existing NGLPs and the temperature levels that ARCs usually can provide, the patterns of replacement or addition of ARCs based on multi-cycle MR*x*V processes are limited, as mentioned above. Unfortunately, many studies focused more on the performance of ARCs, and only a few conducted thorough analyses of the whole modified MR-NGLPs. Therefore, only two sets of operational parameters and performance indicators of ARC precooled MR*x*V processes are listed in Table 7. No experimental study was found.

4.2.2 Multi-cycle MR*x* processes with not only JT expansion in the liquefaction stage (multi-cycle MR*x*E processes)

In Section 3.2.2, a few cases of single-cycle MR*x*E processes were introduced, which established the foundation for multi-cycle processes. Precooling cycles usually act as a refrigeration supplement in the few cases of multi-cycle MR*x*E processes in which configurations have not yet been highlighted.

Based on his proposal of a single-cycle MR1E process introduced in Section 3.2.2, Paradowski (1982) also came up with a modification involving adding an MR-VCRC precooling stage to a single-cycle MR2E process (Fig. 42). The low-level MR is further cooled by the high-level MR before entering separators. In particular, the expansion units in the precooling cycle are also hydraulic turbines. This modification appears in his other designs that use hydraulic turbines, but it remains to be tested in practical applications.

Herron and Chatterjee (1990) proposed a similar MR-VCRC precooled MR1E process (Fig. 43), using the expansion work to further pump or compress the same liquid or gaseous streams prior to cooling. Such use of expansion work requires mechanical coupling of the expander/hydraulic turbine and gas compressor/liquid pump, which enables a 1.5% increase in

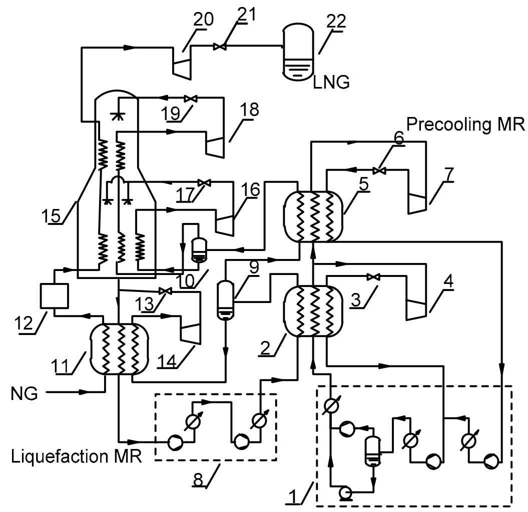

Fig. 42 A multi-cycle MR2E process adapted from Paradowski (1982)

1, 8: multi-stage compressors and after-coolers; 2, 5, 11, 15: HEXs; 3, 6, 13, 17, 19, 21: additional expansion valves; 4, 7, 14, 16, 18, 20: cryogenic hydraulic expansion turbines; 9, 10: liquefaction stage MR separators; 12: NG treatment unit; 22: LNG storage tank

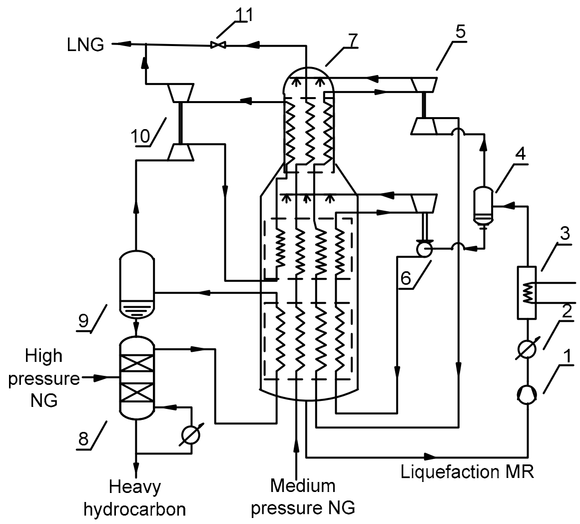

Fig. 43 A multi-cycle MR1E process adapted from Herron and Chatterjee (1990)

1: liquefaction stage compressor; 2: liquefaction stage condenser; 3: precooling stage evaporator; 4: liquefaction stage MR separator; 5, 6, 10: expanders linked with the compressor or pump; 7: HEX; 8: NG scrub column; 9: NG separator; 11: expansion valve liquefaction capacity under constant power consumption, or helps reduce power consumption by 6.3% under constant liquefaction capacity.

We found two cases of open type multi-cycle MR*x*E processes in our literature survey. Foglietta (1998) proposed to obtain 75% of the cooling capacity by NG expansion and 25% by a two-stage C_3H_8 VCRC (Fig. 44). Generally, a portion of NG above 6 MPa, which is cooled to −40 °C in the HEX (Fig. 44, item 4), is extracted to be expanded to a two-phase fluid of 1.4 MPa and −112 °C in the expander (item 9). The two-phase fluid is then separated or rectified in the MR (NG) separator (item 10) to produce a light vapor and a heavy liquid. The liquid is further expanded in the expansion valve (item 11) and releases its coolness in the HEX (item 4), while the gas is cooled in the HEX (item 4) and recompressed to join the recycle stream. The remaining portion of NG continues going through the HEX (item 4) to −112 °C and passes through an expansion valve to reach −156 °C at atmospheric pressure (Foglietta, 1999). Unliquefied gas in the NG separator (item 7) is also recovered as a recycle stream. Due to the separation and recycling, there is a difference in composition between the portion of NG that serves as the refrigerant at the compressor outlet and the expander outlet. However, the ratio of extraction was not stated clearly.

The other case was an MR precooled MR1E process (Fig. 45) put forward by Maunder and Skinner (2003, 2007). In this process, an NG feed, slightly lower than its critical pressure, is cooled to −20–−40 °C in the first HEX (Fig. 45, item 1) and goes through an MR (NG) separator (item 2), from which the liquid is expanded in a valve (item 6) as the natural gas liquid (NGL) by-product after recovering its cooling capacity. The separated vapor is mixed with the recycled gas and cooled to slightly higher than its dew point in the next HEX (item 3) before entering the expander (item 4). The expanded mixture is separated again in a separator (item 5), from which the liquid is extracted as LNG product, while the vapor is recycled as the refrigerant. The first and second separations both lead to a composition shift in the refrigerant. Another closed type MR0V cycle is adopted to provide additional cooling capacity down to a temperature of −100 °C, operating with another set of MRs derived from the NGL by-product. Analysis results showed that the net power consumption was increased by 5% when the expander inlet temperature was 1 °C above the dew point, so the expander inlet temperature should be maintained close to the dew point, but not below it.

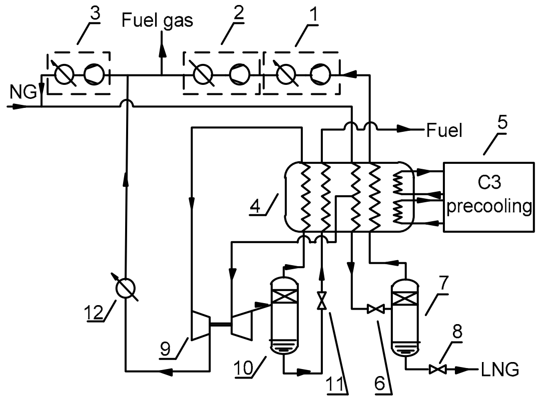

Fig. 44 A multi-cycle MR1E process adapted from Foglietta (1998)

1, 2, 3: 1st–3rd recycle compressors and condensers; 4: HEX; 5: C_3H_8 precooling system; 6, 8, 11: expansion valves; 7: NG separator or distillation column; 9: expander linked with booster compressor; 10: MR (NG) separator or distillation column; 12: condenser

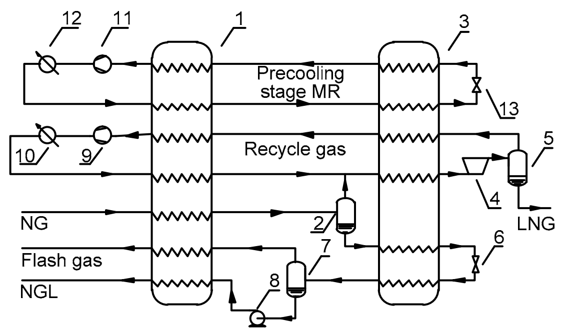

Fig. 45 A multi-cycle MR1E process adapted from Maunder and Skinner (2007)

1, 3: HEXs; 2, 5: MR (NG) separators; 4: expander; 7: NG separator; 6, 13: expansion valves; 8: pump; 9, 11: compressors; 10, 12: condensers

For multi-cycle MR*x*E processes, simulation results were reported only in one paper (Foglietta, 1999). Detailed operating parameters are summarized in Table 8.

4.2.3 Discussion

Multi-cycle MR*x*V and MR*x*E processes were introduced in Sections 4.2.1 and 4.2.2.

Table 8 Available operating parameters from studies of multi-cycle MRxE processes

Reference	Process	Study type	NG feed conditions, [p_{NG} (MPa), T_{NG} (°C)]	Expansion stage pressures, [p_{low}, $p_{interstage}$, p_{high}] (MPa)	Temperatures, [MITA, T_{stage1}, …, T_{stagen}][a] (°C)	Numbers of [evaporating pressure level, separation stage]	Mole percent of MR (%)	SPC (kW·h/kg)
Foglietta, 1999	Open type multi-cycle MR1E	S	[6.79, 37.78]	Precooling: N.F. Liquefaction: [1.38, 6.8]	Precooling: [N.F., 1.7, −37.2] Liquefaction: [N.F., −112.2]	Precooling: [2, N.A.] Liquefaction: [1, 1]	Precooling: [C3]=[100] Liquefaction: [NG]=[CO_2, N_2, C1, C2, C4, C5]=[0.53, 0.51, 95.15, 3.05, 0.61, 0.12, 0.03]	N.F.

The multi-cycle MRxV processes include PR-VCRC precooled types (30 references), MR-VCRC precooled types (18 references), and ARC precooled types (7 references). Most attention has been paid to the first two types. Among the PR-VCRC precooled MRxV processes, C_3H_8 was the most commonly studied, and also the most adopted in the NG liquefaction industry (C3MR process). In C3MR processes, the liquefaction MRs were suggested to contain 50%–60% of N_2+CH_4. Their simulated SPCs lay in the range of 0.234–0.408 kW·h/kg. As for the MR-VCRC precooled MRxV processes (the DMR processes), the liquefaction MRs usually required nearly 50% of N_2+CH_4, while the composition of precooling MRs varied greatly among studies. The simulated SPCs of the DMR processes lay mainly in the range of 0.245–0.375 kW·h/kg, a level similar to that of the C3MR processes. ACRs were also found to serve the precooling purpose well. Without electricity consumption in the precooling stage, ACR precooled MRxV processes had more competitive SPCs, ranging from 0.207–0.257 kW·h/kg. N_2+CH_4 in their liquefaction MRs also accounted for 50%–60%.

In comparison, there were far fewer multi-cycle MRxE processes (6 references), most of which were patented designs. There were no comprehensive simulations or practical applications, so it was difficult to sum up operational parameters and SPC ranges. Specific studies on the precooling cycles were rarely found in the multi-cycle MRxE processes, which were usually added to provide additional cooling capacity.

In multi-cycle MRxV and MRxE processes, multiple compression and evaporating pressures were both adopted. Multiple evaporating pressures were more often used in precooling stages. There were contrary opinions on whether single or multiple evaporating pressures should be used in the precooling stage; therefore, more convincing studies are needed.

Open type processes were not found in multi-cycle MRxV processes. There may be no great advantage in adding an extra precooling cycle to open type single-cycle MRxV processes. Two cases of open type multi-cycle MRxE processes were found, both currently without practical applications.

5 Current summary and future potential

From the literature discussed above, various MR-NGLPs were introduced and categorized based on the proposed novel classification framework. The characteristics of typical MR-NGLPs in each category are summarized and listed in Table 9, including their representative processes, SPC ranges, relevant literature, research maturity, MR component selections, features, and applications. In particular, these processes were graded according to the lower limits of their simulated SPC ranges (low: SPC≤0.25 kW·h/kg; medium: 0.25 kW·h/kg<SPC≤0.5 kW·h/kg; high: SPC>0.5 kW·h/kg). The comparison among these MR-NGLPs led to several findings:

1. MR components and composition varied among different MR-NGLP configurations. In closed type MR0V and MRxV processes, N_2 and HCs (C1–C5) were universally adopted as the MR. In closed type MR0E and MRxE processes, the above MRs were also used occasionally, but a mixture of N_2 and CH_4 was mainly used. In open type MR0 and MRx processes, NG itself was often used as the MR, as well as a mixture of NG and some existing components. The patterns that could be obtained from

Table 9 Summaries of MR-NGLPs in this paper

Category			Representative process	SPC range and grade[a] (kW·h/kg)	Number of publications	Research maturity[b]	Mixed refrigerant	Feature and applications
Single-cycle MR-NGLPs	Single-cycle MR0 process	Single-cycle MR0V process	PRICO process	0.27–0.4 (S), medium 1.35–1.81 (E)	33	Commercialized	N_2-HC (N_2+C1: 30%–45%)	Simple structure and low cost Suitable for small-scale to medium-scale plants, or those insensitive to power consumption
		Single-cycle MR0E process	N_2-CH_4 expander process	N_2-HC: 0.318–0.399 (S), medium N_2-CH_4: 0.567–1.317 (S), high	13	Only theoretical researches	N_2-CH_4 (N_2: 40%–74%) N_2-HC (N_2>35%) NG	With expander: simple structure and easy start-up, but high initial cost and sensitive to the dryness Suitable for offshore plants, pipeline pressure energy utilization and plants insensitive to power consumption With vortex tube: no moving parts itself and lower initial cost than expanders Suitable for pipeline pressure energy utilization
	Single-cycle MR*x* process	Single-cycle MR*x*V process	With phase separators: Kleemenko process	0.243–0.411 (S), low-medium 0.65 (E)	18	Commercialized	N_2-HC (N_2+C1≈35%)	Simple structure, low initial cost for single-cycle MR*x*V processes when separators were fewer than 3 Suitable for small-scale to medium-scale plants, or those insensitive to power consumption
			With rectifying units: MRrV process with a rectifying column	0.846 (S), high 0.69–1.61 (E)	10	Both theoretical and experimental researches	N_2-HC (N_2+C1≈40%)	
		Sigle-cycle MR*x*E process	MR2E process with an expander in place of the last expansion valve	1.029 (S), high	3	Only theoretical studies	N_2-HC	With expander: same as the single-cycle MR0E processes with expanders, but rarely reported With ejector: low initial cost and lifting compressor suction pressure Both suitable for small-scale to medium-scale plants

To be continued

Table 9

Category			Representative process		SPC range and grade[a] (kW·h/kg)	Number of publications	Research maturity[b]	Mixed refrigerant	Feature and applications
Multi-cycle MR-NGLPs	Multi-cycle MR0 process	Multi-cycle MR0V process	Two-cycle	DMR process	0.296–0.34 (S), medium 0.753 (E)	7	Commercialized	Precooling: halogenated HC/HC (C2+C3: 50%–60%) Liquefaction: N_2-HC (N_2+C1: 40%–50%)	Lower power consumption and larger production than the single-cycle MR0V process, but higher initial cost Suitable for medium-scale to large-scale plants, hereinto MFC especially suitable for plants in cold climate
			Three-cycle	MFC process	0.169–0.266 (S), low	12	Commercialized	Precooling: HC (C2+C3>80%) Liquefaction: HC (C1: 5%–10%, C2>60%) Subcooling: N_2-HC (N_2+C1>60%)	
		Multi-cycle MR0E process	C_3H_8 precooled N_2-CH_4 expander process		0.369–0.774 (S), medium	5	Only theoretical studies	Precooling: C3 Liquefaction: N_2-CH_4	Same as the single-cycle MR0E process
	Multi-cycle MRx process	Multi-cycle MRxV process	PR-VCRV pre-cooling	APCI C3MR process	0.234–0.408 (S), low	23	Commercialized	Precooling: C3 Liquefaction: N_2-HC (N_2+C1: 50%–60%)	For MRxV processes precooled by compression refrigeration cycle: Smaller temperature differences between the hot and cold streams in the precooling stages, lower power consumption and larger LNG production than the single-cycle MRxV processes, but high initial cost and complexity Suitable for large-scale plants (typical production: C3MR: around 5MTPA AP-X: 7–10 MTPA DMR: slightly larger than C3MR PMR: up to 8 MTPA). For MRxV processes precooled by ARC: Full utilization of waste heat, but needing for both cleanliness and continuity of exhaust gas
				APCI AP-X process	0.248 (S), low	7	Commercialized	Precooling: C3 Liquefaction: N_2-HC Subcooling: N_2	
			MR-VCRC pre-cooling	Shell DMR process	0.245–0.375 (S), low	14	Commercialized	Precooling: HC Liquefaction: N_2-HC (N_2+C1≈50%)	
				Shell PMR process	–	4	Commercialized	Precooling: HC Liquefaction: N_2-HC	

To be continued

Table 9

Category			Representative process	SPC range and grade[a] (kW·h/kg)	Number of publications	Research maturity[b]	Mixed refrigerant	Feature and applications
Multi-cycle MR-NGLPs	Multi-cycle MR*x* process	Multi-cycle MR*x*V process	ACR precooling –	0.207–0.257 (S), low	7	Only theoretical studies	Precooling: NH_3-H_2O/LiBr-H_2O Liquefaction: N_2–HC (N_2+C1: 50%–60%)	Suitable for occasions with continuous waste gas such as gas turbines
		Multi-cycle MR*x*E process	C_3H_8 precooled open type expander process with separators	–	6	Only theoretical studies	Precooling: C3 Liquefaction: N_2-HC/NG	Same as the single-cycle MR*x*E processes, but rarely reported

[a]: the SPC grades for the simulated SPCs were classified by the lower limit (low: SPC≤0.25 kW·h/kg; medium: 0.25 kW·h/kg<SPC≤0.5 kW·h/kg; high: SPC>0.5 kW·h/kg); [b]: the research maturity was comprehensively classified by the quantity of literature and practical industrial applications

comparisons of the composition of different kinds of process were related mainly to volatile components in those processes operating with JT expansion, which could serve as a reference. (a) The fraction requirements of N_2 and CH_4 in single-cycle MR0V and single-cycle MR*x*V processes were found to be at a similar level (about 30%–45%). (b) The fraction requirements of N_2 and CH_4 in the liquefaction stages of multi-cycle MR0V and MR*x*V processes (the subcooling stage of the MFC process) were also similar (40%–60%). (c) The difference in the composition of volatile components between single-cycle and multi-cycle processes came from the different temperature ranges in which the liquefaction MRs worked. With a precooling stage sharing heat loads, the liquefaction MRs needed more volatile components to reach lower temperatures in multi-cycle processes.

2. The separation units can change the MR composition, thus providing extra DOFs for optimization and improvement. The tabulated SPCs of MR*x* processes were usually lower than those of MR0 processes, indicating the efficiency advantage of MR separation. Oil-lubricated compressors were suitable for small-scale systems in consideration of simplicity and economy, where the use of multiple separation or rectification was effective in avoiding oil block in the low temperature section.

3. Expanders had an advantage of less irreversibility than expansion valves, so it was appropriate to use expanders in place of expansion valves to reduce exergy losses. However, the processes with expanders have been much less studied, and are also less competitive than those with expansion valves in terms of SPCs (single-cycle MR0E>single-cycle MR0V, multi-cycle MR0E>multi-cycle MR0V, single-cycle MR*x*E>single-cycle MR*x*V). The reason might be related to the different MRs used in different categories of processes. In MR0E and MR*x*E processes, expanders usually deal with an N_2-CH_4 mixture in contrast to common MRs which contain heavier HCs, as in MR0V and MR*x*V processes, because an N_2-CH_4 mixture usually stays in gaseous phase in the operational range. Therefore, it might require more energy to liquefy the same amount of NG without the efficient phase-change heat transfer in MR0E and MR*x*E processes. If two-phase expanders or hydraulic turbines are used to deal with MRs containing heavier HCs in MR0E or MR*x*E processes, the performance might be greatly improved. However, it remains to be tested whether they could function normally during start-up or under conditions with dramatic changes in dryness. Another attempt to use gas expanders to deal with MRs containing heavier HCs was to expand only the separated vapor MR stream in an MR*x*E process, in which heavier HCs improved the temperature profile in the warmer temperature section and were removed to avoid liquid expansion. Additionally, the use of other non-JT expansion units was rarely reported, and there was only one case that used ejectors, and one that used vortex tubes. It might be difficult to determine their effectiveness due to the complicated operation mechanism of these two expansion units, as well as the unclear system performance after they are coupled.

4. The coupling of precooling or subcooling was beneficial in reducing SPC at a constant production

rate or at increased LNG production with a given power, by decreasing the exergy loss at the hot or cold ends of the HEXs. The overall efficiency and increased LNG production were preferred in large-scale industrial applications, while simplicity and low cost were preferred in small-scale or medium-scale ones, which reflects the comparison of typical processes such as the MFC and PRICO processes. The reduced equipment requirement and lower cost have made the PRICO process popular in small-scale applications even with a higher SPC, while the MFC process sacrifices its simplicity to seek larger production and a lower SPC.

5. The addition of separation units and coupled precooling/subcooling stages would inevitably increase the complexity and cost. Therefore, the production scale, the SPC level, and the cost should all be taken into consideration in process selection.

Several potential developments in MR-NGLPs in the future should be considered:

1. The search for the optimum MR composition in different configurations remains important and necessary. The composition ranges listed in Tables 1–8 can help determine the composition boundaries in future optimizations. Except for conventional N_2-HC mixtures, other environmentally friendly natural or synthetic working fluids can also be taken into consideration in NGLPs.

2. The use of multiple separation or rectification of MRs is effective in avoiding oil block when oil-lubricated compressors are used, which is an option worth considering, especially in small-scale applications.

3. JT expansion units have been more widely used than non-JT ones. From a thermodynamic point of view, the efficiency advantage of non-JT expansion units, especially expanders, has not been fully exploited. With the development of cryogenic fluid equipment, hydraulic turbines seem to be a promising choice in the two-phase expansion of conventional N_2-HC mixtures in MR0E or MR*x*E processes.

4. Precooling and subcooling, as conventional methods, are still effective for performance improvement of MR-NGLPs. In particular, precooling is a dominant solution for reducing the exergy loss at the hot end of the heat exchanger. Thus, it is possible to construct new multi-cycle processes with better thermodynamic performances on the basis of various single-cycle schemes.

5. Most published theoretical and experimental studies emphasize minimizing indicators related to power consumption, such as total or specific power consumption. This review also suggests that specific power consumption is the most important performance indicator. However, it is also meaningful to consider other performance indicators in future optimizations, such as exergy related parameters (the exergy efficiency of specific components or the overall system) and economy related indexes (operational or capital cost).

6 Conclusions

MRs have been widely used in the field of NG liquefaction and have promoted the configuration development of MR-NGLPs. In this paper, we have presented a review of the development of MR-NGLPs, and conducted analyses of the evolution and optimization of the featured process configurations. Various MR-NGLPs were classified based on a new classification framework from a configurative perspective, based on the following criteria: (1) employing a single or cascaded refrigeration cycle, (2) absence or presence of component separation, and (3) employing only JT expansion or other expansion types. The operating parameters and ranges of energy consumption of typical MR-NGLPs were collected and tabulated, using the SPC as the main performance indicator. This review will be helpful for scientific and industrial practitioners in revealing the featured characteristics of different kinds of MR-NGLPs, explaining their development from basic refrigeration cycles, and clarifying the configurative differences among MR-MGLPs. Additionally, the rough SPC ranges of different kinds of MR-NGLPs can serve as references for engineers when selecting an appropriate process under given power consumption requirements. The proposed framework is also beneficial for further optimizations and constructions of MR-NGLP configurations.

Contributors

Qi SONG conducted the literature survey, wrote the first draft of the manuscript, and revised and edited the final version.

Jing-peng ZHANG, Zhen ZHAO, and Jie-lin LUO assisted with the literature survey, and document delivery and arrangement. Qin WANG put forward the original idea of the proposed classification framework and supervised the research activities. Guang-ming CHEN provided suggestions on the classification framework.

Conflict of interest

Qi SONG, Jing-peng ZHANG, Zhen ZHAO, Jie-lin LUO, Qin WANG, and Guang-ming CHEN declare that they have no conflict of interest.

References

Air Products and Chemicals, Inc, 2005. Air Products to Provide New AP-X® Liquefaction Process Technology to RasGas II LNG Facility in Qatar. http://www.airproducts.com/Company/news-center/2005/09/0906-new-apx-liquefaction-process-qatar.aspx

Alabdulkarem A, Mortazavi A, Hwang Y, et al., 2011. Optimization of propane pre-cooled mixed refrigerant LNG plant. *Applied Thermal Engineering*, 31(6-7):1091-1098. https://doi.org/10.1016/j.applthermaleng.2010.12.003

Alfeev VN, Brodyanski VM, Yogadin VM, et al., 1973. Refrigerant for a Cryogenic Throttling Unit. UK Patent GB 1336892.

Ali W, Qyyum MA, Qadeer K, et al., 2018. Energy optimization for single mixed refrigerant natural gas liquefaction process using the metaheuristic vortex search algorithm. *Applied Thermal Engineering*, 129:782-791. https://doi.org/10.1016/j.applthermaleng.2017.10.078

Ali W, Qyyum MA, Khan MS, et al., 2019. Knowledge-inspired operational reliability for optimal LNG production at the offshore site. *Applied Thermal Engineering*, 150:19-29. https://doi.org/10.1016/j.applthermaleng.2018.12.165

Ansarinasab H, Mehrpooya M, 2017a. Advanced exergoeconomic analysis of a novel process for production of LNG by using a single effect absorption refrigeration cycle. *Applied Thermal Engineering*, 114:719-732. https://doi.org/10.1016/j.applthermaleng.2016.12.003

Ansarinasab H, Mehrpooya M, 2017b. Evaluation of novel process configurations for coproduction of LNG and NGL using advanced exergoeconomic analysis. *Applied Thermal Engineering*, 115:885-898. https://doi.org/10.1016/j.applthermaleng.2017.01.019

Aspelund A, Gundersen T, Myklebust J, et al., 2010. An optimization-simulation model for a simple LNG process. *Computers & Chemical Engineering*, 34(10):1606-1617. https://doi.org/10.1016/j.compchemeng.2009.10.018

Austbø B, Wahl PE, Gundersen T, 2013. Constraint handling in stochastic optimization algorithms for natural gas liquefaction processes. *Computer Aided Chemical Engineering*, 32:445-450. https://doi.org/10.1016/B978-0-444-63234-0.50075-0

Bach WA, 2002. Developments in the mixed fluid cascade process (MFCP) for LNG base load plants. *Linde Reports on Science and Technology*, 63:25-28.

Baek S, Hwang G, Jeong S, 2010. Development of the hybrid JT-expander cycle for NG liquefaction cycle. *AIP Conference Proceedings*, 1218(1):1113-1120. https://doi.org/10.1063/1.3422273

Barclay M, Shukri T, 2000. Enhanced single mixed refrigerant process for stranded gas liquefaction. Proceedings of the 79th Annual GPA Convention.

Bin Omar MN, Morosuk T, Tsatsaronis G, 2012. Exergy analyses applied to an AP-X process for the liquefaction of natural gas. Proceedings of ASME International Mechanical Engineering Congress and Exposition. https://doi.org/10.1115/IMECE2012-87572

Boyarsky M, Yudin B, Mogorychny VI, et al., 1995. Cryogenic Mixed Gas Refrigerant for Operation within Temperature Ranges of 80 K-100 K. US Patent 5441658.

Brendeng E, Neksa P, 2010. Method for Liquefaction of Gas. US Patent 2010058802A1.

British Petroleum, 2017. BP Statistical Review of World Energy. British Petroleum Company, London, UK.

Buijs C, Pek JJB, Meiring WJ, 2006. The PMR process, an innovative technology for large LNG trains. *The APPEA Journal*, 46(1):127-134. https://doi.org/10.1071/AJ05008

Buijs K, Pek B, Nagelvoort R, 2005. Shell's LNG technology for 7-10 MTPA LNG trains. Proceedings of International Petroleum Technology Conference. https://doi.org/10.2523/IPTC-10681-MS

Bukowski J, Liu YN, Boccella S, et al., 2011. Innovations in natural gas liquefaction technology for future LNG plants and floating LNG facilities. Proceedings of International Gas Union Research Conference.

Caetani E, Paradowski H, 1982. Method of and System for Liquefying a Gas with Low Boiling Temperature. US Patent 4339253.

Cao L, Liu JP, Xu XW, 2016. Robustness analysis of the mixed refrigerant composition employed in the single mixed refrigerant (SMR) liquefied natural gas (LNG) process. *Applied Thermal Engineering*, 93:1155-1163. https://doi.org/10.1016/j.applthermaleng.2015.10.072

Cao WS, Lu XS, Lin WS, et al., 2006. Parameter comparison of two small-scale natural gas liquefaction processes in skid-mounted packages. *Applied Thermal Engineering*, 26(8-9):898-904. https://doi.org/10.1016/j.applthermaleng.2005.09.014

Castillo L, Dorao CA, 2012. Consensual decision-making model based on game theory for LNG processes. *Energy Conversion and Management*, 64:387-396. https://doi.org/10.1016/j.enconman.2012.06.014

Castillo L, Dorao CA, 2013. On the conceptual design of pre-cooling stage of LNG plants using propane or an ethane/propane mixture. *Energy Conversion and Management*, 65:140-146. https://doi.org/10.1016/j.enconman.2012.07.015

Castillo L, Majzoub Dahouk M, Di Scipio S, et al., 2013. Conceptual analysis of the precooling stage for LNG

processes. *Energy Conversion and Management*, 66:41-47.
https://doi.org/10.1016/j.enconman.2012.09.021

Сердюков СГ, 2000. Лентрансгаз Производство и применение СПГ. *Газовая промышленность*, 8:66-67 (in Russian).

Chang HM, 2015. A thermodynamic review of cryogenic refrigeration cycles for liquefaction of natural gas. *Cryogenics*, 72:127-147.
https://doi.org/10.1016/j.cryogenics.2015.10.003

Charles PJ, 1968. Method and Apparatus for the Cooling and Low Temperature Liquefaction of Gaseous Mixtures. US Patent 3364685.

Chen GM, Zhang SZ, Wang JF, et al., 2000. Cryogenic Refrigerator. CN Patent 2364403Y (in Chinese).

Coers DH, Sudduth JW, 1976. Refrigerant Apparatus and Process Using Multicomponent Refrigerant. US Patent 3932154.

Darredeau B, 1973. Method of Cooling a Gaseous Mixture and Installation Therefor. US Patent 3780535.

Davis RN, Newton CL, 1990. Natural Gas Liquefaction Process Using Low Level High Level and Absorption Refrigeration Cycles. US Patent 4911741.

Ding H, Sun H, He M, 2016. Optimisation of expansion liquefaction processes using mixed refrigerant N_2–CH_4. *Applied Thermal Engineering*, 93:1053-1060.
https://doi.org/10.1016/j.applthermaleng.2015.10.004

Ding H, Sun H, Sun SJ, et al., 2017. Analysis and optimisation of a mixed fluid cascade (MFC) process. *Cryogenics*, 83:35-49.
https://doi.org/10.1016/j.cryogenics.2017.02.002

Etzbach V, Förg W, 1972. Refrigeration Cycle for the Al-iquefaction of Natural Gas. US Patent 3702063.

Finn AJ, Johnson GL, Tomlinson TR, 1999. Developments in natural gas liquefaction. *Hydrocarbon Processing*, 78(4): 47-59.

Fischer B, Martin P, Rojey A, 2004. Liquefaction of Natural Gas with Natural Gas Recycling. US Patent 6763680B2.

Foglietta JH, 1998. Use of a Turboexpander Cycle in Liquefied Natural Gas Process. US Patent 5755114.

Foglietta JH, 1999. New LNG process scheme. Proceedings of the 78th Annual GPA Convention.

Förg W, 1978. Liquefaction of Natural Gas. US Patent 4112700.

Foss MM, 2012. Introduction to LNG: an Overview on Liquefied Natural Gas (LNG), Its Properties, the LNG Industry, and Safety Considerations. Center for Energy Economics (US), Houston, USA.

Garier C, Paradowski H, 1981. Method and Plant for Liquefying a Gas with Low Boiling Temperature. US Patent 4274849.

Gaumer Jr LS, Newton CL, 1971. Liquefaction of Natural Gas Employing Multiple-component Refrigerants. US Patent 3593535.

Gaumer Jr LS, Newton CL, 1972. Process for Liquefying Natural Gas Employing a Multicomponent Refrigerant for Obtaining Low Temperature Cooling. US Patent 3645106.

Gaumer Jr LS, Newton CL, 1973. Combined Cascade and Multicomponent Refrigeration System and Method. US Patent 3763658.

Geist JM, 1983. The role of LNG in energy supply. *International Journal of Refrigeration*, 6(5-6):283-297.
https://doi.org/10.1016/0140-7007(83)90008-7

Ghorbani B, Hamedi MH, Shirmohammadi R, et al., 2016. Exergoeconomic analysis and multi-objective Pareto optimization of the C3MR liquefaction process. *Sustainable Energy Technologies and Assessments*, 17:56-67.
https://doi.org/10.1016/j.seta.2016.09.001

Ghorbani B, Hamedi MH, Amidpour M, et al., 2017. Implementing absorption refrigeration cycle in lieu of DMR and C3MR cycles in the integrated NGL, LNG and NRU unit. *International Journal of Refrigeration*, 77:20-38.
https://doi.org/10.1016/j.ijrefrig.2017.02.030

Gong MQ, Wu JF, Luo EC, et al., 2004. Study of the single-stage mixed-gases refrigeration cycle for cooling temperature-distributed heat loads. *International Journal of Thermal Sciences*, 43(1): 31-41.
https://doi.org/10.1016/S1290-0729(03)00097-8

Gong MQ, Wu JF, Sun ZH, et al., 2012. Development and performance test of a small trailer-mounted moveable natural gas liquefier. *Energy Conversion and Management*, 57:148-153.
https://doi.org/10.1016/j.enconman.2011.10.027

Gong MQ, Guo H, Sun ZH, et al., 2015. Advances in mobile natural gas mini-liquefiers. *CIESC Journal*, 66(S2):10-20 (in Chinese).
https://doi.org/10.11949/j.issn.0438-1157.20150699

Gou YJ, Jiang XX, Chen JL, et al., 2015. Optimization and comparison of the pre-cooled mixed refrigerant LNG process. *Petrochem Industry Application*, 34(2):112-116 (in Chinese).
https://doi.org/10.3969/j.issn.1673-5285.2015.02.031

Gu AZ, Lu XS, Wang RS, et al., 2004. Liquefied Natural Gas Technology. China Machine Press, Beijing, China (in Chinese).

Hampson W, 1896. Apparatus for Separating Mixed Gases by Refrigeration, Especially Applicable to Separation of Oxygen from Air. US Patent 620312.

Hanson TC, Kun LC, 1988. Process to Produce Liquid Cryogen. US Patent 4778497.

Hatcher P, Khalilpour R, Abbas A, 2012. Optimisation of LNG mixed-refrigerant processes considering operation and design objectives. *Computers & Chemical Engineering*, 41:123-133.
https://doi.org/10.1016/j.compchemeng.2012.03.005

He TB, Ju YL, 2013. Design and optimization of natural gas liquefaction process by utilizing gas pipeline pressure energy. *Applied Thermal Engineering*, 57(1-2):1-6.
https://doi.org/10.1016/j.applthermaleng.2013.03.044

He TB, Karimi IA, Ju YL, 2018. Review on the design and optimization of natural gas liquefaction processes for onshore and offshore applications. *Chemical Engineering Research and Design*, 132:89-114. https://doi.org/10.1016/j.cherd.2018.01.002

He TB, Liu ZM, Ju YL, et al., 2019. A comprehensive optimization and comparison of modified single mixed refrigerant and parallel nitrogen expansion liquefaction process for small-scale mobile LNG plant. *Energy*, 167:1-12. https://doi.org/10.1016/j.energy.2018.10.169

Helgestad DE, 2009. Modelling and Optimization of the C3MR Process for Liquefaction of Natural Gas. Report No. TKP 4550, Norwegian University of Science and Technology, Stavanger, Norway.

Herron DM, Chatterjee N, 1990. Liquefaction of Natural Gas Using Process-loaded Expanders. US Patent 4970867.

Husnil YA, Lee M, 2014. Synthesis of an optimizing control structure for dual mixed refrigerant process. *Journal of Chemical Engineering of Japan*, 47(8):678-686. https://doi.org/10.1252/jcej.14we098

Hwang JH, Roh MI, Lee KY, 2013. Determination of the optimal operating conditions of the dual mixed refrigerant cycle for the LNG FPSO topside liquefaction process. *Computers & Chemical Engineering*, 49:25-36. https://doi.org/10.1016/j.compchemeng.2012.09.008

Jacobsen MG, Skogestad S, 2013. Active constraint regions for a natural gas liquefaction process. *Journal of Natural Gas Science and Engineering*, 10:8-13. https://doi.org/10.1016/j.jngse.2012.10.002

Jensen JB, Skogestad S, 2006. Optimal operation of a mixed fluid cascade LNG plant. *Computer Aided Chemical Engineering*, 21:1569-1574. https://doi.org/10.1016/S1570-7946(06)80271-3

Jensen JB, Skogestad S, 2009a. Single-cycle mixed-fluid LNG process part I: optimal design. Proceedings of the 1st Annual Gas Processing Symposium. https://doi.org/10.1016/B978-0-444-53292-3.50028-6

Jensen JB, Skogestad S, 2009b. Steady-state operational degrees of freedom with application to refrigeration cycles. *Industrial & Engineering Chemistry Research*, 48(14): 6652-6659. https://doi.org/10.1021/ie800565z

Johanson ES, 1965. Natural Gas Liquefaction and Separation. US Patent 3182461.

Kalinowski P, Hwang Y, Radermacher R, et al., 2009. Application of waste heat powered absorption refrigeration system to the LNG recovery process. *International Journal of Refrigeration*, 32(4):687-694. https://doi.org/10.1016/j.ijrefrig.2009.01.029

Khan MS, Lee M, 2013. Design optimization of single mixed refrigerant natural gas liquefaction process using the particle swarm paradigm with nonlinear constraints. *Energy*, 49:146-155. https://doi.org/10.1016/j.energy.2012.11.028

Khan MS, Lee S, Lee M, 2012. Optimization of single mixed refrigerant natural gas liquefaction plant with nonlinear programming. *Asia-Pacific Journal of Chemical Engineering*, 7(S1):S62-S70. https://doi.org/10.1002/apj.642

Khan MS, Lee S, Rangaiah GP, et al., 2013. Knowledge based decision making method for the selection of mixed refrigerant systems for energy efficient LNG processes. *Applied Energy*, 111:1018-1031. https://doi.org/10.1016/j.apenergy.2013.06.010

Khan MS, Karimi IA, Lee M, 2016. Evolution and optimization of the dual mixed refrigerant process of natural gas liquefaction. *Applied Thermal Engineering*, 96:320-329. https://doi.org/10.1016/j.applthermaleng.2015.11.092

Khan MS, Karimi IA, Wood DA, 2017. Retrospective and future perspective of natural gas liquefaction and optimization technologies contributing to efficient LNG supply: a review. *Journal of Natural Gas Science and Engineering*, 45:165-188. https://doi.org/10.1016/j.jngse.2017.04.035

Kleemenko AP, 1959. One flow cascade cycle. Proceedings of the 10th International Congress of Refrigeration, p.34-39.

Krieger H, 1978. Arrangement for Cooling Fluids. US Patent 4094655.

Lee GC, Smith R, Zhu XX, 2002. Optimal synthesis of mixed-refrigerant systems for low-temperature processes. *Industrial & Engineering Chemistry Research*, 41(20): 5016-5028. https://doi.org/10.1021/ie020057p

Lee I, Moon I, 2016. Total cost optimization of a single mixed refrigerant process based on equipment cost and life expectancy. *Industrial & Engineering Chemistry Research*, 55(39):10336-10343. https://doi.org/10.1021/acs.iecr.6b01864

Lee I, Tak K, Lim W, et al., 2013. Deterministic optimization of pure refrigerant system in C3MR process. Proceedings of the 6th International Conference on Process Systems Engineering (PSE ASIA).

Lee I, Tak K, Lee S, et al., 2015. Decision making on liquefaction ratio for minimizing specific energy in a LNG pilot plant. *Industrial & Engineering Chemistry Research*, 54(51):12920-12927. https://doi.org/10.1021/acs.iecr.5b03687

Lee W, An J, Lee JM, et al., 2018. Design of single mixed refrigerant natural gas liquefaction process considering load variation. *Chemical Engineering Research and Design*, 139:89-103. https://doi.org/10.1016/j.cherd.2018.09.017

Little WA, 1978a. Design and construction of microminiature cryogenic refrigerators. *AIP Conference Proceedings*, 44(1):421-424. https://doi.org/10.1063/1.31375

Little WA, 1978b. Scaling of miniature cryocoolers to microminiature size. Proceedings of NIST (NBS) Cryocoolers Conference, p.75-80.

Little WA, 1988. Recent developments in Joule-Thomson cooling: gases, coolers and compressors. Proceedings of the 5th Cryocoolers Conference, p.3-11.

Little WA, 1990. Advances in Joule-Thomson cooling. *In*: Fast

RW (Ed.), Advances in Cryogenic Engineering. Springer, Boston, USA, p.1305-1314.
https://doi.org/10.1007/978-1-4613-0639-9_155

Little WA, 1997. Self-cleaning Low-temperature Refrigeration System. US Patent 5617739.

Little WA, Sapozhnikov I, 1997. Low cost cryocoolers for cryoelectronics. *In*: Ross RG (Ed.), Cryocoolers 9. Springer, Boston, USA, p.509-513.
https://doi.org/10.1007/978-1-4615-5869-9_58

Liu R, 2013. Theoretical and Experimental Studies on an Auto-cascade Natural Gas Liquefier Using a Rectifying Column. MS Thesis, Zhejiang University, Hangzhou, China (in Chinese).

Liu X, Luo YY, Karney BW, et al., 2015. A selected literature review of efficiency improvements in hydraulic turbines. *Renewable and Sustainable Energy Reviews*, 51:18-28.
https://doi.org/10.1016/j.rser.2015.06.023

Liu YN, Pervier JW, 1985. Dual Mixed Refrigerant Natural Gas Liquefaction. US Patent 4545795.

Liu YN, Newton CL, 1988. Feed Gas Drier Precooling in Mixed Refrigerant Natural Gas Liquefaction Processes. US Patent 4755200.

Longsworth RC, 1994. Cryogenic Refrigerator with Single Stage Compressor. US Patent 5337572.

Longsworth RC, Boiarski MJ, Klusmier LA, 1995. 80 K closed-cycle throttle refrigerator. *In*: Ross Jr RG (Ed.), Cryocoolers 8. Springer, Boston, USA, p.537-541.
https://doi.org/10.1007/978-1-4757-9888-3_55

Longsworth RC, Boiarsky MJ, Khatri A, 1996. Cryostat Refrigeration System Using Mixed Refrigerants in a Closed Vapor Compression Cycle Having a Fixed Flow Restrictor. US Patent 5579654.

Lu Z, Zhong Z, Wang Y, et al., 2009. Medium and Small Scale Mixed Refrigerant Natural Gas Liquefaction System with Ejector. CN Patent 100552322C (in Chinese).

Luo SL, Gai JQ, Jiang H, et al., 2015. PRICOOR natural gas liquefaction technology and practical application. *Chemical Engineering of Oil & Gas*, 44(1):50-53 (in Chinese).
https://doi.org/10.3969/j.issn.1007-3426.2015.01.011

Maher JB, Sudduth JW, 1975. Method and Apparatus for Liquefying Gases. US Patent 3914949.

Maunder AD, Skinner GF, 2003. Method for Liquefying Methane Rich Gas. WO Patent 03/019095 A1.

Maunder AD, Skinner GF, 2007. Method for Liquefying Methane-rich Gas. US Patent 7234321 B2.

Mazyan W, Ahmadi A, Ahmed H, et al., 2016. Market and technology assessment of natural gas processing: a review. *Journal of Natural Gas Science and Engineering*, 30:487-514.
https://doi.org/10.1016/j.jngse.2016.02.010

Mehrpooya M, Omidi M, Vatani A, 2016. Novel mixed fluid cascade natural gas liquefaction process configuration using absorption refrigeration system. *Applied Thermal Engineering*, 98:591-604.
https://doi.org/10.1016/j.applthermaleng.2015.12.032

Mehrpooya M, Sharifzadeh MMM, Ansarinasab H, 2018. Investigation of a novel integrated process configuration for natural gas liquefaction and nitrogen removal by advanced exergoeconomic analysis. *Applied Thermal Engineering*, 128:1249-1262.
https://doi.org/10.1016/j.applthermaleng.2017.09.088

Missimer DJ, 1972. Control System for Low Temperature Refrigeration System. US Patent 3698202.

Moein P, Sarmad M, Khakpour M, et al., 2016. Methane addition effect on a dual nitrogen expander refrigeration cycle for LNG production. *Journal of Natural Gas Science and Engineering*, 33:1-7.
https://doi.org/10.1016/j.jngse.2016.04.061

Mokhatab S, Economides MJ, 2006. Process selection is critical to onshore LNG economics. *World Oil*, 227(2):95-99.

Morosuk T, Tesch S, Hiemann A, et al., 2015. Evaluation of the PRICO liquefaction process using exergy-based methods. *Journal of Natural Gas Science and Engineering*, 27:23-31.
https://doi.org/10.1016/j.jngse.2015.02.007

Mortazavi A, Rodgers P, Al-Hashimi S, et al., 2008. Enhancement of LNG propane cycle through waste heat powered absorption cooling. Proceedings of the 2nd International Energy 2030 Conference.

Mortazavi A, Somers C, Alabdulkarem A, et al., 2010. Enhancement of APCI cycle efficiency with absorption chillers. *Energy*, 35(9):3877-3882.
https://doi.org/10.1016/j.energy.2010.05.043

Na J, Lim Y, Han CH, 2017. A modified DIRECT algorithm for hidden constraints in an LNG process optimization. *Energy*, 126:488-500.
https://doi.org/10.1016/j.energy.2017.03.047

Nagelvoort RK, 2002. Plant for Liquefying Natural Gas. US Patent 6389844 B1.

Nawaz A, Qyyum MA, Qadeer K, et al., 2019. Optimization of mixed fluid cascade LNG process using a multivariate Coggins step-up approach: overall compression power reduction and exergy loss analysis. *International Journal of Refrigeration*, 104:189-200.
https://doi.org/10.1016/j.ijrefrig.2019.04.002

Neeraas BO, Brendeng E, 2004. Method and Device for Small Scale Liquefaction of a Product Gas. US Patent 6751984 B2.

Nekså P, Brendeng E, 2007. Small scale natural gas liquefaction plants. Proceedings of the 22nd International Congress of Refrigeration.

Nelson WL, Garcia L, 1991. Method of Liquefying Natural Gas. US Patent 5036671.

Newton CL, 1985. Dual Mixed Refrigerant Natural Gas Liquefaction with Staged Compression. US Patent 4525185.

Nezhad SA, Shabani B, Soleimani M, 2012. Thermodynamic analysis of liquefied natural gas (LNG) production cycle in APCI process. *Journal of Thermal Science*, 21(6): 564-571.
https://doi.org/10.1007/s11630-012-0582-x

Nibbelke R, Kauffman S, Pek B, 2002. Double mixed refrigerant LNG process provides viable alternative for tropical conditions. *Oil and Gas Journal*, 100(27):64-66.

Paradowski H, 1982. Method of and System for Refrigerating a Fluid to be Cooled Down to a Low Temperature. US Patent 4334902.

Park K, Won W, Shin D, 2016. Effects of varying the ambient temperature on the performance of a single mixed refrigerant liquefaction process. *Journal of Natural Gas Science and Engineering*, 34:958-968. https://doi.org/10.1016/j.jngse.2016.07.069

Pek JJB, van Driel A, de Jong ECJN, et al., 2004. Large capacity LNG plant development. Proceedings of 14th International Conference on Liquefied Natural Gas.

Pereira C, Lequisiga D, 2014. Technical evaluation of C3-MR and cascade cycle on natural gas liquefaction process. *International Journal of Chemical Engineering and Applications*, 5(6):451-456. https://doi.org/10.7763/IJCEA.2014.V5.427

Podbielniak WJ, 1936. Art of Refrigeration. US Patent 2041725.

Price BC, 1997. Closed Loop Single Mixed Refrigerant Process. US Patent 5657643.

Pu L, Sun SX, Li YZ, et al., 2007. Calculation and thermodynamic analysis on liquefaction processes of natural gas with expanders. *Journal of Xi'an Jiaotong University*, 41(9):1115-1118 (in Chinese). https://doi.org/10.3321/j.issn:0253-987x.2007.09.025

Pu L, Sun SX, Cheng XH, et al., 2008. Calculations and exergy analysis on several kinds of liquefaction processes of natural gas. *Chemical Engineering*, 36(2):54-58 (in Chinese). https://doi.org/10.3969/j.issn.1005-9954.2008.02.014

Qyyum MA, Qadeer K, Lee M, 2017. Comprehensive review of the design optimization of natural gas liquefaction processes: current status and perspectives. *Industrial & Engineering Chemistry Research*, 57(17):5819-5844. https://doi.org/10.1021/acs.iecr.7b03630

Qyyum MA, van Duc Long N, Minh LQ, et al., 2018a. Design optimization of single mixed refrigerant LNG process using a hybrid modified coordinate descent algorithm. *Cryogenics*, 89:131-140. https://doi.org/10.1016/j.cryogenics.2017.12.005

Qyyum MA, Ali W, van Duc Long N, et al., 2018b. Energy efficiency enhancement of a single mixed refrigerant LNG process using a novel hydraulic turbine. *Energy*, 144:968-976. https://doi.org/10.1016/j.energy.2017.12.084

Qyyum MA, Minh LQ, Ali W, et al., 2018c. Feasibility study of environmental relative humidity through the thermodynamic effects on the performance of natural gas liquefaction process. *Applied Thermal Engineering*, 128:51-63. https://doi.org/10.1016/j.applthermaleng.2017.08.090

Qyyum MA, Qadeer K, Lee S, et al., 2018d. Innovative propane-nitrogen two-phase expander refrigeration cycle for energy-efficient and low-global warming potential LNG production. *Applied Thermal Engineering*, 139:157-165. https://doi.org/10.1016/j.applthermaleng.2018.04.105

Rao HN, Karimi IA, 2017. A superstructure-based model for multistream heat exchanger design within flow sheet optimization. *AIChE Journal*, 63(9):3764-3777. https://doi.org/10.1002/aic.15714

Remeljej CW, Hoadley AFA, 2006. An exergy analysis of small-scale liquefied natural gas (LNG) liquefaction processes. *Energy*, 31(12):2005-2019. https://doi.org/10.1016/j.energy.2005.09.005

Ren B, Chen FS, Wang H, et al., 2014. Concentration optimizations on small scale auto-cascade natural gas liquefier using rectifying column. *CIESC Journal*, 65(S2): 169-174 (in Chinese).

Roberts MJ, 2006. Integrated Multiple-loop Refrigeration Process for Gas Liquefaction. US Patent 7086251 B2.

Roberts MJ, Agrawal R, 2001a. Dual Mixed Refrigerant Cycle for Gas Liquefaction. US Patent 6269655 B1.

Roberts MJ, Agrawal R, 2001b. Hybrid Cycle for the Production of Liquefied Natural Gas. US Patent 6308531 B1.

Roberts MJ, Bronfenbrenner JC, Liu YN, et al., 2002a. Large capacity single train AP-X^{TM} hybrid LNG process. Proceedings of GASTECH 2002.

Roberts MJ, Agrawal R, Daugherty TL, 2002b. Single Mixed Refrigerant Gas Liquefaction Process. US Patent 6347531 B1.

Roberts MJ, Liu YN, Bronfenbrenner JC, et al., 2004. Technology selection. *Hydrocarbon Engineering*, 9:81-84.

Rodgers P, Mortazavi A, Eveloy V, et al., 2012. Enhancement of LNG plant propane cycle through waste heat powered absorption cooling. *Applied Thermal Engineering*, 48:41-53. https://doi.org/10.1016/j.applthermaleng.2012.04.031

Sanavandi H, Ziabasharhagh M, 2016. Design and comprehensive optimization of C3MR liquefaction natural gas cycle by considering operational constraints. *Journal of Natural Gas Science and Engineering*, 29:176-187. https://doi.org/10.1016/j.jngse.2015.12.055

Sanaye S, Ghoreishi SMS, 2019. Energy, exergy and economic analyses of two modified and optimized small-scale natural gas liquefaction (LNG) cycles using N_2 and N_2/CH_4 refrigerants with CO_2 precooling. *Cryogenics*, 102:66-76. https://doi.org/10.1016/j.cryogenics.2019.07.003

Sarsten JA, 1977a. Fractional Condensation of an NG Feed with Two Independent Refrigeration Cycles. US Patent 4057972.

Sarsten JA, 1977b. Natural Gas Liquefaction Process. UK Patent GB 1472196.

Shell Internationale Research Maatschappij NV, 1962. Improvements in or Relating to Process and Apparatus for Liquefying Natural Gas. UK Patent GB 895094.

Shirazi MMH, Mowla D, 2010. Energy optimization for liquefaction process of natural gas in peak shaving plant. *Energy*, 35(7):2878-2885. https://doi.org/10.1016/j.energy.2010.03.018

Siemens CW, 1857. Improvements in Refrigerating and Producing Ice, and in Apparatus or Machinery for That Purpose. UK Patent GB 2064.

Simon J, Etzbach V, Grimm P, et al., 1974. One Flow Cascade Cycle with Buffer Volume Bypass. US Patent 3855810.

Song C, Tan S, Qu FC, et al., 2019. Optimization of mixed refrigerant system for LNG processes through graphically reducing exergy destruction of cryogenic heat exchangers. *Energy*, 168:200-206.
https://doi.org/10.1016/j.energy.2018.11.105

Stockmann R, Forg W, Bolt M, et al., 2001. Method for Liquefying a Stream Rich in Hydrocarbons. US Patent 6253574 B1.

Streich M, 1971. Liquefaction Process for Gas Mixtures by Means of Fractional Condensation. US Patent 3596473.

Streich M, 1973. Gas Liquefaction by a Fractionally Condensed Refrigerant. US Patent 3747359.

Sun H, Ding H, 2014. Plant simulation and operation optimisation of SMR plant with different adjustment methods under part-load conditions. *Computers & Chemical Engineering*, 68:107-113.
https://doi.org/10.1016/j.compchemeng.2014.05.011

Sun H, Ding DH, He M, et al., 2016. Simulation and optimisation of AP-X process in a large-scale LNG plant. *Journal of Natural Gas Science and Engineering*, 32:380-389.
https://doi.org/10.1016/j.jngse.2016.04.039

Swenson LK, 1977. Single Mixed Refrigerant, Closed Loop Process for Liquefying Natural Gas. US Patent 4033735.

Vatani A, Mehrpooya M, Palizdar A, 2014. Energy and exergy analyses of five conventional liquefied natural gas processes. *International Journal of Energy Research*, 38(14): 1843-1863.
https://doi.org/10.1002/er.3193

Venkatarathnam G, 2008. Natural gas liquefaction processes. *In*: Timmerhaus KD, Rizzuto C (Eds.), Cryogenic Mixed Refrigerant Processes. Springer, Berilin, Germany, p.149-220.
https://doi.org/10.1007/978-0-387-78514-1

Vink KJ, Nagelvoort RK, 1998. Comparison of baseload liquefaction processes. Proceedings of the 12th International Conference on Liquefied Natural Gas.

von Linde C, 1895. Gasverflüssigungs-maschine (Machine for the Liquefaction of Gas). CH Patent 10704 (in German).

Wahl PE, Løvseth SW, Mølnvik MJ, 2013. Optimization of a simple LNG process using sequential quadratic programming. *Computers & Chemical Engineering*, 56:27-36.
https://doi.org/10.1016/j.compchemeng.2013.05.001

Wang H, Chen FS, Song Q, et al., 2015. Performance optimizations on a new small scale auto-cascade natural gas liquefier using a rectifying column. *CIESC Journal*, 66(S2):231-237 (in Chinese).
https://doi.org/10.11949/j.issn.0438-1157.20150710

Wang K, Pu LM, Han SY, et al., 2014. Optimization of a small scale natural gas liquefaction process with N_2-CH_4 expansion refrigeration. *Natural Gas Chemical Industry*, 39(1):27-31 (in Chinese).
https://doi.org/10.3969/j.issn.1001-9219.2014.01.006

Wang MQ, Zhang J, Xu Q, et al., 2011. Thermodynamic-analysis-based energy consumption minimization for natural gas liquefaction. *Industrial & Engineering Chemistry Research*, 50(22):12630-12640.
https://doi.org/10.1021/ie2006388

Wang MQ, Zhang J, Xu Q, 2012. Optimal design and operation of a C3MR refrigeration system for natural gas liquefaction. *Computers & Chemical Engineering*, 39:84-95.
https://doi.org/10.1016/j.compchemeng.2011.12.003

Wang MY, Khalilpour R, Abbas A, 2013. Operation optimization of propane precooled mixed refrigerant processes. *Journal of Natural Gas Science and Engineering*, 15:93-105.
https://doi.org/10.1016/j.jngse.2013.09.007

Wang MY, Khalilpour R, Abbas A, 2014. Thermodynamic and economic optimization of LNG mixed refrigerant processes. *Energy Conversion and Management*, 88:947-961.
https://doi.org/10.1016/j.enconman.2014.09.007

Wang Q, Wang J, Chen G, et al., 2012a. An Auto-cascade Gas Liquefaction System with a Rectifying Column. CN Patent 10214317B (in Chinese).

Wang Q, Wang J, Chen G, et al., 2012b. A Variable Concentration Auto-cascade Gas Liquefaction System with a Rectifying Column. CN Patent 102147162B (in Chinese).

Wang Q, Liu R, Wang JP, et al., 2012c. An investigation of the mixing position in the recuperators on the performance of an auto-cascade refrigerator operating with a rectifying column. *Cryogenics*, 52(11):581-589.
https://doi.org/10.1016/j.cryogenics.2012.08.003

Wang Q, Liu R, Wang JP, et al., 2013. The influence types of the mixing position in the recuperators of an auto-cascade refrigerator operating with a rectifying column. *Journal of Engineering Thermophysics*, 34(5):802-807 (in Chinese).

Wang Q, Song Q, Zhang JP, et al., 2019a. Performance analyses on four configurations of natural gas liquefaction process operating with mixed refrigerants and a rectifying column. *Cryogenics*, 97:13-21.
https://doi.org/10.1016/j.cryogenics.2018.11.005

Wang Q, Song Q, Zhang JP, et al., 2019b. Experimental studies on a natural gas liquefaction process operating with mixed refrigerants and a rectifying column. *Cryogenics*, 99:7-17.
https://doi.org/10.1016/j.cryogenics.2019.02.007

Watson HAJ, Vikse M, Gundersen T, et al., 2018. Optimization of single mixed-refrigerant natural gas liquefaction processes described by nondifferentiable models. *Energy*, 150:860-876.
https://doi.org/10.1016/j.energy.2018.03.013

Wu JF, Gong MQ, Liu JL, 2002. A new type mixture refrigeration auto-cascade cycle with partial condensation and separation reflux exchanger and its preliminary experimental test. *AIP Conference Proceedings*, 613(1):887-892. https://doi.org/10.1063/1.1472108

Wu JF, Gong MQ, Luo EC, 2003. Multi-component Mixed Refrigerant Throttling Cryogenic System with Partial Condensation. CN Patent 1122797C (in Chinese).

Xu WY, 2005. Small scale liquefied natural gas production plant. *Chemical Engineering of Oil and Gas*, 34(3):161-164 (in Chinese). https://doi.org/10.3969/j.issn.1007-3426.2005.03.004

Xu XW, Liu JP, Jiang CS, et al., 2013. The correlation between mixed refrigerant composition and ambient conditions in the PRICO LNG process. *Applied Energy*, 102:1127-1136. https://doi.org/10.1016/j.apenergy.2012.06.031

Xu XW, Liu JP, Cao L, 2014. Optimization and analysis of mixed refrigerant composition for the PRICO natural gas liquefaction process. *Cryogenics*, 59:60-69. https://doi.org/10.1016/j.cryogenics.2013.11.001

Yoon JI, Lee HS, Oh ST, et al., 2009. Characteristics of cascade and C3MR cycle on natural gas liquefaction process. *International Journal of Chemical and Molecular Engineering*, 3(11):620-624. https://doi.org/10.5281/zenodo.1080259

Zhang AM, Chen GM, Wang Q, 2008. Experimental study on a small-scale liquefied natural gas apparatus. *Journal of Zhejiang University (Engineering Science)*, 42(11):1973-1976 (in Chinese). https://doi.org/10.3785/j.issn.1008-973X.2008.11.024

Zhang SZ, Wang JF, Zhang HX, et al., 2001. Analysis of an auto-refrigerating cascade system utilizing a rectifying column. *Journal of Engineering Thermophysics*, 22(1): 25-27 (in Chinese). https://doi.org/10.3321/j.issn:0253-231x.2001.01.008

中文概要

题　目：混合工质天然气液化流程的特色结构与性能综述

概　要： 天然气的运输与储存均以液态（LNG）为宜。近几十年来，随着混合制冷剂天然气液化流程的飞速发展，出现了种类繁多的结构形式，为业界提供了丰富的选择。针对种类繁多的混合制冷剂天然气液化流程，本文提出了一个新的分类框架，并在此基础上介绍了每一类中具有特色的商业化流程或专利设计中的结构特点；同时，整理和讨论了这些流程所采用的制冷剂组合和运行参数（包括运行压力、每一级的制冷温度和蒸发压力位的数量等），并将单位液化功作为最重要的性能指标。本综述旨在从流程结构的角度厘清混合制冷剂天然气液化流程的发展历程，以及展示流程之间结构性的区别，为从业人员选择合适流程提供参考，同时也为已有流程性能的优化以及新流程的构建提供依据与建议。

关键词： 天然气；液化；混合制冷剂；结构；性能